



Sonoma Technology Inc.

5510 Skylane Blvd., Suite 101
Santa Rosa, CA 95403-1083
707 / 527-9372

NAVAJO GENERATING STATION
VISIBILITY CONTRIBUTION STUDY

STATUS REPORT #2

WORKING DRAFT NUMBER 4
FOR REVIEW PURPOSES

Edited by
L. Willard Richards and Donald L. Blumenthal

Contributing Authors:

Aerosol Dynamics
Susanne Hering

AeroVironment Inc.
Robert Nininger
Ivar Tombach

Salt River Project
Joe Sutherland

Ted B. Smith & Associates
Ted Smith

Sonoma Technology Inc.
Donald Blumenthal
Jun Chen
Corinne Cottle
Tim Dye
Charles (Lin) Lindsey
Jeff Prouty
Willard Richards

Systems Applications Inc.
Andrew Gray

University of Minnesota
Peter McMurry
Barbara Turpin
Xinqiu Zhang

Prepared for:

Prem Bhardwaja
Salt River Project
P.O. Box 52025
Phoenix, AZ 85072

STI-99284-1019-WD4
November 7, 1990





Sonoma Technology Inc.

NAVAJO GENERATING STATION VISIBILITY STUDY

STATUS REPORT #2

WORKING DRAFT NUMBER 4 FOR REVIEW PURPOSES

EDITED BY L. WILLARD RICHARDS AND DONALD L. BLUMENTHAL
SONOMA TECHNOLOGY INC. WITH CONTRIBUTIONS
FROM:

AEROSOL DYNAMICS

AEROVIRONMENT INC.

SALT RIVER PROJECT

TED B. SMITH & ASSOCIATES

SONOMA TECHNOLOGY INC.

SYSTEMS APPLICATIONS INC.

UNIVERSITY OF MINNESOTA

**GCES OFFICE COPY
DO NOT REMOVE!**

Prepared for
Prem Bhardwaja
Salt River Project
P.O. Box 52025
Phoenix, AZ 85072

STI-99284-1019-WD4
November 7, 1990

5510 Skylane Blvd., Suite 101 • Santa Rosa, CA 95403-1083

707/527-9372

120.01

5/20/91

N318

21391

7/1/91



PLEASE READ BEFORE READING REPORT

PREFACE

This document is an interim working document and should be considered as work in progress. The data, analyses, and results presented here should be considered as preliminary. They will continue to evolve as additional data are processed and additional analyses are performed.

The analysis and modeling efforts described here have been performed by independent research teams. In general, the results of these analyses are self-consistent. In a few cases, however, the results of analyses performed by different methods and with different portions of the data base may not be totally consistent with one another. Discrepancies between the analyses will be investigated as they are identified or brought to our attention.

Readers of this report are encouraged to suggest changes or additions which will improve the analyses, help to better meet the objectives, or which will correct errors, omissions, misinterpretations, or misrepresentations.

ACKNOWLEDGEMENTS

This work was funded by the Salt River Project and the participants in the Navajo Generating Station. The cooperation and assistance of the National Park Service and the staff of the Grand Canyon National Park have made this project possible and are greatly appreciated. The authors would like to thank the employees of all of the organizations involved in the study for their tremendous efforts in both the field program and in the preparation of the status reports.

The major participating organizations and their roles in the study are listed below:

- Salt River Project: Sponsor, NGS operation, emissions measurements, air quality measurements, forecasting, meteorological analysis.
- AeroVironment Inc.: Member of the study design and coordination team, field program management, construction and operation of the ground sampling network, operation of Doppler acoustic sounders, data management, data analysis.
- Sonoma Technology Inc.: Member of the study design and coordination team, coordination and operation of sampling aircraft, operation of meteorological stations, upper air soundings, data analysis, data analysis coordination.
- Systems Applications Inc.: Member of the study design and coordination team, deterministic modeling.
- Tracer Technologies: Tracer release, tracer analysis.
- Desert Research Institute: Quality assurance, quality assurance coordination, data analysis.

Additional participants in the field study and/or data analyses are:

Aerosol Dynamics	NOAA Environmental Research Laboratory
Asea Brown Boveri Environmental	NOAA Wave Propagation Laboratory
Battelle Northwest Laboratories	Sunset Labs
Caltech	Ted B. Smith and Associates
ENSR	Unisearch
G ₂ Environmental Inc.	University of California at Davis
Lantern Corporation	University of Minnesota
NEA Laboratories, Inc.	Weather Network Inc.

TABLE OF CONTENTS

<u>Section</u>	<u>Page</u>
PREFACE	ii
ACKNOWLEDGEMENTS	iii
LIST OF FIGURES	vi
LIST OF TABLES	viii
1. INTRODUCTION AND OBJECTIVES	1-1
2. OVERVIEW OF THE STUDY	2-1
3. SUMMARY OF INITIAL RESULTS AND CONCLUSIONS	3-1
3.1 SUMMARY OF INITIAL RESULTS	3-1
3.1.1 Transport Categories	3-1
3.1.2 Conditions When the NGS Emittants Were Present at Hopi Point	3-2
3.1.3 Effect of Humidity on Light Scattering	3-3
3.1.4 Long-Range Transport	3-4
3.1.5 Aerosol Optical Properties	3-5
3.1.6 Dispersion Modeling	3-5
3.1.7 Trace Data	3-6
3.1.8 Representativeness	3-6
3.2 INITIAL CONCLUSIONS	3-7
4. TRAJECTORY AND STREAKLINE ANALYSES OF NGS EMITTANT TRANSPORT	4-1
5. DESCRIPTIVE AND STATISTICAL ANALYSES	5-1
5.1 RELATIONSHIPS OF LIGHT SCATTERING AT HOPI POINT TO TRANSPORT CATEGORY AND RELATIVE HUMIDITY	5-1
5.2 TIME SERIES ANALYSES	5-6
5.3 ANALYSIS OF TIMES OF HIGH LIGHT SCATTERING BY PARTICLES WHEN EMITTANTS MAY BE PRESENT	5-15
5.4 DILUTION OF NGS EMITTANTS	5-17
5.5 MATRIX OF SELECTED DAILY PARAMETERS	5-20
6. PARTICLE SIZE DISTRIBUTIONS AND OPTICAL PROPERTIES	6-1
6.1 SULFUR AEROSOL SIZE DISTRIBUTIONS	6-1
6.2 AEROSOL OPTICAL EFFECTS	6-1
6.2.1 Approach	6-1
6.2.2 Aerosol Model: Hygroscopicity Classes and Single Particle Composition	6-2
6.2.3 Model Visibility Calculations for Hopi Point	6-4
6.3 PRELIMINARY ESTIMATES OF THE LIGHT SCATTERING BY AMMONIUM SULFATE WHEN NGS EMITTANTS WERE PRESENT AT HOPI POINT	6-5
7. SYNOPTIC METEOROLOGY AND REPRESENTATIVENESS OF THE STUDY PERIOD	7-1
7.1 SYNOPTIC ANALYSIS OF NGS STUDY EPISODES	7-1
7.2 SYNOPTIC COMPARISONS WITH HISTORICAL EPISODES	7-3
7.3 METEOROLOGICAL REPRESENTATIVENESS OF THE 1990 AND WHITEX STUDY PERIODS	7-5
7.3.1 The 1990 Study Period	7-6

TABLE OF CONTENTS (Concluded)

<u>Section</u>	<u>Page</u>
7.3.2 The 1987 WHITEX Study Period	7-7
7.4 REPRESENTATIVENESS OF AIR QUALITY MEASUREMENTS	7-8
8. DETERMINISTIC MODELING	8-1
9. QUALITY ASSURANCE AND UNCERTAINTIES	9-1
9.1 PERFLUOROCARBON TRACER DATA	9-1
9.2 SURFACE AIR QUALITY AND OPTICAL DATA	9-5
9.2.1 QC/QA Tests	9-5
9.2.2 Validation and Estimation of Precision	9-6
10. REFERENCES	10-1
APPENDIX A	A-1
APPENDIX B	B-1

LIST OF FIGURES

<u>Figure</u>	<u>Page</u>
2-1. Study Region and Monitoring Sites	2-2
5-1. Frequency Distribution of Light Scattering by Particles at Hopi Point for Each Transport Category	5-4
5-2. Cumulative Frequency Distributions for the Four-Hour Average Light Scattering by Particles at Hopi Point for Times when the NGS Emittants were Probably Present, Probably Absent, and Uncertain and Additional Analysis is Required	5-5
5-3. Hour Average Light Scattering by Particles as a Function of Relative Humidity	5-7
5-4. Time Series Plot of Hopi Point Hourly Light Scattering by Particles and Eight-Hour Average Particulate Sulfur Concentrations Measured by the Low Pressure Impactor in January.	5-8
5-5. Time Series Plot of Hopi Point Hourly Light Scattering by Particles and Eight-Hour Average Particulate Sulfur Concentrations Measured by the Low Pressure Impactor in February	5-9
5-6. Time Series Plot of Hopi Point Hourly Light Scattering by Particles and Eight-Hour Average Particulate Sulfur Concentrations Measured by the Low Pressure Impactor in March	5-10
5-7. Time Series Plot of Hopi Point Hourly Light Scattering by Particles and Relative Humidity in January	5-11
5-8. Time Series Plot of Hopi Point Hourly Light Scattering by Particles and Relative Humidity in February	5-12
5-9. Time Series Plot of Hopi Point Hourly Light Scattering by Particles and Relative Humidity in March	5-13
5-10. Cumulative Frequency Distributions Showing the Dilution of the NGS Emittants Indicated by Tracer Concentrations Reported by WHITEX and This Study	5-18
6-1. Particle Size and Light Scattering Coefficient as a Function of Relative Humidity Corresponding to the 24 h MOUDI Sample Beginning at 1800 MST on January 21	6-3
6-2. Sulfate Scattering Efficiency and Fractional Reduction in Scattering Coefficient as a Function of Fractional Reduction in Sulfate Loadings for the 24 h MOUDI Sample Beginning at 1800 MST on January 21	6-3
6-3. Light Scattering Efficiency for Ammonium Sulfate as a Function of Relative Humidity	6-7

LIST OF FIGURES (Concluded)

<u>Figure</u>	<u>Page</u>
8-1. SO ₂ Concentrations Predicted by Inert SO ₂ Model Showing Wind Vectors for 2300 Hours 19 January 1990	8-2
8-2. SO ₂ Concentrations Predicted by Inert SO ₂ Model Showing Wind Vectors for 1100 Hours 20 January 1990	8-3
8-3. SO ₂ Concentrations Predicted by Inert SO ₂ Model Showing Wind Vectors for 2300 Hours 20 January 1990	8-4
8-4. (a) SO ₂ Concentrations Predicted by Inert SO ₂ Model at Hopi Point With and Without NGS SO ₂ Emissions; (b) SO ₄ Measured at Hopi Point (AVSI Sampler)	8-6
8-5. (a) SO ₂ Concentrations Predicted by Inert SO ₂ Model at Desert View With and Without NGS SO ₂ Emissions; (b) SO ₄ Measured at Desert View (AVSI Sampler)	8-7
8-6. (a) Sulfate Concentrations Predicted by Linear Chemistry Model at Hopi Point With and Without NGS SO ₂ Emissions; (b) Same as (a), Except Including SO ₄ Measured at Hopi Point (AVSI Sampler)	8-8
9-1. Scatter Diagrams Comparing Perfluorocarbon Tracer Concentrations Measured by Collocated Samplers at Hopi Point for Tracer 1, PMCP, and Tracer 2, PMCH	9-2
9-2. Scatter Diagrams Comparing Perfluorocarbon Tracer Concentrations Measured by Collocated Samplers at Hopi Point for Tracer 3, PDCH, and Tracer 4, PTCH	9-3
9-3. Scatter Diagram Comparing Fine-Particle Sulfur Concentrations Measured by Collocated Samplers at Hopi Point	9-8
9-4. Scatter Diagram Comparing Fine-Particle Sulfur Concentrations Measured by Collocated Samplers at Indian Gardens	9-9
9-5. Scatter Diagram Comparing Sulfur Dioxide Concentrations Measured by Collocated Samplers at Hopi Point	9-10
9-6. Scatter Diagram Comparing Sulfur Dioxide Concentrations Measured by Collocated Samplers at Indian Gardens	9-11

LIST OF TABLES

<u>Table</u>	<u>Page</u>
4-1. Frequency of Occurrence of NGS Emittants at Hopi Point	4-1
5-1. Statistics for Four-Hour Average Light Scattering by Particles and Relative Humidity at Hopi Point for the Three Transport Categories	5-2
5-2. Tabulation of Category 1 and 2p Measurement Periods with Light Scattering by Particles Greater than 10 Mm^{-1a}	5-16
6-1. Calculated Light Scattering Coefficients and Efficiencies	6-6
6-2. Light Scattering by Ammonium Sulfate During Episodes When NGS Emissions Were Present ^a	6-8
7-1. Comparison of 1990 Categories with Three Year Period	7-3
7-2. Number of Reported Hours/Month with Low Clouds at GCN	7-4
9-1. Estimated Precision in Surface Air Quality and Optical Data	9-7



1. INTRODUCTION AND OBJECTIVES

From January 10, 1990 through March 31, 1990, a large scale visibility field study was conducted in northern Arizona and southern Utah. The study addressed the issues of visibility impairment in the Grand Canyon during winter months and the improvement to visibility which might be obtained if the SO₂ emissions of the nearby Navajo Generating Station (NGS) were to be reduced. This report is the second in a series which describes the results of the NGS Visibility Study. Detailed discussions of the issues which led to the study, the participating organizations, the field measurements, and the results of preliminary data analyses were presented in a prior status report published in August 1990 (Richards et al., 1990). This report provides a brief summary of the results of additional analyses performed since then and presents some initial conclusions regarding the potential NGS effects on visibility in the Canyon. These conclusions were derived from analysis of a data set that is still undergoing validation, but, except as specifically noted below, we feel the conclusions will not change meaningfully as a result of further validation. When appropriate, the results are compared to an earlier study by the National Park Service (NPS) called WHITEX. A final report scheduled for January 1991 will describe the procedures and results of the analyses and modeling in more detail.

The principal objective of the NGS Visibility Study is to estimate what the improvement in visibility in the Grand Canyon during the winter months would be if NGS sulfur emissions were reduced. The primary issue of concern regarding NGS is its contribution to visibility impairment resulting from sulfates formed from its emittants.* The study addresses the above objective by focusing on the contribution of NGS to light extinction by sulfates.

* "Emittants" refers to the chemical species emitted from the NGS stacks as particles or gases. The effects of these emittants include both their direct effects and the effects of particulate and gaseous chemical species derived from or induced by them.



2. OVERVIEW OF THE STUDY

The field measurements were designed to support both data analysis and deterministic modeling. To meet the objectives, various data analysis techniques are being used to examine the relationships between NGS emittants, meteorology, air quality, and visibility in the study region. A deterministic model is being used to simulate the contribution of NGS and other SO₂ sources in the southwestern U.S. to the sulfate levels in the study area during episode conditions.

The major components of the field study are summarized below and described in more detail in the August Status Report (Richards et al., 1990). Routine emissions, air quality, tracer, and meteorology measurements were made on all days of the study. About one-third of the study days were selected as Intensive Operations Periods (IOPs). On those days, aircraft measurements, special studies, and additional upper air soundings were performed. The study region and sampling sites are shown in Figure 2-1.

Emissions Measurements and Tracer Releases

Continuous source measurements of SO₂, NO_x, plant load, etc. were made. Four different perfluorocarbon tracers were released, one at a time, at a rate proportional to plant load from the NGS stacks in Page, Arizona and changed daily at 1800 MST, cycling through the four tracers.

Surface Air Quality and Tracer Measurements

Air quality and tracer measurements were made daily at 26 locations and tracer only was measured at one additional site. Three types of sites were operated: three Grand Canyon Receptor Sites, seven Research Sites, and 16 Regional Characterization Sites. All sites collected four-hour samples of fine particles, SO₂, and tracer. The cutpoint for the fine particle samplers was about 3.7 μm diameter. Filter samples were analyzed for mass, sulfur and SO₂. Additional aerosol, gas, and visibility measurements were made at the Receptor and Research Sites. The haze in the region and the cloud cover were documented by daily photographs or time lapse movies at four sites.

Measurements at the three Receptor Sites, Hopi Point, Indian Gardens, and Desert View, were used to characterize the effects of the NGS emittants in the Grand Canyon.

Meteorological Measurements

Wind, temperature, and humidity were measured at the three Receptor Sites, six of the Research Sites, and at 10 additional locations throughout the region. Upper air wind, temperature, and humidity soundings were made at seven study sites plus the standard NWS sites. Additional tethered sonde soundings were made at two sites. Approximately 1400 balloon soundings were made during the study. In addition, continuous (hourly) upper wind measurements were made by Doppler sodar (to 0.5 km) at four sites and by radar profiler (to 2 km) at three sites.

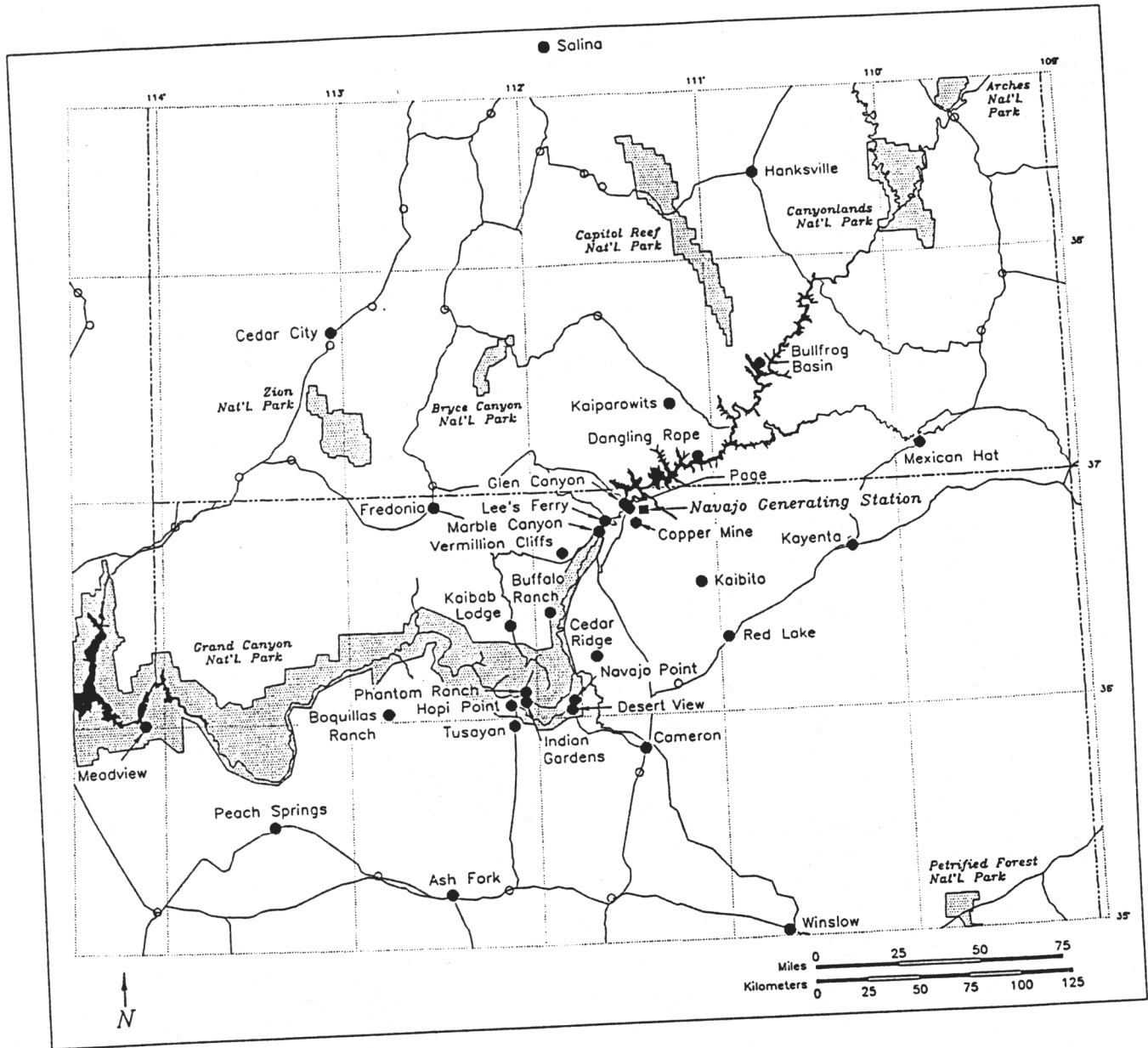


Figure 2-1. Study Region and Monitoring Sites.

Aircraft Measurements

Two aircraft were used to document the chemical and physical characteristics of the pollutants and their three-dimensional distribution in the region and in the NGS plume.

Special Studies

Several special studies were performed at Grand Canyon Receptor Sites. At Hopi Point, measurements of aerosol chemical composition as a function of size were made on intensive study days, and aerosol sulfur size distribution measurements were made with eight-hour time resolution throughout the study. Tandem Differential Mobility Analyzer (TDMA) measurements were made on selected days to examine the effects of water on aerosol size distribution. Electron microscopy analyses were performed to determine the composition of individual particles. Two switched inlet nephelometers were used to determine the effect of coarse particles and water on light scattering. At Desert View, continuous H₂O₂ measurements were made throughout the study, and fog water sampling was attempted. Doppler LIDAR measurements were made at Navajo Point, near Desert View, to examine the spatial distribution of aerosol and winds in the Canyon.

Forecasting and Selection of Intensive Operations Periods (IOPs)

A forecast office was operated in Page by SRP. Forecasts were prepared twice daily to aid in the daily sampling decisions and selection of IOP days.

Laboratory Analysis

Laboratory analyses have been done for tracers, mass, sulfate, nitrate, trace elements, carbon, SO₂, size-fractionated sulfur, and other species.

Data Base Management

All data from the study are being assembled into a common, validated, and internally consistent data base. Data will be in a format that is easy for modelers and analysts to access.

Quality Assurance

Standard procedures were developed for all aspects of the study. Contractors who did not otherwise participate in the field study conducted independent systems and performance audits for all study components.



3. SUMMARY OF INITIAL RESULTS AND CONCLUSIONS

Although the data analysis and modeling efforts are still in progress, some initial results and conclusions which address the study objectives are now available. These results will be refined and expanded in the next few months, but it is expected that the general thrust of the conclusions will not change significantly. Due to the short time available, the location of the special experiments at Hopi Point, and the availability of data from that site from prior studies, the analyses performed to-date focus primarily on Hopi Point, so most of the results and conclusions presented here are limited to that location.

3.1 SUMMARY OF INITIAL RESULTS

Some initial results of the NGS Visibility Study are presented below. Most of these results are from analyses performed since the August Status Report (Richards et al., 1990). These analyses are briefly described in the succeeding sections of this report.

3.1.1 Transport Categories

- Surface and upper air meteorological data, tracer data, and SO₂ data were used to identify whether or not NGS emittants were in the vicinity of Hopi Point for each four-hour sampling period of the 81-day study. The emittants were estimated to be:
 - Present about 21% of the periods (Transport Category 1);
 - Uncertain, additional analysis required for about 19% of the periods (Transport Category 2); and
 - Absent about 60% of the 486 four-hour measurement periods (Transport Category 3).
- The four-hour periods in each category were approximately evenly distributed throughout the day. No significant differences were evident between day and night.
- Additional analyses will be performed to confirm the absence or presence of the emittants for the 19% uncertain periods. A preliminary evaluation indicates that the uncertain cases may be approximately equally divided between times when the emittants are present and absent. Thus, it is estimated that the NGS emittants are:
 - Absent at Hopi Point during $70 \pm 10\%$ of the four-hour measurement periods, and
 - Present during $30 \pm 10\%$ of the four-hour measurement periods.

- For comparison, WHITEX reported that the NGS emittants were present at Hopi Point on 29 out of 40 days and on 56 out of 79 selected six-hour periods, or 72% and 71% of the time intervals, respectively.

3.1.2 Conditions When the NGS Emittants Were Present at Hopi Point

- During the periods when NGS emittants were present at Hopi Point, the average light scattering was smaller and the frequency of occurrence of high light scattering values was no greater than when the emittants were absent.
 - The frequency of occurrence of low light scattering values (clean periods) was higher for periods when the NGS emittants were estimated to be present than for other periods.
 - For the four-hour periods when NGS emittants were estimated to be present (Category 1), the median light scattering by particles b_{sp} was 2.7 Mm^{-1} and the average was 5.4 Mm^{-1} , compared with a median of 5.3 Mm^{-1} and an average of 6.9 Mm^{-1} for periods when the emittants were estimated to be absent or uncertain (Categories 3 and 2).
- For many of the times when the NGS emittants were present at Hopi Point, the visibility effects of the emittants were so small that the arrival and departure of the emittants were not indicated by the transmissometers (which measure total light extinction) or by the nephelometers (which measure light scattering by particles).
- The high humidity conditions associated with clouds and high light scattering readings did not occur as frequently when the emittants were estimated to be present at Hopi Point as when they were estimated to be absent:
 - The relative humidity at Hopi Point was less than 70% for 82% of the four-hour periods during which NGS emittants were estimated to be present compared to 64% of the periods when they were estimated to be absent or uncertain.
 - The average relative humidity was 44% when the emittants were estimated to be present at Hopi Point compared with 54% when they were estimated to be absent or uncertain.
- The above three results are consistent with calculations presented in a review of WHITEX by the National Research Council. The NRC committee calculated the amount of sulfate that might be formed from NGS emissions in the absence of clouds and high humidities and concluded that "aerosol concentrations of this magnitude should have little effect on haze at Hopi Point" (NRC, 1990, p. 35).
- The lower average b_{sp} values and relative humidities for the periods when emittants were estimated to be present than for those times when the emittants were estimated to be absent was associated with the greater frequency of transport of relatively haze-free, dry air to the

Grand Canyon during times when the emittants were estimated to be present.

3.1.3 Effect of Humidity on Light Scattering

- The times of worst visibility at Hopi Point (e.g., 1/20, 2/13, 3/5) were associated with relative humidity over 70% (in agreement with WHITEX). These poor visibility events usually were associated with storms or with transport from the southwest or west.
- Other studies have shown that sulfate formation can occur much more rapidly in clouds than in dry air (e.g., see NAS, 1990). On January 19 and 20, and March 31, 1990, NGS emittants arrived at Hopi Point along with clouds and may have been a significant or even dominant contributor to high sulfate concentrations.
 - For the January event, the dispersion modeling results show that sulfur from sources other than NGS also contributed significantly to the sulfur concentrations at Hopi Point.
 - For March 31, the background sulfur concentrations have not yet been examined, but no other source was evident from the meteorology data.
 - During these two periods of high sulfate, clouds were present in the transmissometer sight paths some of the time on March 31 and most of the time on January 19. Clouds both increase the sulfate formation rate and mask the effects of sulfate on visibility.
- On January 20, NGS emittants which had passed through clouds were measured by aircraft 16 km from NGS. Neither particle sulfur nor light scattering by particles were measurably above the background values. Thus, rapid sulfate formation does not always take place in clouds. During this period, the H_2O_2 concentrations at Hopi Point were generally less than 0.1 ppb (See the August Status Report, Richards et al., 1990).
- During the 4% of the four-hour periods when emittants were "estimated to be present" with RH greater than 70%, the average b_{sp} was 16.4 Mm^{-1} versus 10.7 Mm^{-1} for all other four-hour periods with RH exceeding 70%.
 - These periods were equally divided between day (0600 through 1800 MST) and night, so the emittants were estimated to be present and the RH was greater than 70% for 4% of the daytime measurement periods, or nine measurement periods. The average b_{sp} for these daytime periods was 18 Mm^{-1} .
 - For six of these nine daytime periods, clouds or precipitation were present in at least one transmissometer sight path and the average b_{sp} was 21 Mm^{-1} .
 - For three of these nine daytime periods, no clouds or precipitation were present in any transmissometer sight path and the average b_{sp} was 11 Mm^{-1} .

- An upper limit to the fraction of the time the combination of clouds and emittants capable of causing rapid sulfate formation might have been present at Hopi Point can be estimated as follows:
 - The relative humidity exceeded 70% when NGS emittants might have been present at Hopi Point during 4 to 7% of the four-hour periods of the study. This range includes 4% for the "estimated to be present" periods exceeding 70% RH and 3% for the "uncertain" periods.
 - If all the "estimated to be present" periods and the half of the "uncertain" periods when the emittants are more likely to have been present are added together, the "best estimate" is that the NGS emittants might have been in the vicinity of Hopi Point during conditions of RH greater than 70% on 5.3% of the four-hour periods.
 - There were seven days (9% of the study days) on which one or more of these "best estimate" measurement periods (see preceding paragraph) occurred between the hours of 0600 and 1800 MST.
- Of the top 20% of reduced visibility episodes that occurred at the Grand Canyon during the 1990 study, all but one were associated with the passage of a synoptic-scale low pressure system. The only episode that was not accompanied by a trough passage occurred under conditions of low humidity. The four episodes with greatest visibility reduction during the 1990 study were all associated with the passage of closed low systems.

3.1.4 Long-Range Transport

- The highest light scattering due to particles b_{sp} at Hopi Point during the study (2/13, 3/5) occurred when NGS emittants were not in the vicinity and hazy air was being transported into the region from the southwest. The February 13 event followed a period of high winds and dust storms in the California deserts.
- The number of episodes with light scattering by particles greater than 15 Mm^{-1} that occurred during each transport category was approximately proportional to the number of measurement periods in each category. Episodes with readings above 20 Mm^{-1} occurred with slightly higher frequency in measurement periods during which the emittants were estimated to be absent from Hopi Point (Transport Category 3) than in an equal number of measurement periods in other categories. (Here an episode was defined to begin when the b_{sp} was above the threshold for two successive measurement periods and end when below the threshold for two successive measurement periods.)

3.1.5 Aerosol Optical Properties

- The results of detailed measurements of properties of the ambient aerosol at Hopi Point which influence their effect on light scattering include:
 - The aerosol was typically composed of a less-hygroscopic fraction and a more-hygroscopic fraction.
 - Size-resolved microscopy and elemental analyses showed that the less-hygroscopic fraction was predominantly carbon species and soil dust and that carbon species also occurred in the more hygroscopic fraction.
 - The growth curves for the more hygroscopic fraction showed about 20% less growth with increasing humidity than is observed for pure ammonium sulfate, and for about 30% of the measurements, deliquescence occurred at relative humidities of 75 to 80%, as for ammonium sulfate.
 - The mean size of the particulate sulfur was variable, was usually smaller than 0.3 μm , and was larger than 0.5 μm about 5% of the time. (The particles have a maximum light scattering efficiency when the mean size is somewhat greater than 0.5 μm and are less efficient for smaller mean sizes.)
- Size-resolved aerosol samples have been chemically analyzed for inorganic compounds, organic species, and trace elements for 13 24- or 48-hour periods at this time. Model calculations, including water equilibrium, gave ammonium sulfate light scattering efficiencies ranging from 3 to 6.6 m^2/g for relative humidities between 30 and 70%, and efficiencies as high as 16 m^2/g at 92% relative humidity. The calculated reduction in light scattering by particles if all the sulfate were removed ranged from 21 to 84% on these 13 periods.
- Model calculations were made for the percentage improvement in total scattering (by particles and by clean air) which would occur if all ammonium sulfate were removed from the aerosol for three 24- or 48-hour periods. These periods were times when NGS emittants were likely to have been present at Hopi Point and the particle light scattering averaged over 10 Mm^{-1} . This percentage improvement represents an upper bound for the possible improvement if only NGS-related sulfate were removed. For these three episodes, the percentage improvements in total scattering were 45, 50, and 29%.

3.1.6 Dispersion Modeling

- A deterministic model was run with simple linear chemistry for the period from January 18 through January 23, 1990. The model region covered most of the southwest U.S., and the model used the study data as input. The model indicates that NGS emittants were in the vicinity of Hopi Point for only a limited portion of this episode period and that

emittants from northern Utah were also at Hopi Point at the same time as the NGS emittants.

- The model showed that for a period between noon on January 20 and early January 21, NGS contributed a large portion of the sulfur arriving at Hopi Point. During this time, there was an increase in sulfate levels and the model indicates that NGS emittants might have contributed up to 60% of the sulfate present at this time. Although sulfate increased during this time, the measured light scattering by particles decreased rapidly, indicating a decrease in the light scattering efficiency of the particles.

3.1.7 Tracer Data

- Data from collocated samplers at Hopi Point and Desert View indicate that the perfluorocarbon tracer (PFT) data from this study are dominated by noise for concentrations in the range observed at these sites. Elevated tracer concentrations for measurement periods in which the emittants were estimated to be absent indicated a positive bias in many of these tracer readings.
- Comparison of the PFT data with meteorological calculations and sulfur dioxide concentrations show that the PFT data, when taken as a whole, give a reliable indication of the general location of the NGS emittants.
- Comparison of the WHITEX CD₄ tracer data with the PFT data from this study showed that the CD₄ data indicated significantly higher and more persistent concentrations of NGS emittants at Hopi Point than indicated by the PFT data. The WHITEX CD₄ data show evidence of false positive readings, and insufficient QA data were obtained to estimate their quality, so the conclusions based on the CD₄ data can be questioned.

3.1.8 Representativeness

- Seven reduced visibility episodes occurred during January to March, 1990 compared to an average of seven per season for the three-year sample from December to February, 1984 through 1987. The meteorology of the 1990 episodes was analogous to the meteorology that accompanied the principal WHITEX episodes.
- The average number of cloudy days at the Grand Canyon during the 1990 winter study was comparable to the average number of cloudy days from the three-year sample of winter conditions. Average temperatures and moisture aloft also were comparable to climatological norms, based on six years of upper air soundings collected at Page and twenty-seven years of upper air data collected at Winslow.
- Based on the results of three separate surveys of climatological conditions spanning six, ten, and seventeen years, respectively, the synoptic meteorology of the winter of 1990 was characterized by fewer conditions producing northerly flow patterns and more frequent occurrences of southwesterly flow patterns compared to previous years. The opposite conditions occurred during WHITEX in that northerly flow

patterns occurred more often than usual while southwesterly flow patterns occurred less frequently than the climatological norms.

- The four episodes with greatest visibility reduction during the 1990 study were all associated with the passage of closed low systems. Likewise, the top 50 days of reduced visibility episodes that occurred in a three year sample from the winters of 1984-85, 1985-86 and 1986-87 also were associated with passage of a synoptic-scale trough, except for approximately one episode per year that occurred under conditions of low humidity.

3.2 INITIAL CONCLUSIONS

The following conclusions are drawn from the work summarized in this report.

- For 60 to 79% of the four-hour periods of the study, NGS emittants were estimated to be absent from the vicinity of Hopi Point, and thus could not have affected light extinction at Hopi Point.
- On some occasions, NGS emittants interacted with clouds en route to Hopi Point. During 4 to 7% of the four-hour periods of the study or during the "daytime" on seven calendar days of the study, they may have been present at Hopi Point while the RH was greater than 70%. For times when they were present under high humidity conditions, NGS emittants probably contributed to sulfate concentrations at Hopi Point, and during at least one event may have been the dominant contributor. Since sulfates are usually the largest contributors to light extinction in the region, NGS emittants probably affected visibility in the Canyon on some occasions.
- For most of the remaining four-hour periods, the contribution of NGS emittants to light extinction at Hopi Point was probably insignificant due to the absence of interactions with clouds.
- When the NGS emittants interact with clouds, they may not always affect visibility. In-cloud reaction rates may be minimized due to the prior depletion of H_2O_2 , visibility effects can be masked due to the presence of clouds in the sight path, or the effects may occur at night.
- Long range transport of pollutants from outside the study region was a major source of visibility impairment at the Canyon on several occasions during the study and caused the highest haze levels observed during the study.
- NGS sulfur controls will have no measurable effect on light extinction at Hopi Point on most days, including some of the days of highest light extinction. Controls probably will result in improved visibility at Hopi Point during times that NGS emittants which have been processed by clouds are present. If one assumes that sulfur controls on NGS might reduce light extinction at Hopi Point for those times when NGS emittants are present at Hopi Point and the RH is greater than 70%, then controls might be beneficial on about 4% to 7% of the four-hour periods. This range includes the 4% for the "estimated to be present" periods and an

additional 3% for the "uncertain" periods. However, clouds were present during parts of almost half of these periods.

- Initial deterministic model results for the period of January 18 through January 23 indicate that emittants from northern Utah mixed with NGS emittants en route to Hopi Point. During this episode, NGS emittants could only have contributed to sulfate concentrations for less than 24 hours. However, during the period when the model predicted that NGS emittants were important, those emittants may have been responsible for up to 60% of the sulfate at Hopi Point.
- Optical model results for the percentage improvement in total light scattering which might occur if all ammonium sulfate were removed from the aerosol during three periods of high b_{sp} ($\geq 10 \text{ Mm}^{-1}$) when NGS emittants might be present at Hopi Point ranged from 29 to 50%. These estimates are an upper bound on the improvement during these times if only NGS-related sulfate were removed.
- Overall, 1990 represented an average year in terms of the number of visibility episodes and the weather conditions associated with reduced visibility at the Grand Canyon. The weather conditions that accompanied episodes of reduced visibility during 1990 were similar to the conditions that occurred during the WHITEX episodes.
- With one exception per year on average in a three-year sample from 1984 through 1987, and one exception in the 1990 study, the greatest visibility reduction during episodes occurred on the day of a trough passage through the area. These episodes were accompanied by synoptic-scale troughing, an increase in moisture and cloud cover, the likelihood for precipitation, enhanced vertical mixing of pollutants, and southerly to southwesterly winds accompanying the passage of the trough.
- The primary uniqueness in the meteorology that accompanied visibility episodes during the 1990 study (compared to the three-year sample) was the tendency for the area to be influenced by closed low pressure systems rather than traveling waves in the westerlies. Closed lows tend to be slow moving, with marked effects on cloudiness and humidity.
- The winters of 1990 and 1987 were characterized by synoptic-scale flow patterns over the western U.S. that differed somewhat from expected conditions based on long-term averages. Given that northerly flow patterns may have occurred more frequently than normal in 1987 and less frequently than normal in 1990, emissions from NGS may have been in the vicinity of the Grand Canyon more often in 1987 and less often in 1990 than longer-term averages would predict.

4. TRAJECTORY AND STREAKLINE ANALYSES OF NGS EMITTANT TRANSPORT

In order to determine those times when NGS emittants were likely to be in the vicinity of Hopi Point and to estimate the frequency of occurrence of such events, trajectory and streakline analyses were performed. These analyses used simple diagnostic models to prepare interpolated, mass-consistent wind fields from the dense network of surface and upper air measurements.

Four-hour average tracer and filter samples were collected throughout the study. For each four-hour period from January 10 through March 31, 1990, the streakline analyses and the tracer and SO₂ data were used to assess whether or not NGS emittants were in the vicinity of Hopi Point. Data from each time period were reviewed to determine whether the emittants were: "probably present," "uncertain, additional analysis required," or "probably absent." These categories, along with selected Hopi Point air quality data for each time period, are included in Appendix A. These categories were used for further analyses summarized in Section 5. The distribution of categories is shown in Table 4-1. The breakdown between daytime and nighttime periods is not indicated because the measurement periods in each category are nearly always divided between day and night in proportion to the number of measurement periods. For example, if the sampling periods between 0600 MST and 1800 MST are considered daytime and between 1800 MST and 0600 MST nighttime, then the measurement periods in each category are nearly always equally divided between daytime and nighttime.

A further breakdown in these categories became necessary in an analysis described in Section 6. To improve the estimate of an upper limit for the average contribution of the NGS emittants to light extinction, Category 2 was divided into time periods in which it was more likely that further analysis would show that the emittants were present (Category 2P) or were absent (Category 2A). Each of these categories contained 47 four-hour measurement periods, and they are tabulated in Appendix A.

Table 4-1. Frequency of Occurrence of NGS Emittants at Hopi Point

Transport Category	Percent of Four-Hour Periods	Number of Four-Hour Periods
1. Probably present	21	100
2. Uncertain, additional analysis required	19	94
3. Probably absent	<u>60</u>	<u>292</u>
Total	100	486

For comparison purposes, the NPS concluded in the WHITEX report (Malm et al., 1989) that:

"Out of 40 days analyzed during WHITEX, the NGS plume was estimated to be impacting Hopi Point on 29 days, or 71 percent of the time." (From Section 9.4.2, Page 9-5, Trajectory and Streakline Analysis Conclusions.)

Also, in Chapter 6, Page 6-32 of the WHITEX report, a similar result is reported: 56 out of the 79 six-hour periods indicated a "hit" (NGS plume impacted Hopi Point). These 79 six-hour periods were chosen such that they occurred during episodes of poor visibility.

The process used to calculate and review the streaklines in this study is described below.

The analyses of the transport of NGS emissions involved preparing objectively analyzed, mass consistent wind fields for each hour of the study period from January 10, 1990 through March 31, 1990. The models used were developed at the California Institute of Technology by Goodin, et al. (1980) and later modified by the California Air Resources Board. Data used in the analyses included surface winds and winds aloft measured by the Doppler radar profilers, Doppler SODARs, and rawinsonde sounding stations. Only data validated at Level 1 were used in these analyses. The domain over which the wind fields were prepared is comparable to the study region shown in Figure 2-1. This domain was 500 km (East - West) by 400 km (North - South), roughly centered on Page, Arizona. A horizontal grid of 100-by-80 grid points was defined over this area with horizontal spacing of 5000 m (5 km) in both the North-South and East-West directions. Ten vertical levels were specified: 10 m, 150 m, 300 m, 450 m, 600 m, 750 m, 900 m, 1200 m, 1500 m, and 2000 m (all heights above ground level). The objective analysis routines included very simple parameterizations for the effects of atmospheric stability, mixing depth, and topographical forcing on the horizontal winds.

Once the wind field analyses were completed, forward trajectories from Page were computed for each hour of the study period. To date, trajectories have been calculated for 600 m and 750 m agl to encompass the likely average plume rise from NGS. Trajectories at additional levels and more explicit information on plume altitudes are currently being evaluated but are not included in the results presented here. From the hourly trajectories, streaklines were prepared to represent the "centerline" of the plume. In the strictest sense, a streakline defines the line connecting all air parcels at a particular moment in time that have passed a given geometric point, in this case 600 m and 750 m agl above Page.

To facilitate analyses of emissions transport, a PC-based computer animation was prepared that displays the streaklines, the four-hour tracer and SO₂ data from the surface sampling network, and the hour-average nephelometer readings taken at Hopi Point, all superimposed on a map similar to that in Figure 2-1. This animation was used to determine when emissions from NGS may have reached Hopi Point.

The animation begins at 0000 MST on January 10, 1990 and updates hourly through 2300 MST on March 31, 1990. The streaklines are represented by circles which are "emitted" every two hours at Page and whose position is updated hourly. Horizontal spread of the "plume" is roughly represented by the size of the circles, which have a diameter given by:

$$\text{Diameter} = 2\sigma_y = 2(x^{0.8})$$

where x is the integrated distance travelled by the trajectories that underlie the streaklines. This very simple parameterization was chosen based on the results of aircraft data collected in the NGS plume during WHITEX and VISTTA (Smith, 1981). We are investigating more sophisticated representations of the transport and dispersion of the emittants for a future version of the animation.

Tracer and SO_2 data are shown in the animation as bar graphs at each of the surface sampling sites. The bar graphs are updated every four hours, corresponding to the sampling times used during the field study. For clarity, the tracer and SO_2 data are color-coded.

The streaklines, tracer, and SO_2 data were used to assign each four-hour period to one of the three categories summarized earlier. There was a large amount of noise in individual tracer values, so there were times when there were contradictions between the three data sets. For these times, the regional distributions of tracer and SO_2 were examined to assess whether an individual tracer reading might be erroneous. In some cases a tracer data point might be discounted, and the categorization would be supported only by the streakline and/or SO_2 data.

In general, the assignment of the categories was conservative. If either the meteorology or the air quality data provided a reliable indication that NGS emittants were in the vicinity of Hopi Point, the time period was classified as "probably present." If the edge of a circle was within about 25 km of Hopi Point in any of the four hours of a time period, the period was classified as "probably present."

In some cases the streakline analyses showed transport away from Hopi Point, but the regional SO_2 and tracer data indicated that surface transport might be carrying emittants to Hopi Point. For these cases, the time period was also classified as "probably present."

During some time periods, the streaklines showed transport aloft away from Hopi Point. At the same time, SO_2 or tracer concentrations were elevated at sites between NGS and Hopi Point, but not at Hopi Point. For these cases and other similar situations, the period was classified as "uncertain, additional analysis required."

The efforts to evaluate mechanisms that may transport emissions from NGS to the Grand Canyon are continuing. An important goal of these analyses is to resolve the uncertainties indicated by use of the second category and to re-assign those time periods to the appropriate category. The animation provides important insight into time periods that require further investigation. In particular, the following conditions can be observed in the animation:

- Fumigation of the NGS plume due to growth of the convective boundary layer appears to be indicated by a rapid increase in tracer and/or SO_2 concentrations around 1400 MST on many days, especially in the Lake Powell Basin. Once emissions have been mixed to the ground, it is necessary to investigate possible conditions of de-coupling of the lower level winds from the winds at plume height, which may result in transport towards the Grand Canyon by terrain-induced circulations.
- Stagnation conditions are indicated at times when the streaklines move slowly and accumulate over the domain. The possibility of low-level, terrain-induced circulations forming is being investigated for these time periods. In particular, the February 28 - March 1 time period appears to be a case of stagnation that persisted for several days.
- There are three episodes when the tracer and/or SO_2 data suggest that NGS emissions may have reached the Grand Canyon via a transport pathway that carried emissions outside the analysis domain and then back when the winds reversed direction. Additional analysis of the meteorology, tracer, and chemistry data sets is required to determine if in fact this process occurred.
- The Hopi Point nephelometer data are being correlated with humidity and cloud cover data. There is a diurnal variation in the b_{sp} data that is probably associated with diurnal variations in relative humidity. The average b_{sp} readings are highest near dawn and lowest near sunset, with the result that the daytime and nighttime averages are nearly the same. There also is an indication that peak b_{sp} readings are associated with low-level cloud cover or precipitation.

5. DESCRIPTIVE AND STATISTICAL ANALYSES

The data from the study have been sorted and classified in a variety of ways to help provide a better understanding of the causes of light extinction at Hopi Point. This section presents several analyses which illustrate different physical phenomena. A listing of the data on which these analyses are based appears in Appendix A.

5.1 RELATIONSHIPS OF LIGHT SCATTERING AT HOPI POINT TO TRANSPORT CATEGORY AND RELATIVE HUMIDITY

Several analyses were performed to assess the relationships among light scattering by particles (b_{sp}) at Hopi Point, the transport categories described in Section 4, and relative humidity (RH). Above about 70% RH, the light scattering due to sulfates tends to increase rapidly (see Figure 6-3) and clouds are frequently present in the transmissometer sight paths (see Figures 5-7 through 5-9), so this humidity was selected as a reasonable dividing line for the analyses.

Table 5-1 provides Hopi Point four-hour b_{sp} statistics sorted by transport category and by RH. The statistics are not given separately for daytimes and nighttimes because it was found that the statistics for each of these divisions are essentially the same as for all data combined. Several results are apparent from this table.

- The highest four-hour average light scattering by particles occurred when NGS emittants were probably absent from Hopi Point.
- On average, Category 1, when NGS emittants were probably present, is characterized by drier air than Category 3, when the emittants were probably absent. This is reflected by the lower average RH and higher percentage of time periods with RH less than 70% for Category 1.
- For those periods when the RH was less than 70%, when the emittants were probably present at Hopi Point, the average four-hour b_{sp} was 3.0 Mm^{-1} compared to 5.0 Mm^{-1} when the emittants were probably absent or uncertain.
 - The times when the NGS emittants were transported to Hopi Point in the absence of high humidities were associated with the transport of air with low b_{sp} readings to Hopi Point.
 - The effects of the NGS emittants appear to be very small when the relative humidity was below 70%, in agreement with the calculations by the NRC Committee (NRC, 1990).
- The median b_{sp} was 2.7 Mm^{-1} when the NGS emittants were probably present at Hopi Point. If the light scattering by clean air is taken into account, this implies that light scattering by all fine particles was less than about 21% of the total light extinction for half of these time periods.

Table 5-1. Statistics for Four-Hour Average Light Scattering by Particles and Relative Humidity at Hopi Point for the Three Transport Categories

Statistical Parameter	Category 1	Category 2	Category 3	Categories 2 & 3
	Probably Present	Uncertain	Probably Absent	Probably Absent + Uncertain
Median b_{sp} (Mm^{-1})	2.7	5.1	5.5	5.3
Average b_{sp} (Mm^{-1})	5.4	6.8	7.0	6.9
90th percentile b_{sp} (Mm^{-1})	15	13	15	14
Maximum b_{sp} (Mm^{-1})	29	30	37	37
Minimum b_{sp} (Mm^{-1})	0.3	0.5	0.2	0.2
Average RH (%)	43.8	43.8	57.6	54.3
Percent of Study with RH $\geq 70\%$ ^a	3.8	3.0	25.5	28.5
Percent of Study with RH $< 70\%$ ^a	17.4	16.1	34.2	50.3
Average b_{sp} for RH $\geq 70\%$ (Mm^{-1})	16.4	13.2	10.4	10.7
Average b_{sp} for RH $< 70\%$ (Mm^{-1})	3.0	5.7	4.6	5.0

a Fifteen four-hour periods had missing relative humidity; percent computed with 471 four-hour periods instead of 486 four-hour periods. A four-hour period is considered to have RH $\geq 70\%$ if the RH exceeded 70% for one or more hours in the period.

- When the RH exceeded 70%, the average four-hour b_{sp} was 16.4 Mm^{-1} for those periods when NGS emittants were probably present at Hopi Point, compared to 10.7 Mm^{-1} for other days with RH above 70%. This indicates that when the emittants are transported to Hopi Point on high humidity days (when they may have been processed by clouds), they may have had a significant effect on light extinction. Approximately 3.8% of the four-hour periods during the study were in this category. This 3.8% number is 18% of the time periods in Category 1.
- If one assumes that sulfur controls on NGS might reduce light extinction at Hopi Point for those times when NGS emittants are present at Hopi Point and the RH is greater than 70%, then controls might be beneficial on about 3.8 to 6.8% of the four-hour periods. This range includes the 3.8% calculated above for the "probably present" periods and an additional 3% for the "uncertain" periods.
- An alternative way to examine the potential effects of controls is to estimate the number of calendar days on which controls might have an effect on visibility. Since visibility is only important during daylight hours, we determined the number of days during which the RH was over 70% for measurement periods beginning at 0600 MST through 1800 MST for categories 1 and 2. The following results were obtained.
 - For category 1 (probably present) there were six days meeting these criteria: January 18 through 21, February 5, and March 31.
 - For category 2 (uncertain) there were four days. Two of these days included times when recent analyses have indicated that NGS emittants were more likely to be present than absent: February 20 and March 1. On the other two days, February 6 and 8, NGS emittants were more likely to be absent.
 - The total for categories 1 and 2 is ten days or 12% of the study days. The total for category 1 and one-half of category 2 is eight days or 10% of the study days.

Figure 5-1 shows the frequency distribution of b_{sp} values at Hopi Point for each transport category. A few additional factors are apparent in this figure.

- The highest four-hour average b_{sp} readings occurred when NGS emittants were probably absent.
- The time periods when NGS emittants were probably present did not dominate any category. Clean and hazy days both occurred when the emittants were probably present and probably absent.

Figure 5-2 shows the cumulative frequency distribution of b_{sp} at Hopi Point for each transport category. The lowest 10 to 20% of the readings for all categories are small enough that they are less than the measurement uncertainty. This figure shows that:

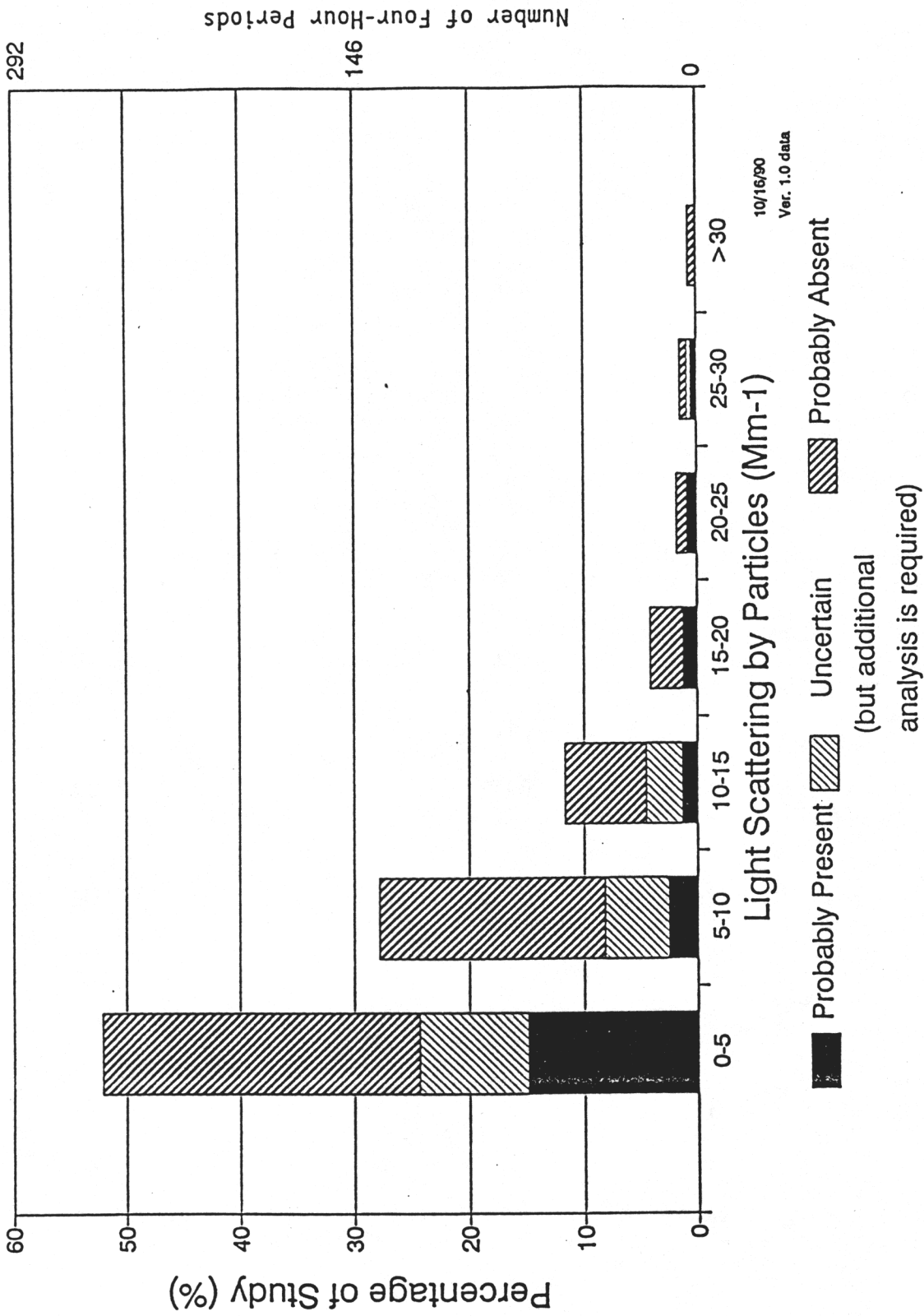


Figure 5-1. Frequency Distribution of Light Scattering by Particles at Hopi Point for Each Transport Category.

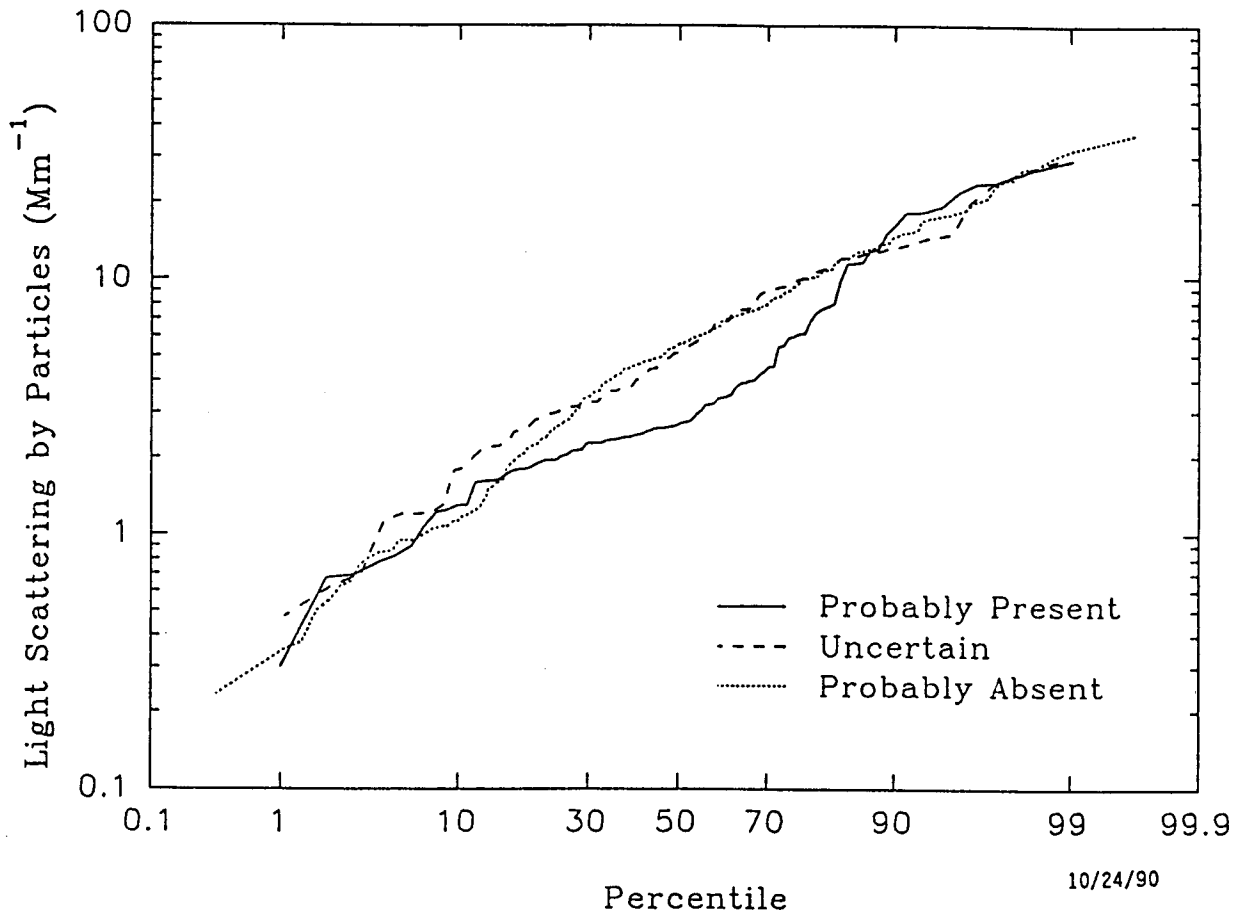


Figure 5-2. Cumulative Frequency Distributions for the Four-Hour Average Light Scattering by Particles at Hopi Point for Times when the NGS Emittants were Probably Present, Probably Absent, and Uncertain and Additional Analysis is Required. Readings below 1 Mm^{-1} are smaller than the measurement uncertainty.

- The frequency of occurrence of low light scattering values was higher during periods when the emittants were probably present than for other periods.
 - Over much of the midrange of the distributions, the b_{sp} readings were about a factor of two lower when the emittants were probably present than for the other two categories.
 - About 75% of the time the emittants were probably present, the b_{sp} reading was smaller than the average reading of 6.6 Mm^{-1} .
- In the 85 to 96 percentile range, the b_{sp} readings are 15 to 20% higher when the emittants are probably present than for the other cases.
- The frequency distribution for "uncertain" times (Category 2) is very similar to that for "probably absent" times (Category 3).

Figure 5-3 shows a scatter plot of hourly averaged b_{sp} at Hopi Point versus relative humidity. This figure shows that:

- Most of the high light scattering values occurred above 70% relative humidity.
- The average four-hour b_{sp} for periods with $\text{RH} \geq 70\%$ was 11.4 Mm^{-1} versus 4.5 Mm^{-1} for RH less than 70% (See Table 5-1).
- The full range of b_{sp} values was observed at relative humidities between 90 and 100%. High humidity is not necessarily accompanied by high b_{sp} .

5.2 TIME SERIES ANALYSES

Figures 5-4 through 5-9 summarize the study results in the form of time series plots of optical, meteorological, and sulfate data measured at or near Hopi Point. The lower panel in Figures 5-4 through 5-6 shows hourly light scattering by particles measured by the nephelometer at Hopi Point and eight-hour-average sulfate measured by the low-pressure impactor (LPI). The heavy bar in the middle of the figure shows when the NGS emissions are probably present at Hopi Point. These are the times in Category 1 in Table 4-1 and Appendix A.

The thin bar in line with the heavy bar in the middle of some of the figures indicates the 47 measurement periods initially classed as "uncertain, additional analysis is required" (Category 2) and then later classed as being more likely to be classed as present than absent when additional analyses are performed (Category 2P). These classifications of the measurement periods are listed in Appendix A.

The three upper bars show times when the hour average transmissometer readings were greater than 100 Mm^{-1} . Readings this large occurred only when the sight path was obscured by fog, clouds, rain, or snow. The top bar shows data from the transmissometer installed for this study on a sight path between Indian Gardens and Kolb Studio, near Hopi Point. The data from this

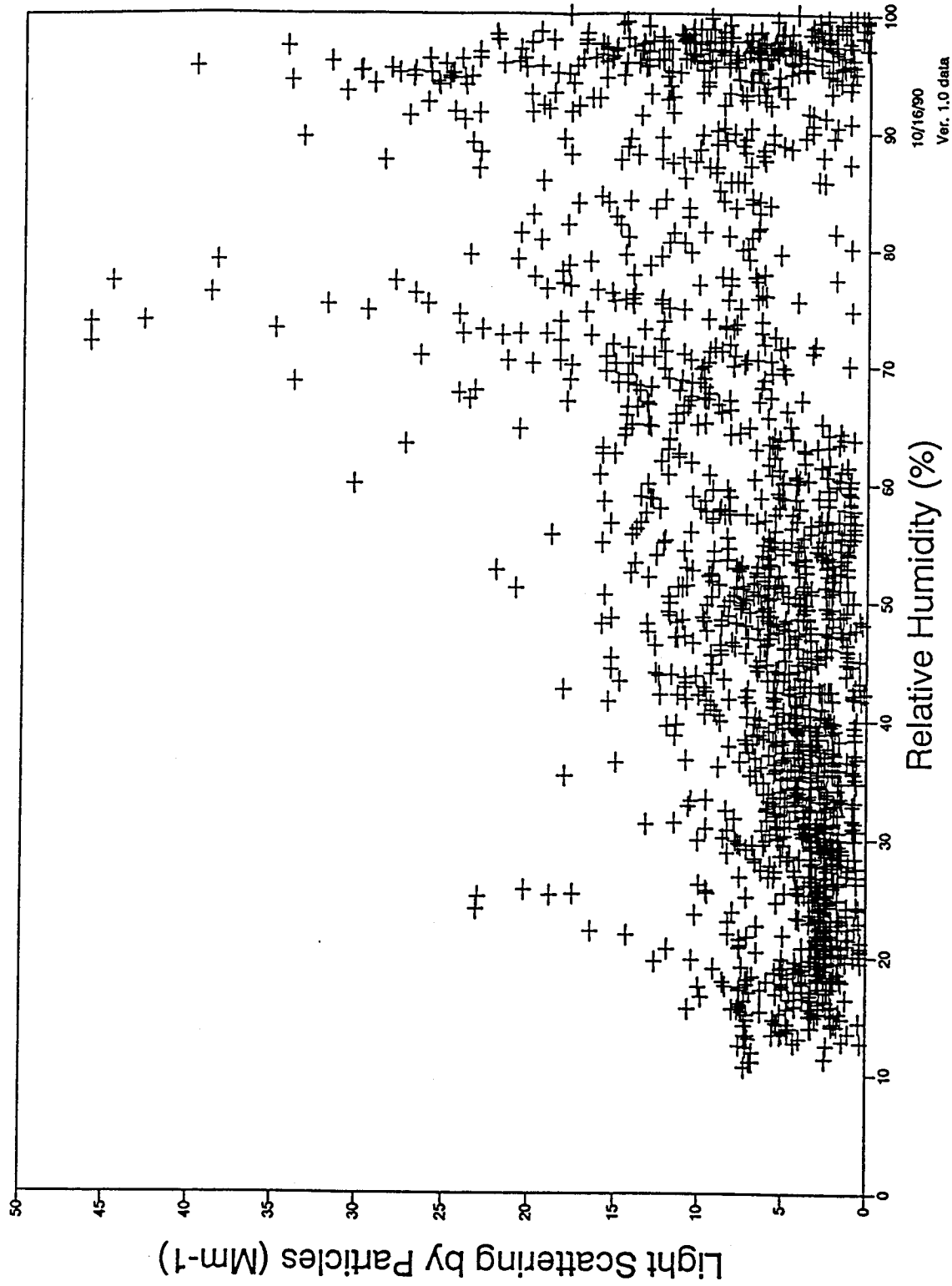
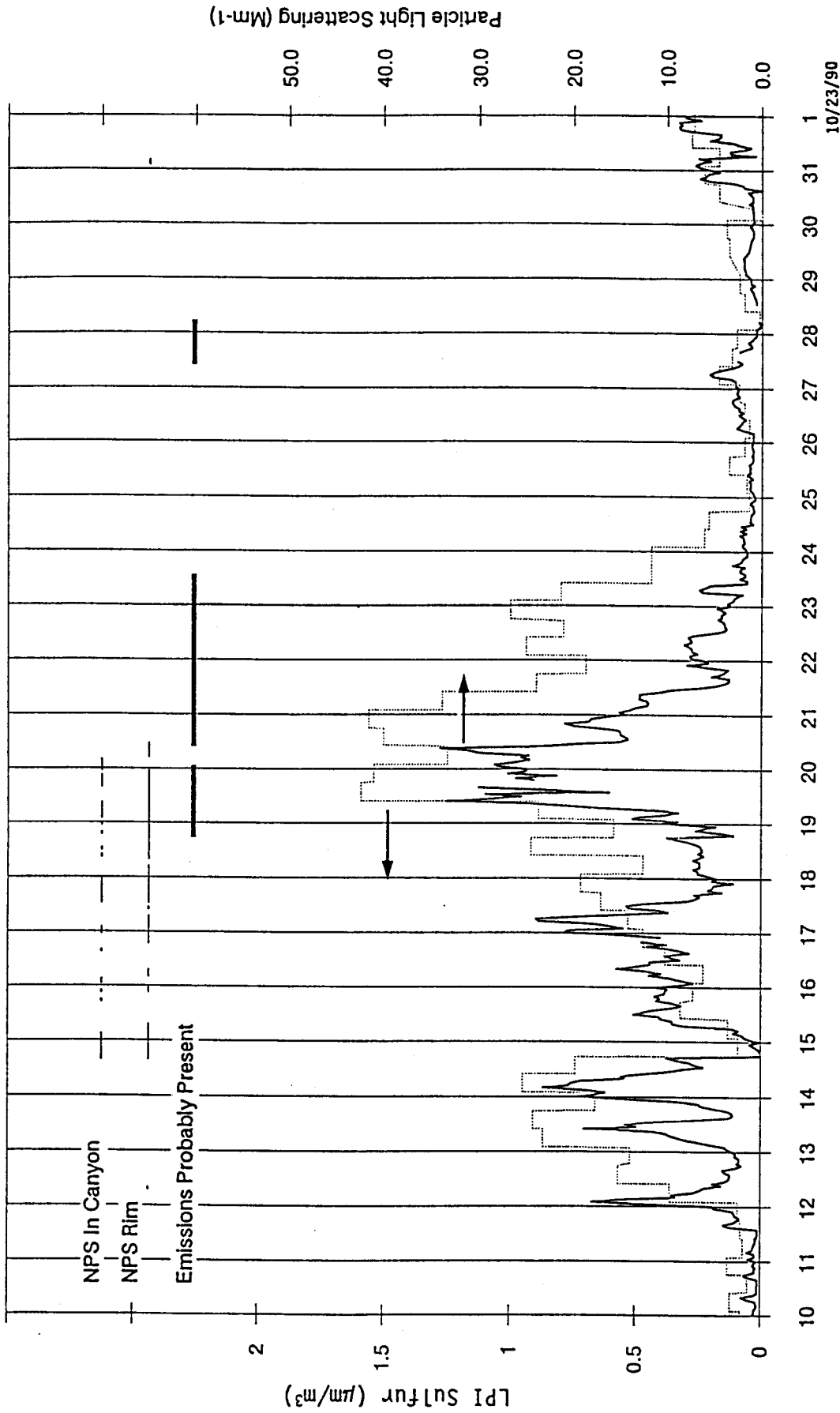
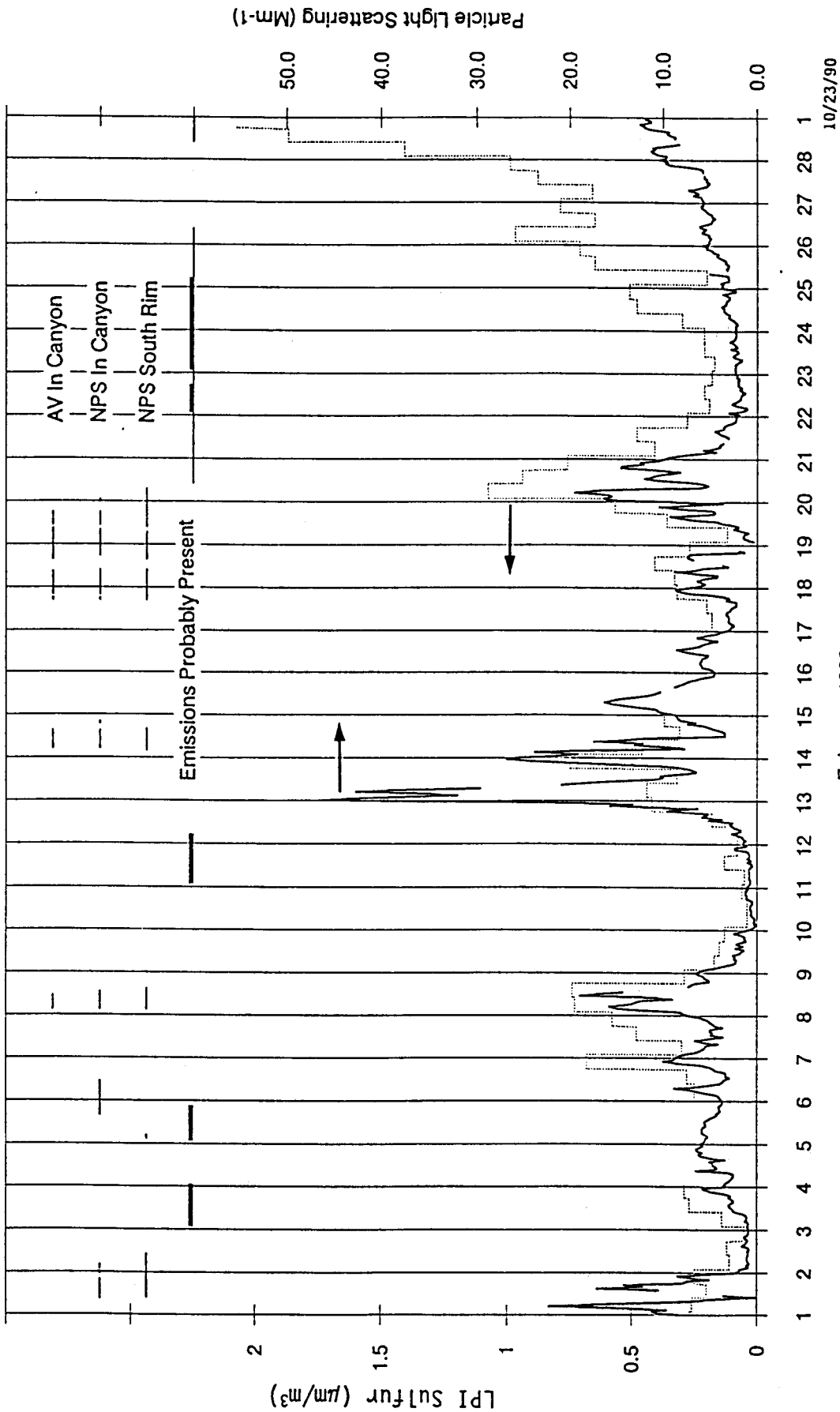


Figure 5-3. Hour Average Light Scattering by Particles as a Function of Relative Humidity.



January 1990

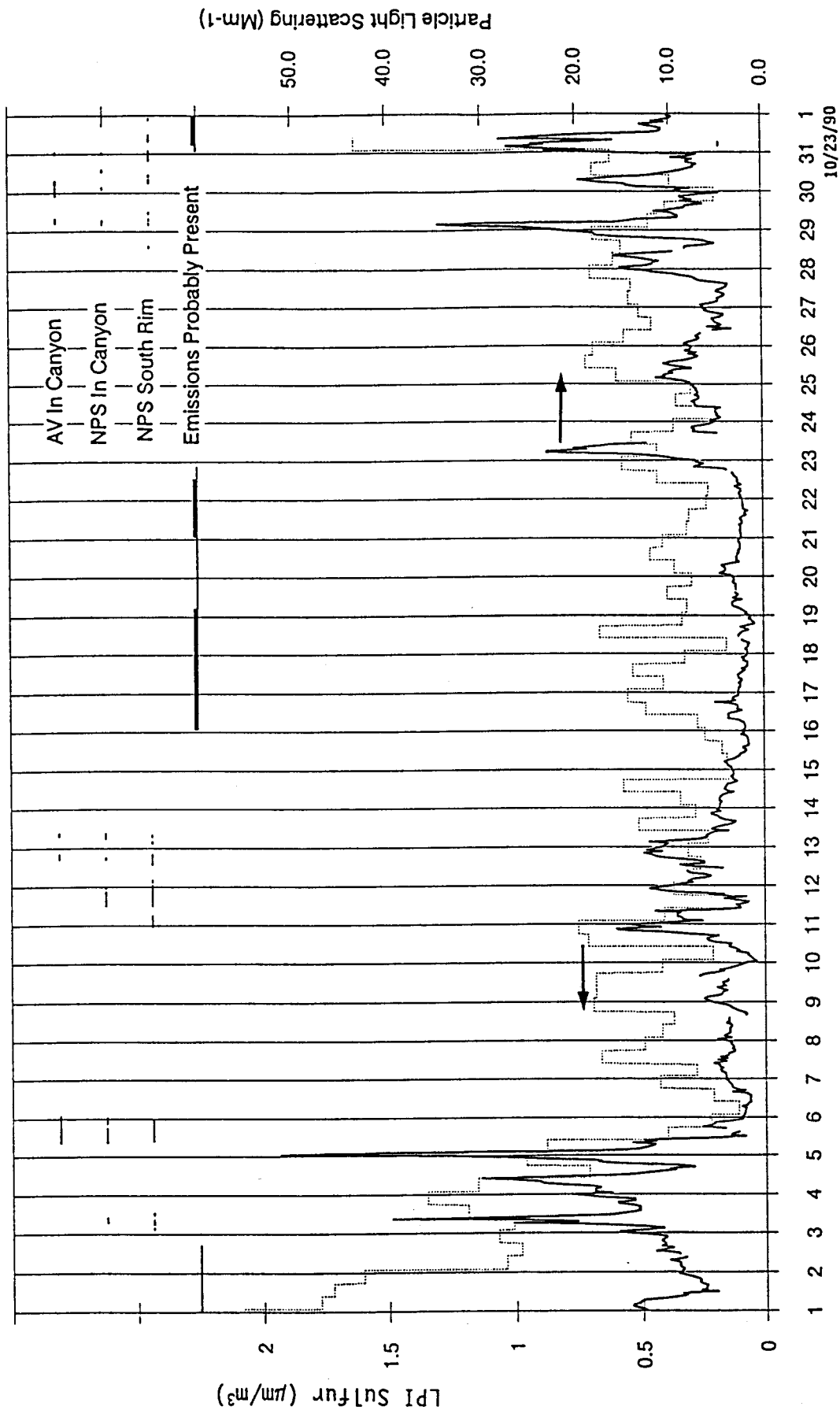
Figure 5-4. Time Series Plot of Hopi Point Hourly Light Scattering by Particles and Eight-Hour Average Particulate Sulfur Concentrations Measured by the Low Pressure Impactor in January. The light bars at the top of the figure indicate when the transmissometer sight paths were obscured by clouds or precipitation and the heavy bar when NGS emissions were probably present at Hopi Point.



February 1990

10/23/90

Figure 5-5. Time Series Plot of Hopi Point Hourly Light Scattering by Particles and Eight-Hour Average Particulate Sulfur Concentrations Measured by the Low Pressure Impactor in February. The light bars at the top of the figure indicate when the transmissometer sight paths were obscured by clouds or precipitation and the heavy bar when NGS emissions were probably present at Hopi Point.



March 1990

Figure 5-6. Time Series Plot of Hopi Point Hourly Light Scattering by Particles and Eight-Hour Average Particulate Sulfur Concentrations Measured by the Low Pressure Impactor in March. The light bars at the top of the figure indicate when the transmissometer sight paths were obscured by clouds or precipitation and the heavy bar when NGS emissions were probably present at Hopi Point.

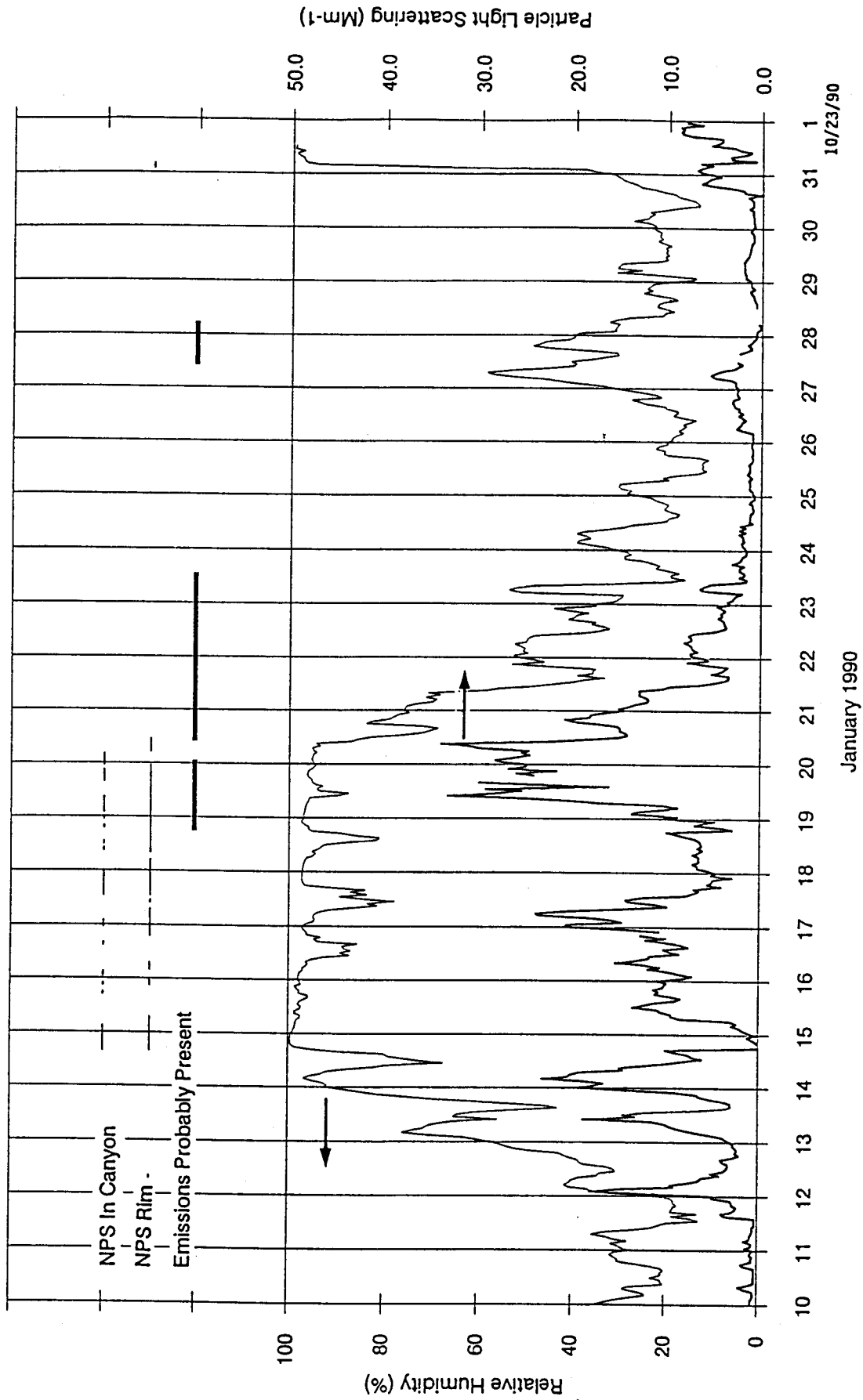


Figure 5-7. Time Series Plot of Hopi Point Hourly Light Scattering by Particles and Relative Humidity in January. The light bars at the top of the figure indicate when the transmissometer sight paths were obscured by clouds or precipitation and the heavy bar when NGS emissions were probably present at Hopi Point.

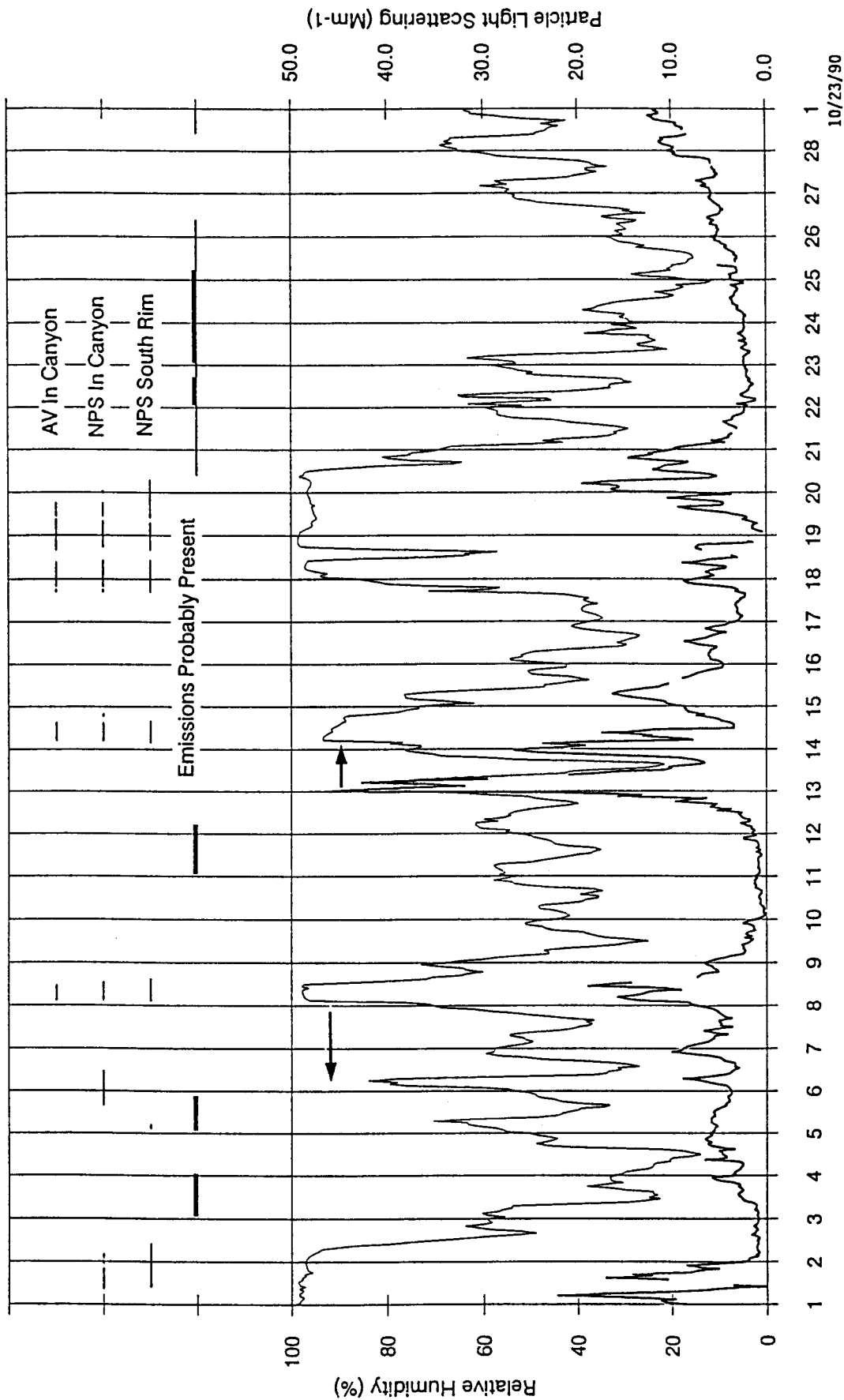
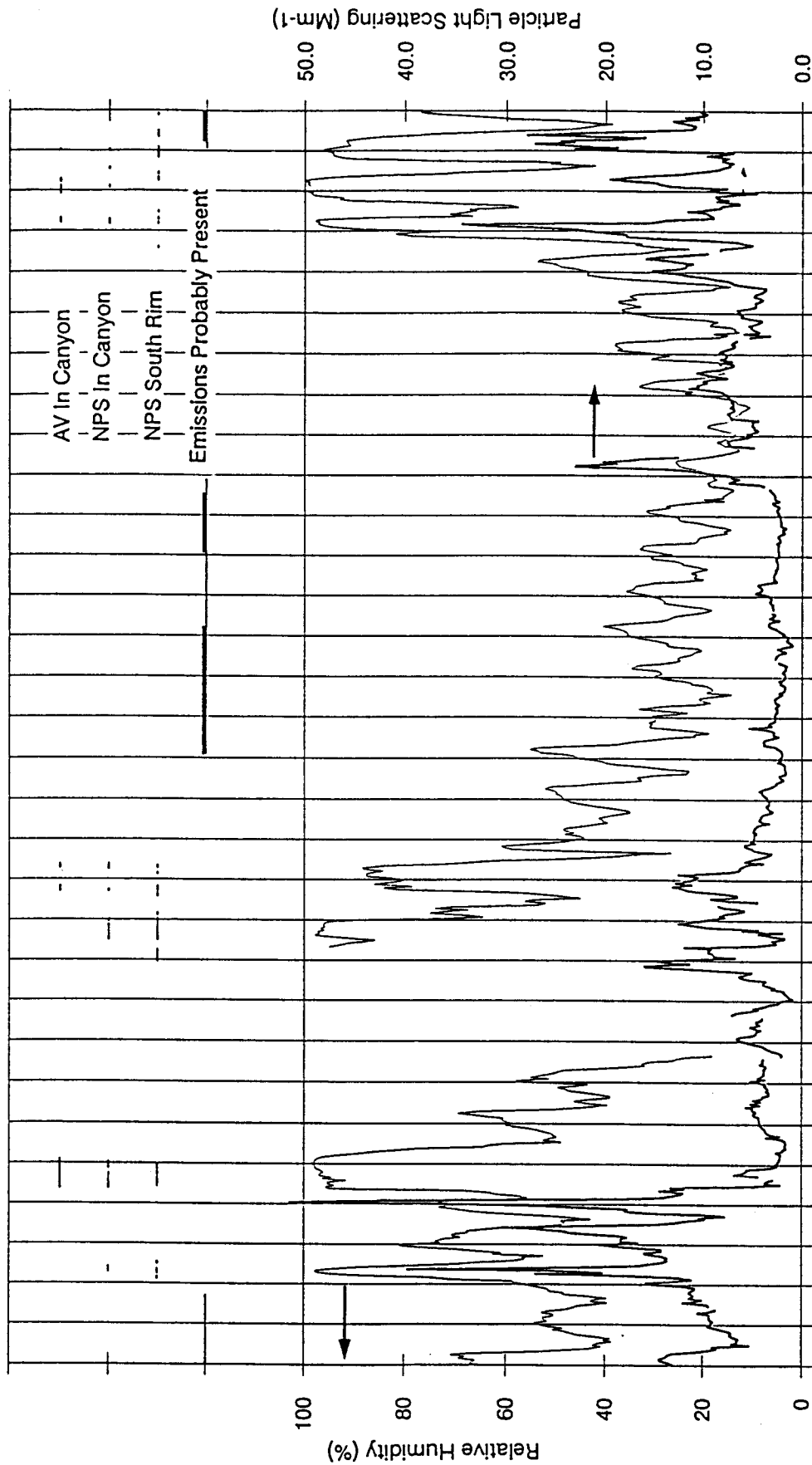


Figure 5-8. Time Series Plot of Hopi Point Hourly Light Scattering by Particles and Relative Humidity in February. The light bars at the top of the figure indicate when the transmissometer sight paths were obscured by clouds or precipitation and the heavy bar when NGS emissions were probably present at Hopi Point.



March 1990
10/23/90

Figure 5-9. Time Series Plot of Hopi Point Hourly Light Scattering by Particles and Relative Humidity in March. The light bars at the top of the figure indicate when the transmissometer sight paths were obscured by clouds or precipitation and the heavy bar when NGS emissions were probably present at Hopi Point.

instrument begin on February 2. The middle bar shows data from the NPS transmissometer between Yavapai Museum on the South Rim and Phantom Ranch in the bottom of the Canyon. The third bar shows data from the NPS transmissometer between Lippan Point and Grandview Points on the South Rim.

Figures 5-7 through 5-9 are the same as Figures 5-4 through 5-6, except that the lower panel shows the hour-average relative humidity and nephelometer readings at Hopi Point. The vertical rulings in these Figures mark midnight MST, and the date on the ruling is for the following day.

The following observations can be made:

- High nephelometer readings tend to be associated with high sulfate concentrations or high humidities, but there are exceptions:
 - An example of a high nephelometer reading in the absence of high sulfate occurred when dust was transported from the southwest on February 13.
 - Low nephelometer readings occurred frequently during periods when the relative humidity was near or above 90% (see also Figure 5-3).
- There were two times when NGS emittants probably arrived while the transmissometers indicated the presence of clouds or precipitation: the evening of January 18 and the morning of March 31. The nephelometer readings and sulfate concentrations increased suddenly both times to values significantly above the study average values.
- These observations lend support to the current consensus that the sulfate formation rate is enhanced in clouds and to the estimate by the NRC Committee that the effects of the NGS emittants could be "significant" at these times (NRC, 1990).
- The nephelometer readings and sulfate concentrations remained high on January 19, but clouds obscured the transmissometer sight path at the South Rim all day. Therefore, the visibility at the South Rim transmissometer site was controlled by the clouds and not directly affected by sulfate.
- For about 75% of the measurement periods during which the NGS emittants were probably present at Hopi Point, they were transported there by cleaner than average ($b_{sp} < 6.6 \text{ Mm}^{-1}$), dry ($\text{RH} < 70\%$) air. When the Category 1 (probably present) times began and ended on February 11 and 12, February 22 through 25, and March 16 through 23, changes in the nephelometer readings were not evident. Thus, the visibility effects of the emittants on these occasions when the atmosphere was clean and dry were too small to be discerned in the readings of the optical instruments at the Receptor Sites.
- Tracer, continuous monitor, and plume animation data show that the highest concentrations of NGS emittants at Hopi Point during the study were observed the night of January 20-21. Time series and regression analyses of this event appear in Section 11 of the August Status Report

(Richards et al., 1990). The fresh NGS emittants were present for a few hours centered around 2100 MST, which is a time when the relative humidity and nephelometer readings were declining rapidly. Even though the relative humidity was high, the optical effects of the fresh emittants were smaller than the uncertainties in the optical measurements.

- Many excursions of the Hopi Point nephelometer reading above 10 Mm^{-1} were observed. (For comparison, when the nephelometer reads 10 Mm^{-1} , the light scattering by particles is equal to the light scattering by particle-free air.) The animation discussed in Section 4, the meteorological analyses, and data presented in the August Status Report show that many of these elevated readings, including the highest seen during the study (2/13 and 3/5) were associated with transport from the southwest or west during times when the NGS emittants were classified as probably absent.

5.3 ANALYSIS OF TIMES OF HIGH LIGHT SCATTERING BY PARTICLES WHEN THE EMITTANTS MAY BE PRESENT

Table 5-2 lists the time periods which satisfied two criteria:

- The light scattering by particles was above 10 Mm^{-1} , and
- The measurement periods were assigned to Category 1 (probably present) or Category 2P (uncertain, but it is estimated that further analysis will show the emittants were probably present).

The entries in the table show how the high readings are distributed between day and night and also the number of times clouds or precipitation were present in the transmissometer sight paths when the b_{sp} readings were high.

The presence of a cloud or precipitation in a transmissometer sight path for one reading during a four hour period does not indicate that clouds obscured the scenic views during that period. It is planned to examine photographs to obtain an estimate of the visual effects of clouds. However, these data do indicate times when clouds were present near the viewpoints.

The above criteria were met during four episodes: January 19 through 21, February 20, February 28 through March 2, and March 31. These four episodes were listed at the beginning of this section among the times in Categories 1 and 2P when the relative humidity was above 70%. The only difference between the two listings is February 5, when the relative humidity exceeded 70% but the b_{sp} did not exceed 10 Mm^{-1} .

For the division between day and night, the daytime periods began with the 0600 MST measurement period and ended with the period ending at 1800 MST. Thus, there are an equal number of daytime and nighttime periods, and the data in Table 5-2 are equally divided between day and night.

Table 5-2. Tabulation of Category 1 and 2P Measurement Periods with Light Scattering by Particles Greater than 10 Mm^{-1} ^a

Measurement Periods in Episode		Number of Periods with b_{sp} Greater than 10 Mm^{-1} ^b			Number of Periods with b_{sp} Greater than 20 Mm^{-1}				
First	Last	Total	Night	Days, Obsc.	Day, Not Obscured	Total	Night	Day, Obsc.	Day Not Obscured
0200 MST 1/19	0600 MST 1/21	14	7	5	2	6	3	3	0
1800 MST 2/20	2200 MST 2/20	2	2	0	0	0	0	0	0
1800 MST 2/28	0600 MST 3/1	4	3	0	1	0	0	0	0
1000 MST 3/2	1400 MST 3/2	2	0	0	2	0	0	0	0
0200 MST 3/31	1800 MST 3/31	5	2	2	1	2	1	1	0
Totals		27	14	7	6	8	4	4	0

a Category 1 is "NGS emittants probably present" and Category 2 is "uncertain, but it is estimated that additional analysis will show that the emittants were probably present."

b Both periods with b_{sp} between 10 and 20 Mm^{-1} and with b_{sp} greater than 20 Mm^{-1} are included in these columns.

c Daytime readings are classed as obscured if the NPS transmissometer on the South Rim recorded a one-hour reading greater than 100 Mm^{-1} and not obscured if the highest one-hour reading was less. Not all sight paths will be obscured when clouds or precipitation are present in the South Rim transmissometer sight path for a portion of a four-hour measurement period. Daytime measurement periods extend from 0600 to 1800 MST and nighttime periods from 1800 to 0600 MST.

A daytime measurement period was listed as being obscured by clouds or precipitation if the NPS transmissometer on the South Rim recorded a one-hour reading above 100 Mm^{-1} during the four-hour measurement period. This is an indication of the presence of clouds, but does not give a reliable indication of the extent to which clouds obscured the views.

The b_{sp} readings exceeded 20 Mm^{-1} during eight Category 1 or 2P measurement periods, and all of them were at night or during times when clouds or precipitation were in the South Rim transmissometer sight path for at least part of the measurement period. The b_{sp} readings exceeded 10 Mm^{-1} during 27 Category 1 or 2P measurement periods, so there were 19 cases with readings between 10 and 20 Mm^{-1} . Six of these cases occurred during the day when the South Rim transmissometer gave no indication of the presence of clouds or precipitation.

Entries for eight calendar days appear in Table 5-2, or 10% of the study days. Daytime b_{sp} readings above 10 Mm^{-1} with no indication of clouds or precipitation in the South Rim transmissometer sight path occur on five of these days. The entries in Table 5-2 are for cases in which light scattering by all fine particles is equal to or greater than the light scattering by clean air. The data analysis has not yet progressed to the point that estimates can be made of the NGS contribution to fine particle scattering during these measurement periods. Estimates of the light scattering by sulfate during some of these measurement periods appear in Section 5.

A rough indication of the visibility corresponding to these values of light scattering by particles can be given by calculating the visual range. The following calculations assume that 4% contrast is the threshold for visual detection, that light scattering by air contributes 10 Mm^{-1} , and that light absorption is 10% of b_{sp} . The highest four-hour b_{sp} during a Category 1 time was 30 Mm^{-1} , and the corresponding visual range was 75 km or 47 miles. A b_{sp} of 20 Mm^{-1} corresponds to a visual range of 100 km or 60 miles, and a b_{sp} of 10 Mm^{-1} corresponds to a visual range of 145 km or 90 miles.

5.4 DILUTION OF NGS EMITTANTS

Atmospheric transport and dispersion cause the emittants from a point source to be diluted and to be transported to monitoring sites at surrounding locations. For inert species, the ratio of the ambient concentration χ measured at a monitoring site divided by the rate of emission Q depends only on the properties of the atmosphere. Variations in the emission rates will not affect this ratio (provided such factors as the plume rise are not significantly affected). Cumulative frequency distributions of the χ/Q ratio provide a way of summarizing the observed atmospheric transport and dilution. Figure 5-10 shows χ/Q plots derived from the tracer concentrations measured at Hopi Point in WHITEX and in this study.

The WHITEX χ/Q line was calculated from all reported values of ambient concentrations of CD_4 tracer at Hopi Point during WHITEX (See Figure 4.15 on page 4-20 of the WHITEX Final Report, Malm et al., 1989). The ambient concentrations and emission rates used in these calculations are the same as in the WHITEX Final Report and do not include the rescaling of the Unit 3 data

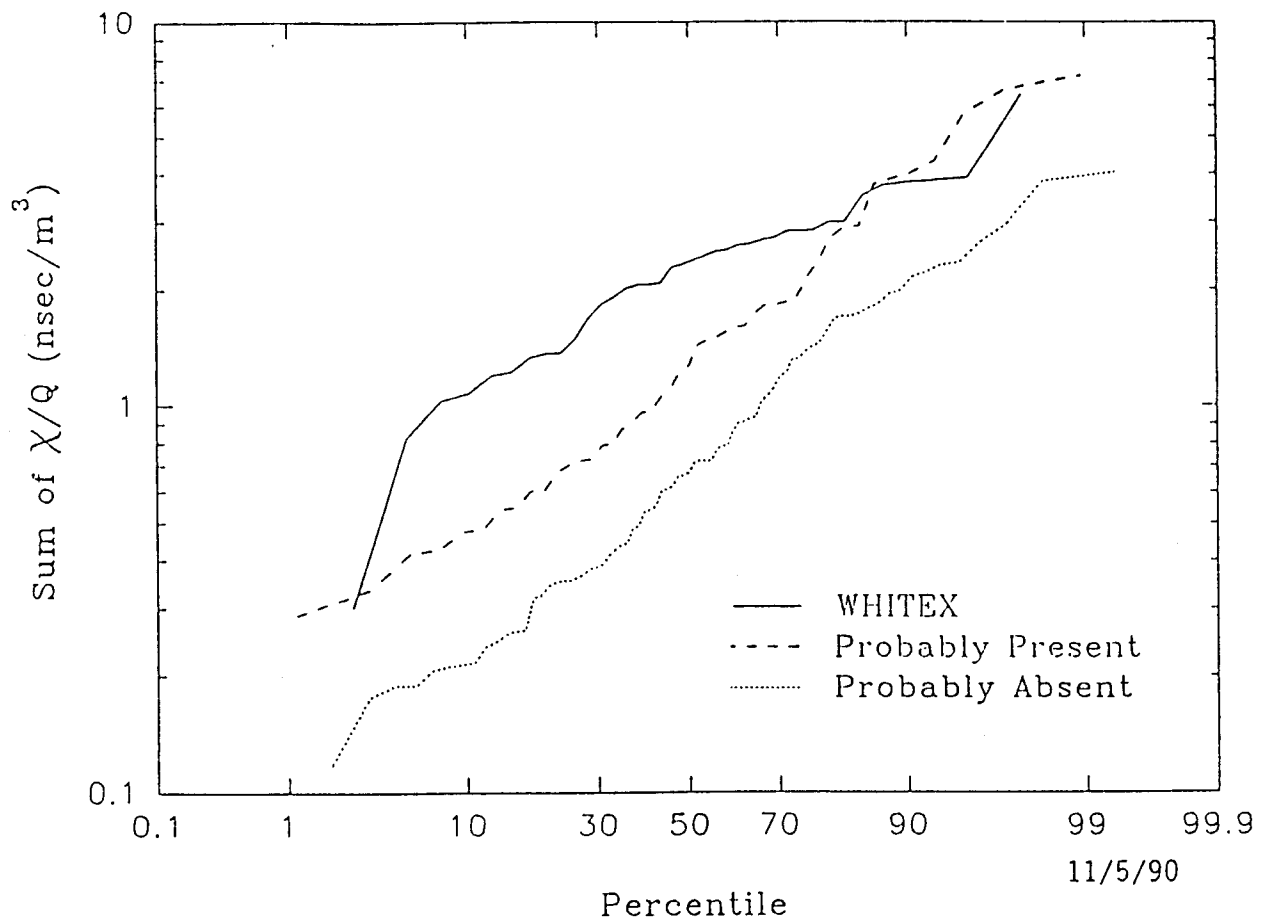


Figure 5-10. Cumulative Frequency Distributions Showing the Dilution of the NGS Emittants Indicated by Tracer Concentrations Reported by WHITEX and this Study. The "probably absent" curve was calculated with June 1990 data and the "probably present" curve was calculated with August 1990 data and plume ages determined from the animation.

used in some of the preliminary WHITEX analyses. The plume ages used to relate ambient concentrations and emission rates were obtained from Table 6.10 on page 6-33 of the WHITEX Final Report. When necessary, linear interpolation was used to determine the plume age for sampling times not included in the table. When a range of plume ages was reported, the average value was used. It is recognized that these calculation procedures contain rough approximations, but it is believed that a more careful analysis would not significantly alter the WHITEX curve in Figure 5-10.

To save analytical costs, WHITEX CD₄ samples were selected for analysis from times when the concentrations of the NGS emittants at Hopi Point were thought to be the highest. The fact that the WHITEX CD₄ data were selected by a procedure that is hard to duplicate complicates any comparison with the perfluorocarbon tracer (PFT) data from this study. However, the dashed line in Figure 5-10 was derived by procedures which gave the highest possible χ/Q values, so the resulting curve is as close as possible to the WHITEX data. Steps in the derivation are:

1. Twelve-hour average ambient concentrations were calculated for each perfluorocarbon tracer for time periods beginning at 0600 and 1800 MST to duplicate the WHITEX averaging time. Differing sample start times in the two studies caused a two hour offset from the 0800 and 2000 MST start times used in WHITEX.
2. Only the 12-hour time periods during which the NGS emittants were probably present during at least two of the three four-hour time periods (Category 1 in Table 4-1) were selected. Forty-seven 12-hour time periods met this criterion.
3. The average χ/Q was calculated for each tracer separately and then the four χ/Q values were added to obtain the reported value. This procedure includes the measurement noise from each of the four measurements. The emission rate Q corresponding to each ambient measurement was calculated using the plume age derived from examination of the animation (See Section 4). For the three tracers that were not being emitted at the time derived from the plume age, the one-day average of the release rate during the most recent release of each tracer was used for Q .

The results are shown by the dashed line in Figure 5-10. For the highest 10% of the data, higher χ/Q ratios were observed in this study than in WHITEX. The WHITEX χ/Q values are higher throughout the remainder of the distribution.

The PFT concentrations reported for Hopi Point at the current level of validation are known to be degraded by noise (See Section 9.1), and are believed to have generally higher values, on average, than the correct ones. The dotted line in Figure 5-10 shows the χ/Q values calculated from the PFT data in this study for times when the NGS emittants are probably absent from the Receptor Sites (Category 3 in Table 4-1). The emission rate used in these calculations is the current or most recent daily average for the observed tracer. If both the classification of the measurement periods in Table 4-1 and the tracer measurements were correct, the dotted line would be off scale at the bottom of the plot, and perhaps only a few measurements due to noise, measurement error, or improper classification would appear at the right of the

diagram. In fact, it is observed that the distribution of χ/Q values is not very different from the distribution calculated for times when the NGS emittants are probably present. This indicates that noise made a substantial contribution to the reported PFT concentrations.

The WHITEX curve corresponds to less dilution of the emittants than the SRP curves. This indicates that the WHITEX CD_4 data may be even more strongly affected by measurement bias and noise than the PFT data from this study. This and the following observations raise questions concerning the use of the WHITEX CD_4 data to quantify the dilution of the NGS emittants:

- The ratios of sulfur dioxide to CD_4 measured at the Glen Canyon site during WHITEX deviated from the emission ratios by more than a factor of ten in both directions, and these deviations were much larger than can be accounted for by the error estimates derived from the reported experimental uncertainties. These large deviations were present in the data even when the sulfur dioxide and CD_4 concentrations were relatively high, when measurement noise should have been minimized.
- The CD_4 concentrations reported for Hopi Point fall in a relatively narrow range, and CD_4 concentrations in this same range are reported for samples collected in locations believed to be well removed from the NGS emittants. For example, CD_4 concentrations similar to those for Hopi Point were reported for aircraft samples collected about 80 km from NGS in the opposite direction from where the plume was being transported (Anderson and Hammarstrand, 1988).

5.5 MATRIX OF SELECTED DAILY PARAMETERS

A day-by-day listing of selected measurements from the 1990 NGS winter study is included in Appendix B. The listing includes tracer, fine mass, and sulfate (calculated as [sulfur] x 4.1) concentrations at Hopi Point; particle scattering coefficients at Hopi Point and Bryce Canyon; surface wind, relative humidity, and stability at Hopi Point; Page afternoon mixing depth relative to the altitude of Hopi Point; NGS plume height winds; winds at Cedar Ridge (about halfway between NGS and Hopi Point); Winslow 700 mb winds; NWS Grand Canyon precipitation; and surface and upper-air synoptic weather types classified by Larry Kalkstein of the University of Delaware. Except for the precipitation and synoptic classification data, all data in the listing are for daytime measurements only (i.e., measurement periods between 0600 and 1800 MST).

Inspection and analysis of the 81-day matrix of variables reveals many patterns in the data, as described below.

1. The scattering coefficients at Hopi Point and Bryce Canyon tend to rise and fall in phase. That is, periods of reduced visibility at Hopi Point were also characterized by reduced visibility at Bryce Canyon.

2. An analysis of stability at Hopi Point (in terms of the temperature lapse rate between Hopi Point and Indian Gardens within the canyon) shows that high scattering coefficients at Hopi Point occurred when the air mass was

neutral. A stable air mass typically resulted in low scattering coefficients. In addition, the surface wind at Hopi Point was more frequently from the southwest when the air mass was neutral and scattering coefficients were high. This result is contrary to the WHITEX hypothesis that haziness at the Grand Canyon occurs primarily during "stagnation." Low altitude locations may be affected by stagnation and increased build-up of pollutants. However, high altitude sites like Hopi Point became hazy during periods of good mixing and southwesterly flow.

3. Scattering coefficients at Hopi Point were positively correlated with relative humidity (correlation coefficient of +0.55).

4. The relationship between Hopi Point scattering coefficient and ammonium sulfate concentration was not consistent. For example, the ratios on January 19 and January 21 differed by more than a factor of two. These data highlight the effects of particle composition, particle size, and relative humidity.

5. Finally, examination of the NGS plume transport directions reveals that Hopi Point tended to have higher scattering coefficients when the NGS emittants were being blown away from the Grand Canyon (in agreement with Item 2, above).



6. PARTICLE SIZE DISTRIBUTIONS AND OPTICAL PROPERTIES

6.1 SULFUR AEROSOL SIZE DISTRIBUTIONS

The size distributions of sulfur containing particles were measured over eight-hour intervals throughout the study period at Hopi Point using a low-pressure impactor (LPI). For most days, four-hour sulfur size distribution data from the U.C. Davis Drum impactors (DRUM) are also available. These data showed that the submicrometer concentrations varied from 0.01 to 2.1 $\mu\text{g}/\text{m}^3$ sulfate, with a geometric mean concentration of 0.3 $\mu\text{g}/\text{m}^3$.

Both the DRUM and LPI samplers show considerable day-to-day variability in the mass median diameter of the sulfur-containing aerosol. Most LPI distributions show sulfur mass median diameters less than 0.3 μm , which are below the size range most effective for light scattering. Only 5% of the distributions have median diameters above 0.5 μm , for which light scattering is more efficient.

The occurrences of larger sulfur mass median diameters did not generally coincide with the periods of the highest sulfate concentrations. Sulfate concentrations greater than 1.0 $\mu\text{g}/\text{m}^3$ were observed for 21 out of 240 or 9% of the eight-hour measurement periods. Of these, only one period had a mass median diameter greater than 0.4 μm . The periods of larger sulfate median diameters were found during periods of high relative humidities (greater than 70% RH), but not all high humidity days showed the large sulfur particle size. For the majority of all study days, and the majority of days of elevated sulfate concentrations (greater than 1 $\mu\text{g}/\text{m}^3$), the aerosol sulfur size in the Grand Canyon was below the range most effective for light scattering.

These data are consistent with previous measurements of desert aerosols (Hering et al., 1981, Ouimette and Flagan, 1982). They differ from measurements in Los Angeles (Hering and Friedlander, 1982, Wall et al., 1988) and the midwest (McMurry and Wilson, 1983, Vossler and Macias, 1986) where the median sulfur particle size was most often in the range between 0.4 and 0.8 μm . This larger particle size is a more efficient light scatterer than that observed for the Grand Canyon. Thus, typical sulfate scattering efficiencies for the Grand Canyon sulfate aerosols are expected to be lower than those derived from these urban areas.

6.2 AEROSOL OPTICAL EFFECTS

6.2.1 Approach

Optical effects of ambient aerosols at Hopi Point were calculated explicitly for 13 days during the Winter 1990 NGS Visibility Study. Particle light scattering coefficients were calculated using a deterministic model which takes into consideration mixing characteristics and hygroscopicity of subfractions within the size-segregated aerosol. Light scattering efficiencies for ammonium sulfate, defined as the change in b_{sp} resulting from a change in the ammonium sulfate concentration, were calculated as a function of relative humidity and the degree of ammonium sulfate removal.

The experimental measurements used as input to the calculations included daily measurements of the response of particle size to changes in relative humidity, scanning electron microscopy analyses of single particle composition, and 24-hour averaged size distributions of carbonaceous aerosols, inorganic ions and elemental composition measured by the micro-orifice uniform deposit impactor (MOUDI). These data were used to formulate an aerosol model which describes the distribution of species and water among particles and the response of particle size to changes in relative humidity. Mie theory was applied to the aerosol model to determine light scattering coefficients and efficiencies.

6.2.2 Aerosol Model: Hygroscopicity Classes and Single Particle Composition

The response of particle size to changes in relative humidity was measured with a Tandem Differential Mobility Analyzer (TDMA). The TDMA selected a monodisperse fraction of the ambient aerosol, exposed it to a known relative humidity, and measured the distribution of particle sizes which resulted. The measurements were made for several relative humidities and repeated for different monodisperse input aerosols. These data were collected at Hopi Point on most days of the NGS Winter Visibility Study.

The TDMA experiments at Hopi Point yielded two distinct growth curves describing the changes in the particle diameter as a function of relative humidity. At high humidities all particles grew, but some grew more than others. This indicated that ambient particles typically included both more-hygroscopic and less-hygroscopic particle types.

For the more-hygroscopic fraction, the water uptake as a function of relative humidity varied significantly from day to day, as did the ratio of the number of particles in each hygroscopicity class. Unlike Los Angeles aerosol (McMurry and Stolzenburg, 1989), the extent of growth was independent of the dry particle size. Aerosol hygroscopicity was described by daily growth curves, one for the more-hygroscopic fraction and one for the less-hygroscopic fraction, as shown by the dashed lines of Figure 6-1.

According to single particle scanning electron microscopy (SEM) of samples collected from the TDMA, the less-hygroscopic particles contained carbonaceous particles and soil dust particles. The more-hygroscopic particles are believed to contain sulfates, but this could not be directly confirmed by microscopy due to sampling difficulties. These particles had a growth factor about 20% less than is found for pure ammonium sulfate. Also, for about 30% of the TDMA measurements, the more-hygroscopic fraction deliquesced at relative humidities of 75% - 80%, which is similar to the deliquescent point for pure ammonium sulfate. SEM analyses of ambient samples which were not segregated according to hygroscopicity indicated that many sulfur-rich particles were present, and many of these also contained carbon.

On the basis of these data, the aerosol was modeled as a combination of three externally mixed particle types. The less-hygroscopic fraction was assumed to be composed of externally mixed (1) carbon and (2) soil dust particles. The more-hygroscopic fraction was assumed to contain (3) all

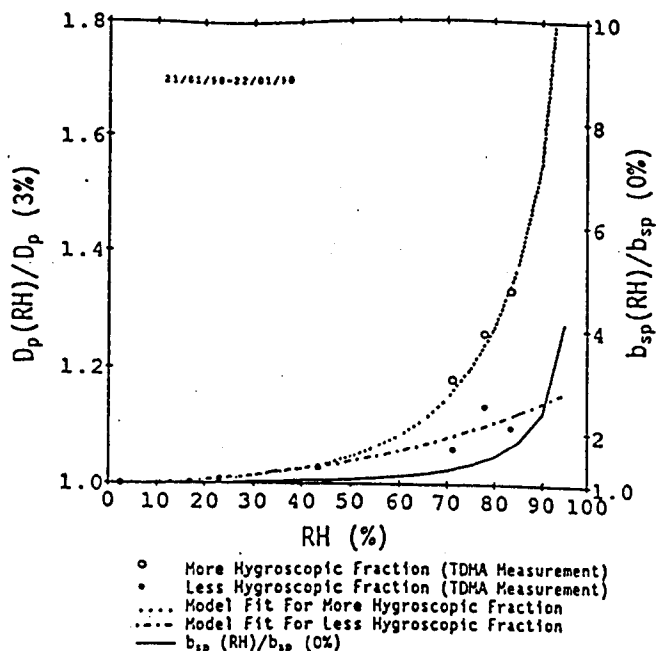


Figure 6-1. Particle Size and Light Scattering Coefficient as a Function of Relative Humidity Corresponding to the 24 h MOUDI Sample Beginning at 1800 MST on January 21.

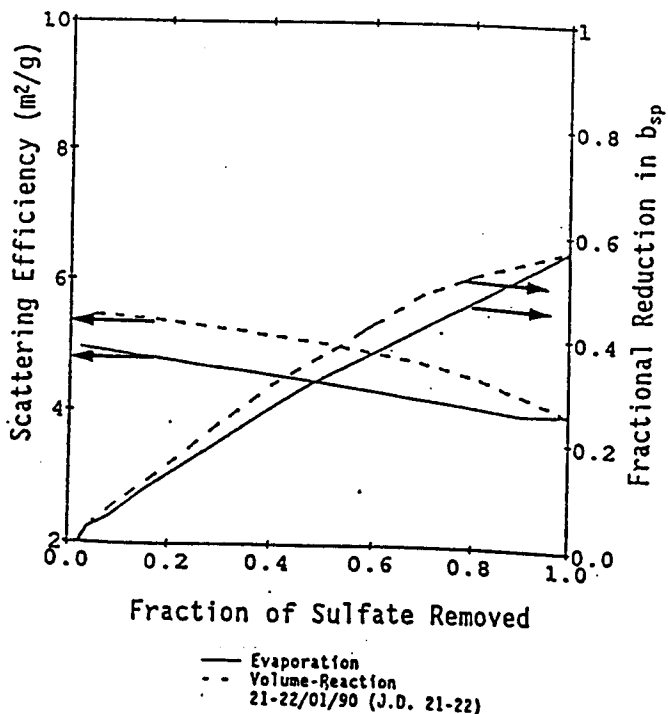


Figure 6-2. Sulfate Scattering Efficiency and Fractional Reduction in Scattering Coefficient as a Function of Fractional Reduction in Sulfate Loadings for the 24 h MOUDI Sample Beginning at 1800 MST on January 21.

sulfate, nitrate and a portion of the carbon. For each day modeled, the carbon was apportioned between the hygroscopic and nonhygroscopic fraction by a particle number balance between the TDMA and micro-orifice impactor (MOUDI) species size distribution data. The associated water was given by the TDMA growth curves and the average ambient relative humidity. Densities and refractive indices of the particle types were estimated from the concentrations of individual species and water by assuming that volume is conserved when species are mixed together.

6.2.3 Model Visibility Calculations for Hopi Point

Average light scattering coefficients and scattering efficiencies were calculated for twelve 24-hour periods and one 48-hour period at Hopi Point. For each period, the size distributions of each of the three particle types described above were calculated as a function of geometric particle diameter and used with volume averaged refractive indices to compute light scattering coefficients, b_{sp} , on the basis of Mie (1908) theory. For 10 of the 13 days modeled, calculated light scattering coefficients agreed well with values measured by nephelometry. The three exceptions were days on which coarse wind-blown dust might have influenced nephelometer data or during which relative humidities were at times near 100% and varied widely.

Light scattering coefficients were also evaluated as a function of relative humidity. TDMA results for January 22, 1990 are shown in Figure 6-1. The dashed lines show the growth curves for the more- and less-hygroscopic aerosol classes. The solid line represents b_{sp} as a function of relative humidity normalized by b_{sp} at 0% relative humidity ($b_{sp}(RH)/b_{sp}(0\%)$). This indicates the calculated effect which the uptake of water from both aerosol fractions has on the light scattering coefficient. The change in b_{sp} with water uptake is relatively small at relative humidities below 70% or 80%. When the same aerosol was exposed to higher values of relative humidity, b_{sp} increased sharply, resulting in much larger reductions in visibility.

Scattering efficiencies for ammonium sulfate, $\Delta b_{sp}/\Delta[(NH_4)_2SO_4]$, were evaluated by comparing the calculated particle scattering for the ambient data with the calculated scattering after removal of a portion of the ammonium sulfate and its associated water. In this model the number of particles is assumed constant, and each sulfate-containing particle is allowed to shrink in proportion to its growth law. Growth laws describe how a species is divided among particles of different sizes during the formation process. Both condensation - evaporation and volume reaction growth laws were used (McMurry and Wilson, 1982, Friedlander, 1977). At high relative humidities the volume growth model is most applicable, whereas at low relative humidities the size distribution is more likely to change according to an evaporation - condensation growth law (McMurry and Grosjean, 1985, McMurry and Wilson, 1982, Heisler and Friedlander, 1977, Hering and Friedlander, 1982). Results for data collected between 1800 MST January 21 and 1800 MST January 22, 1990 are shown in Figure 6-2. This figure shows the calculated ammonium sulfate scattering efficiencies and the fractional reduction in b_{sp} as a function of fraction of the ammonium sulfate removed.

Calculated ammonium sulfate scattering efficiencies at ambient relative humidity were typically 3 to 6 m^2/g and reached 16 m^2/g on a day with a

relative humidity averaging about 92%. Dry scattering efficiencies for ammonium sulfate were estimated to be 2 to 5 m²/g. Values for each day modeled are shown in Table 6-1 and Figure 6-3. The ammonium sulfate scattering efficiency increased with increasing sulfate mass median particle size and with increasing relative humidity. The estimated contribution of ammonium sulfate to fine (less than 2 μm diameter) particle light scattering on the 13 days studied varied between 20% and 80%, with an average of 53%. The remainder of the scattered light was mostly attributable to organic carbon. Soil dust accounted for only 1% to 6% of the light scattering associated with fine particles, although there is some evidence that coarse, wind blown dust may have contributed significantly to scattering on some days.

The curve in Figure 6-3 was fit to the data so ammonium sulfate light scattering efficiencies could be estimated at any relative humidity. The equation for the curve is:

$$\begin{aligned} \text{Ammonium Sulfate Light Scattering Efficiency (m}^2\text{/g)} \\ = 2.32 + 1.01/(1-\text{RH}/100) \end{aligned} \quad (6-1)$$

6.3 PRELIMINARY ESTIMATES OF THE LIGHT SCATTERING BY AMMONIUM SULFATE WHEN NGS EMITTANTS WERE PRESENT AT HOPI POINT

It is not yet possible at this stage in the data analysis to apportion the sulfate concentrations measured at Hopi Point to NGS and to other sources. However, calculations of light scattering by particles and by ammonium sulfate have been completed for 24- or 48-hour sample collection periods overlapping three of the four episodes listed in Section 5.3, which were periods with b_{sp} greater than 10 Mm⁻¹ when NGS emittants were probably present (Categories 1 and 2P) at Hopi Point. Table 6-2 summarizes these results. In the three periods for which the calculations were performed, the calculated period-averaged reductions in light scattering by particles if all ammonium sulfate were removed were 73, 70, and 57%. These values were taken from Table 6-1, in which calculations were done by assuming all sulfate was in the form of ammonium sulfate. The calculated period-averaged reductions in total light scattering (scattering by particles and by air) if all ammonium sulfate were removed were 45, 50, and 29%.

The calculated reduction in b_{sp} if all sulfate were removed may be taken as an upper bound (albeit, a high upper bound) for the expected reduction in b_{sp} if only NGS sulfate were removed. The discrepancy between measured and calculated b_{sp} for the period commencing 1800 MST February 19 appears to have resulted from the rapid change in relative humidity on the 20th (see Figure 5-8).

The actual effects of NGS sulfate on visibility during portions of two of these three episodes may have been much less than implied by these upper bounds because of the presence of clouds, which can obscure views and mask the effects of sulfate on visibility. When results for the apportionment of sulfur from NGS and from other sources become available (such as the preliminary results in Section 8) it will become possible to estimate the apportionment of light extinction between NGS and other sources.

Table 6-1. Calculated Light Scattering Coefficients and Efficiencies

Date ^a 1990	Relative Humidity ^b (%)	Light Scattering by Particles b_{sp} (Mm^{-1}) ^b		Ammonium Sulfate Light Scattering Efficiency ^d (m^2/g)		Calculated Reduction in b_{sp} if all Ammonium Sulfate were Removed (%) ^e
		Measured ^c	Calculated	Ambient Humidity	0% Relative Humidity	
1/18-20 ^f	92.2	19.4	22.5	16.0	3.8	61
1/20-21	63.3	12.1	10.1	6.6	4.8	84
1/21-22	44.8	6.0	6.5	4.6	4.3	57
1/22-23	32.9	3.4	5.1	3.0	2.8	41
1/30-31	72.2	4.6	9.4	5.6	4.5	21
2/12-13	53.6	21.3	5.6	4.3	3.6	21
2/13-14	81.8	13.3	13.1	8.2	4.4	51
2/19-20	92.6	10.3	25.3	15.1	3.1	70
2/28-3/1	55.2	10.7	12.9	5.4	4.5	55
3/1-2	48.0	9.4	7.7	3.0	2.7	59
3/2-3	67.9	16.1	11.6	5.2	4.2	64
3/3-4	63.5	17.7	11.8	5.3	4.5	51
3/4-5	76.5	16.2	11.5	6.3	4.5	49

a The collection of 24 h MOUDI samples began at 1800 MST on the first of the indicated dates.

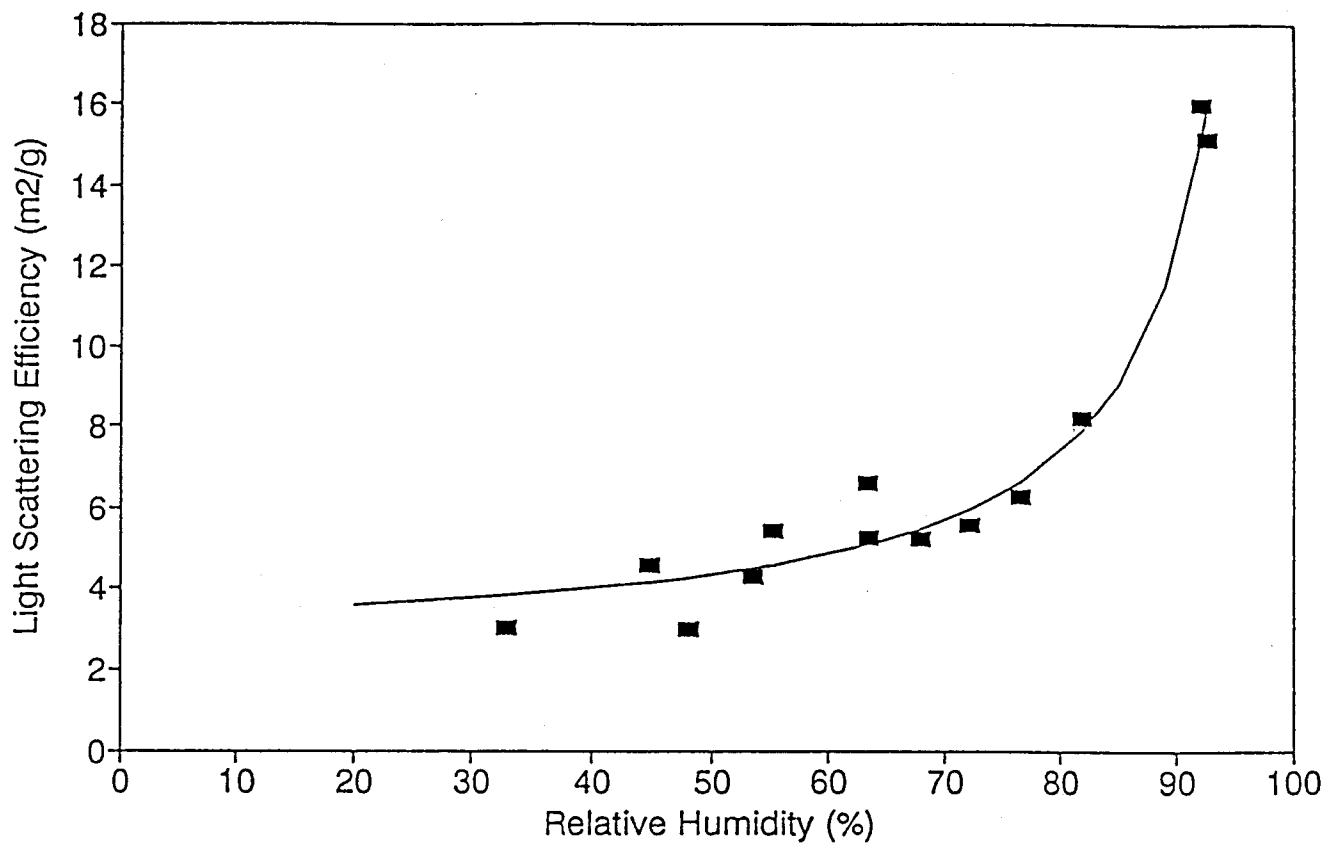
b Average for the 24 h sampling period.

c Measured by the nephelometer at Hopi Point.

d The calculated reduction in particle light scattering divided by the amount of ammonium sulfate removed $\Delta b_{sp}/\Delta[(NH_4)_2SO_4]$. Tabulated values represent the average scattering efficiency for sulfate removal ranging from 0 to 100%.

e $[b_{sp}(\text{with } (NH_4)_2SO_4) - (b_{sp} \text{ without } (NH_4)_2SO_4)]/b_{sp}(\text{with } (NH_4)_2SO_4)$

f 48-hour sample beginning 1800 MST on January 18.



10/12/90

Figure 6-3. Light Scattering Efficiency for Ammonium Sulfate as a Function of Relative Humidity.

Table 6-2. Light Scattering by Ammonium Sulfate During Episodes When NGS Emissions Were Present^a

Sample Collection Start Date ^b 1990	No. Days When NGS Emissions Present	Light Scattering by Particles b_{sp} (Mm ⁻¹) ^c		Calculated Reductions If All Ammonium Sulfate Were Removed (%)	
		Meas.	Calc.	b_{sp} ^d	b_{scat} ^e
Jan 18-20	3	15.8	16.3	73	45
Feb 19 ^f	1	10.3	25.3	70	50
Feb 28-Mar 1 ^g	2	10.1	10.3	57	29
Mar 30-31	>1	- ^h	-	-	-

a These episodes include any periods when NGS emissions were present (see Figures 5-4 through 5-9) and b_{sp} readings in excess of 10 Mm⁻¹ were recorded.

b The collection of 24 hr MOUDI samples began at 1800 MST on the date indicated. The January 18 sample was collected over 48 hours.

c Taken from Table 6-1 as the simple averages of the b_{sp} for each of the days in the period indicated (where each day commences at 1800 MST).

d Taken from Table 6-1 as the simple averages of the percentage b_{sp} reductions for each of the days in the period indicated (where each day commences at 1800 MST).

e Assumes Rayleigh scattering of 10 Mm⁻¹. Computed as:

$$(b_{sp} * \% \text{ reduction in } b_{sp}) / (10 + b_{sp})$$

f The calculation is for 1800 MST February 19 through 1800 MST February 20. However, b_{sp} also exceeded 10 Mm⁻¹ at times from 1800 MST through 2400 MST February 20.

g The calculation is for 1800 MST February 28 through 1800 MST March 2. However, b_{sp} also exceeded 10 Mm⁻¹ at times from 1800 MST February 27 through 1800 MST February 28.

h Calculation was not done for this date because the impactor samples have not yet been analyzed.

The four episodes during which NGS emittants were probably present (Categories 1 and 2P) comprised eight days. During portions of 22 other days, b_{sp} exceeded 10 Mm^{-1} , but NGS emittants were not present. On these days, no improvement in b_{sp} would be expected if only NGS sulfate were removed.



Review

7. SYNOPTIC METEOROLOGY AND REPRESENTATIVENESS OF THE STUDY PERIOD

Several studies were undertaken to characterize the synoptic meteorology of each day of the 1990 study as well as the 1987 WHITEX period and to compare each study to climatological norms. The basic characteristics of the synoptic meteorology that accompanied visibility episodes during the 1990 study are presented in Section 7.1. The meteorology that accompanied episodes during the 1990 study is compared to the meteorology that accompanied historical episodes in Section 7.2. Evaluations of the representativeness of the day-to-day meteorology of the 1990 and WHITEX study periods are discussed in Section 7.3. Finally, Section 7.4 summarizes the findings presented in the August Status Report regarding representativeness of the air quality measurements collected during 1990.

The issue of representativeness has been addressed by estimating the long-term frequency of occurrence of a number of climatological parameters based on multi-year samples. The frequency with which these same parameters occurred during the 1990 and WHITEX study periods then was compared to the estimated long-term climatological norms. The parameters selected for comparison, which are discussed in Section 7.3, are designed to evaluate general synoptic patterns over the western United States and specific processes affecting the transport, diffusion, and possible interaction with moist environments of emissions from NGS. The frequencies of occurrence of these parameters have been averaged over a number of winter seasons to arrive at a description of "average" or "normal" conditions, accompanied by measures of their variability. In reality, the frequencies of occurrence of the parameters in any one season may not exactly match their climatological norms, but they will occur with a frequency that is within acceptable bounds (e.g., one standard deviation). If such is the case, a particular season can be said to be "representative" of climatological conditions.

7.1 SYNOPTIC ANALYSIS OF NGS STUDY EPISODES

Synoptic meteorological conditions associated with reduced visibility at Hopi Point were examined for the 1990 study period. The objective was to identify factors of commonality so that comparisons could be made between 1990 events and previous occurrences. Attention has been focused on episode descriptions rather than single day events. Many of the reduced visibility conditions occur as the result of sequential conditions lasting for several days, and individual days should not be considered separately. In particular, there were indications of aerosol concentrations lingering in the area after the initial, associated conditions no longer existed.

Sixteen days from the 1990 NGS study were considered. These represent the top 20% of the reduced visibility days as indicated by the Hopi Point nephelometer. These sixteen days consisted of seven separate episodes. The time periods examined were:

January 12-14	March 3-5
January 17-20	March 23
February 1	March 29-31

February 13-14

Several interesting characteristics were observed:

- With one exception, the peak visibility reduction events at Hopi Point were associated with high noontime relative humidities at Grand Canyon Airport and the presence of low clouds (at or below 1000 ft. agl). The exception was March 23, which was very dry.
- With the same exception, the greatest visibility reduction during each event occurred on the day of a trough passage through the area. On March 23 there was no significant trough passage.
- The multi-day events (five of seven) were either closed low systems or very slow moving low pressure troughs. Closed low systems are slow-moving and most productive of widespread clouds and high humidities. Three of the low centers moved over or slightly south of the NGS area. The fourth (February 13-14) center passed to the north of the project area and had a shorter duration in terms of cloud effects near the Grand Canyon.
- The episode of March 3-5 began on February 25 with light southerly winds causing slight increases in humidity and slight reductions in visibility. The major impact on visibility did not occur until March 3-5 when the closed low system developed.
- Light winds aloft occurred during three episodes (January 17-20, March 3-5, and March 29-31). These light winds tended to inhibit the rapid removal of pollutants from the area and may have led to recirculation of pollutants from one day to the next. These were three of the four events with the highest light scattering due to particles.

Based on the above characteristics, the 1990 visibility reduction episodes can be divided into the following categories:

- Closed low system - Low center may move over or to the south of NGS or may pass to the north. The track of the low center is significant in determining impact at Hopi Point. Examples are:
 - January 17-20
 - February 13-14 (center to the north)
 - March 3-5
 - March 29-31
- Southwesterly Flow - A basic southwesterly flow aloft exists over Arizona but with occasional minor trough passages which cause brief and temporary occurrences of northwest winds. Examples are:
 - January 12-14
 - February 1
- Low Humidity - Relative humidities are low and low clouds do not exist in the area. Presumably aerosols are formed elsewhere and transported

into the area, whereas aerosols may be formed or grow in the area under the conditions described above. An example is:

- March 23

7.2 SYNOPTIC COMPARISONS WITH HISTORICAL EPISODES

Meteorological conditions occurring during the 1990 study were compared to the top 50 reduced visibility days occurring during the three winter (December-February) seasons: 1984-85, 1985-86, and 1986-87. The 1984-87 data came from nephelometer observations at Hopi Point during the SCENES program. These 50 days represent 16% of all of the sampling days during the period considered and constitute 21 separate episodes.

The three winter (December-February) seasons (1984-85, 1985-86, 1986-87) were classified into the same categories as given above for the 1990 events. Table 7-1 shows a comparison between 1990 and the three year sample.

Table 7-1. Comparison of 1990 Categories with Three Year Period

Category	Jan.-Mar. 1990 No. Cases	Dec.-Feb. 1984-87 No. Cases	Dec.-Feb. 1984-87 Avg. No. Cases
Closed Low	4	8	2.7
Southwesterly Flow	2	9	3.0
Low Humidity	1	4	1.3
TOTAL	7	21	7.0

As indicated in Table 7-1, the average number of episodes in January-March 1990 was the same as the December-February averages for the SCENES data. There were five episodes during the January-February 1987 WHITEX study, compared to four during the January-February portion of the 1990 NGS study.

There was a greater proportion of closed low systems during the 1990 study than is historically evident. The four episodes with greatest visibility reduction during the 1990 study (January 19-20, February 13, March 5, and March 29-31) were all associated with closed low systems. By comparison, in the top 21 reduced visibility episodes of 1984-87, nine of the episodes were southwesterly, eight were closed lows and four were low humidity events.

For comparison, the three principal WHITEX episodes can be classified as follows:

February 9-14, 1987 Southwesterly

January 14-18, 1987 Closed Low
 February 3- 5, 1987 Southwesterly

The January 17-20, 1990 episode was very similar to the January 14-18, 1987 WHITEX episode. A closed low formed in southern California and moved eastward, slightly to the south of the Grand Canyon area. The 1987 low was slightly more intense (at 500 mb) than the 1990 low but its trajectory resulted in extensive low clouds at GCN on only two days (January 15 and 16), compared to five days in 1990 (January 15-19). The duration of the impact in 1990 was consequently longer than in 1987. The remaining three closed low episodes in 1990 were less intense and passed somewhat to the north of the tracks followed in 1987 and 1990. Another example of the January 17-20, 1990 type episode occurred on December 14-15, 1984.

There were two types of synoptic patterns during the 1990 study which were characterized by southwesterly flow over Arizona. January 12-14 had a semi-stationary trough off the California coast which eventually moved inland and from which the closed low system of January 17-20 developed. Similar patterns occurred on January 14-17, 1986, January 29-30, 1986, and February 7-13, 1987. The latter episode was one of the WHITEX events.

The second type of southwesterly pattern occurred on February 1, 1990. This pattern consisted of traveling waves in the westerlies which produced brief periods of southwest winds accompanied by trough passages through northern Arizona. Similar examples can be found on February 7-8, 1985 and February 3, 1987. The 1987 episode was one of the WHITEX events.

It is recognized that humidity and low clouds contribute, in some cases, to the conversion of SO₂ to sulfate and, in other cases, to the hygroscopic growth of existing aerosols. Both factors can be expected to have a visibility reduction effect. Table 7-2 summarizes the number of hours with low clouds (<1000 ft. agl) at Grand Canyon Airport (GCN) for 1990 and for three previous years. Observations were only made during hours when the airport control tower was open (0800 - 1800 local time on most days).

Table 7-2. Number of Reported Hours/Month with Low Clouds at GCN

Year	Jan	Feb	March	Total
1985	101	52	70	223
1986	25	89	75	189
1987	47	43	47	137
Three-Year Average	58	61	64	183
1990	68	54	47	169

Table 7-2 indicates that the number of cloudy hours in 1990 was near or slightly below the average of the three-year comparison sample.

The following comments summarize the comparison between 1990 episodes and those occurring in the December-February period of 1984-85, 1985-86, and 1986-87.

1. Overall, 1990 represented an average year in terms of visibility episodes and associated weather conditions. An average number of episodes occurred, compared to a three-year data sample from 1984-87.
2. There were somewhat more closed low systems associated with the 1990 episodes and fewer southwesterly types than were present in the three-year data set. The closed low systems in 1990 produced the four major visibility episodes during the study.
3. The frequency of occurrence of low clouds at Grand Canyon Airport was near but slightly less than the three-year average.
4. The January 17-20, 1990 episode was very similar to the January 14-18, 1987 WHITEX episode. Another example occurred in December 1984.
5. The other two WHITEX episodes (February 3-5 and February 9-14, 1987) also had analogous cases in the 1990 study.
6. The primary uniqueness in the meteorology for the 1990 study (compared to the three-year period) was the tendency for the area to be influenced by closed low pressure systems rather than traveling waves in the westerlies. Such systems tend to be slow-moving, with marked effects on cloudiness and humidity. These, in turn, contribute to the formation and growth of aerosols.

7.3 METEOROLOGICAL REPRESENTATIVENESS OF THE 1990 AND WHITEX STUDY PERIODS

The previous section discussed basic characteristics of the synoptic meteorology that accompanied visibility episodes during the 1987 WHITEX study and the 1990 NGS study. Based on these results, it appears that the synoptic conditions that accompanied visibility episodes during the winter of 1990 were similar to the conditions associated with episodes in previous years in that the worst episodes coincided with synoptic-scale troughing. The one difference between 1990 and previous years was that more of the episodes accompanied the passage of closed lows and fewer of the episodes were associated with the passage of open-wave troughs during 1990 than in previous years.

Additional studies have been undertaken to characterize the synoptic meteorology of each day of the WHITEX and 1990 studies in terms of long-term climatological norms. In one study (Davis, 1990), the synoptic meteorology of the entire western United States was categorized into 13 synoptic regimes for the period 1979 through 1990. The synoptic indices used in this study were

based on upper air data collected at 21 upper air stations in the western U.S. and Mexico. Temperature, dewpoint, geopotential heights and winds aloft were used to categorize each day of a winter season. In a second study (Kalkstein and Weber, 1990), upper air wind, temperature, moisture and geopotential height data from Winslow and surface data from Flagstaff for the period 1970 through 1990 were used to categorize each winter day over north-central Arizona into one of 15 surface indices and one of 13 upper air indices. In a third study (Muller, et al., 1990), 850 mb and 500 mb upper air charts were used to determine the joint frequencies of geostrophic wind direction and wind speed over north-central Arizona for the period 1984 through 1990, based on gradients of geopotential heights. Additional parameters for evaluating the representativeness of the 1990 and WHITEX study periods were taken from daily Airsondes launched at Page and from the Grand Canyon National Park climate station.

The studies conducted by Kalkstein (1990) and Davis (1990) used discriminate analysis procedures to assign synoptic conditions that occurred during the winters of 1988 through 1990 into synoptic categories that had been defined previously based on conditions that had occurred through 1987. The discriminate analysis technique tended to skew the distribution of category assignments for 1988 through 1990 in favor of categories that one would expect to occur infrequently, based on conditions that had occurred prior to 1988. As a result, both studies found a higher-than-expected frequency of occurrence of categories that are not typical of winter conditions. This result may be an artifact of the discriminate analysis technique rather than a representation of the actual conditions that occurred during the winters of 1988 through 1990. The impact of this problem is that while one can conclude that certain conditions occurred more or less frequently than expected, one can not determine as yet whether such occurrences are "abnormal" or "non-representative". This problem is being addressed by redefining the synoptic categories so that they include conditions experienced during the winters of 1988 through 1990. These results will be presented in the final data analysis report for the SRP study.

7.3.1 The 1990 Study Period

The results of these studies for 1990 can be summarized as follows:

- Over north-central Arizona, the synoptic meteorology of the 1990 study period indicated that southerly to southwesterly flow patterns occurred more often than in previous years, while patterns that produce northerly winds occurred less often.
- Over the entire western U.S., the winter of 1990 was similarly characterized by more frequent occurrences of southerly-to-southwesterly flow patterns and fewer occurrences of northerly-to-northwesterly flow patterns than in previous years. These patterns resulted from the formation of a relatively persistent cold-cone high pressure system over the western U.S., leading to more frequent intrusions of the subtropical jet into the southwestern U.S. and a decline in the frequency of conditions associated with digging of the polar jet and advection of continental polar air into the region.

- The increased frequency of closed lows accompanying reduced visibility conditions during 1990 may reflect the blocking effect of the high pressure system over the western U.S., preventing the polar jet stream digging into the region while favoring the development of slower moving closed lows along the subtropical jet.

Data from the Airsonde launched daily at Page, Arizona indicate:

- Based on six years of winds aloft data at 600 m agl above Page, the frequency of occurrence of northerly-to-northeasterly winds was less during 1990 than in previous years, while there was a greater frequency of occurrence of southwesterly winds in 1990 compared to previous years.
- Based on six years of Airsonde soundings at Page, the average temperature in the lowest kilometer above Page during the 1990 study was slightly warmer than normal; the average relative humidity was about average; and the average temperature lapse rate was slightly less than normal (i.e., less stable).
- These results are in general agreement with the premise that a high pressure ridge formed over the western U.S., which would have reduced the influence of the polar jet over Arizona and favored the intrusion of warmer air from the southwest.

Daily weather reports from the Grand Canyon National Park climate station indicate:

- Grand Canyon temperatures were slightly cooler than the 1977-90 mean during 1990. Precipitation and snowfall were much greater than the mean. This increase in precipitation may be due to the longer duration of adverse weather conditions that accompanied the slow-moving low pressure systems.

7.3.2 The 1987 WHITEX Study Period

The results of the investigations into the representativeness of the January-February, 1987 period can be summarized as follows:

- The synoptic meteorology of the WHITEX study period was characterized by a higher-than-normal frequency of arctic air mass intrusions into north-central Arizona, which were accompanied by northerly flow patterns. The frequency of occurrence of synoptic conditions associated with digging of the polar jet into the southwestern U.S. and the advection of continental polar air into the region was about average during 1987.
- The WHITEX study period experienced a higher-than-normal frequency of patterns producing strong northerly winds over north-central Arizona and a somewhat lower-than-normal frequency of southwesterly flow patterns.

Data from the Airsonde launched daily at Page, Arizona indicate:

- Winds aloft data at 600 m agl above Page show that the frequency of occurrence of northerly winds was higher-than-normal in 1987 with a corresponding lower-than-normal frequency of occurrence of southwesterly winds. These findings are in general agreement with the results of the climatological analyses of synoptic weather patterns.
- Airsonde data at Page indicate that average temperatures in the lowest kilometer above Page were slightly cooler than normal during 1987, whereas relative humidity averaged higher than the mean.

Daily weather reports from the Grand Canyon National Park climate station indicate:

- Grand Canyon temperatures were slightly cooler than the mean during 1987. Precipitation and snowfall were below the mean. This decrease in precipitation may be indicative of the colder, drier air that accompanied the increased frequency of intrusions of arctic air masses into north-central Arizona.

7.4 REPRESENTATIVENESS OF AIR QUALITY MEASUREMENTS

The August Status Report (Richards, et al., 1990) described the results of investigations into the representativeness of air quality conditions that occurred during 1990 compared to previous years, based on cumulative frequency distributions for three measures of air quality. The findings reported in the August Status Report can be summarized as follows:

- The monthly means and cumulative frequency distributions for fine particle sulfur measured by the LPI during January, February, and March, 1990 were close to the means and within the variability observed by the NPS monitoring station at the Grand Canyon for the same months in 1979 through 1986 (see Section 7.4.1 of the August Status Report).
- Cumulative frequency distributions of fine particle sulfur from the 1990 study, based on data acquired by the LPI and by X-ray fluorescence analysis of the fine particle filters from the AVSI sampler, were within the variability of the SCENES data collected at Hopi Point in 1985 through 1988 (see Section 7.4.2 of the August Status Report).
- The cumulative frequency distributions of fine particle mass measured at both Hopi Point and Glen Canyon show generally higher fine particle mass concentrations in January and February, 1990 than do the cumulative frequency distributions from SCENES for 1985 through 1988. The use of a 3.7 μm cutpoint may have contributed to this difference (see Section 7.4.2 of the August Status Report).
- The cumulative frequency distributions for light scattering by particles at Hopi Point for data collected during January and February, 1990 show higher values than during SCENES for percentiles above 30%. A change in the measurement method in the 1990 study to reduce the heating of the sample may have contributed to this difference (see Section 7.4 of the August Status Report).

8. DETERMINISTIC MODELING

A deterministic air quality model was assembled which simulates the transport, transformation, and deposition of emissions of SO₂. The model is designed to account for SO₂ emissions from all sources within a 1350 X 1350 km grid centered around NGS (which includes northern Utah, southern Arizona, and southern California). The rate of sulfate formation computed in the model is dependent on observed atmospheric conditions, including, most notably, the liquid water content (indicating the presence or absence of clouds). The air quality model will be used to determine the impact of NGS SO₂ emissions on sulfate levels during two episodes. The field study data are being used as input to the model.

The model was first used to simulate the period between January 18, 1990 and January 23, 1990. Three-dimensional wind fields were produced using the PSU/NCAR MM4 meteorological model, which utilizes four-dimensional data assimilation, incorporating observational data into a prognostic meteorological model simulation. The resulting wind fields "drive" the transport component of the air quality model.

The air quality model was first run in an "inert" mode, with the chemical mechanism and deposition turned off, in order to observe the transport of "emittants" from NGS and other sources, and to assess the impact of these emittants at Hopi Point. The model run showed that during January 18, a circular pattern of air flow was carrying NGS emissions toward the west. Emissions from northern Utah were being transported toward the southwest, whereas emissions from southern Arizona (smelters) were carried toward northeast Arizona early in the day and eastward later in the day. Southern California emissions were transported in a southeast direction all day. As January 19 began, the winds in the vicinity of NGS shifted slightly toward the south and then directly toward the east, drawing air masses across Hopi Point which were made up of (1) mostly aged emissions from northern Utah, (2) a small amount (about 20 percent) of NGS emissions, and (3) possibly a very small (but aged) contribution from southern Arizona. By the afternoon of January 19, the air mass reaching Hopi Point contained negligible contributions from NGS. This is also when the observed sulfate concentrations and light extinction levels were increasing. By the end of January 19, steady, strong winds were carrying material from NGS directly to the east, and material from northern Utah was being advected southward and then eastward. It appears that almost all the SO₂ emissions impacting Hopi Point during the first half of January 20 were due to sources in northern Utah.

At about the middle of January 20, a shift was observed to take place. Air masses over the south and east of Utah and over NGS and Hopi Point slowed and then for about the next 24 hours flowed steadily toward the southwest and south. This airflow brought SO₂ emissions from northern Utah southward across NGS and the directly to Hopi Point. This shift can be observed by examination of the contour plots in Figures 8-1, 8-2, and 8-3 showing the "inert" SO₂ contours and wind vectors for 2300 MST on January 19, and 1100 and 2300 MST on January 20.

SO2 (PPM)*1.0E-5 WITH WIND VECTORS AT LEVEL 4
2300 MST 900119

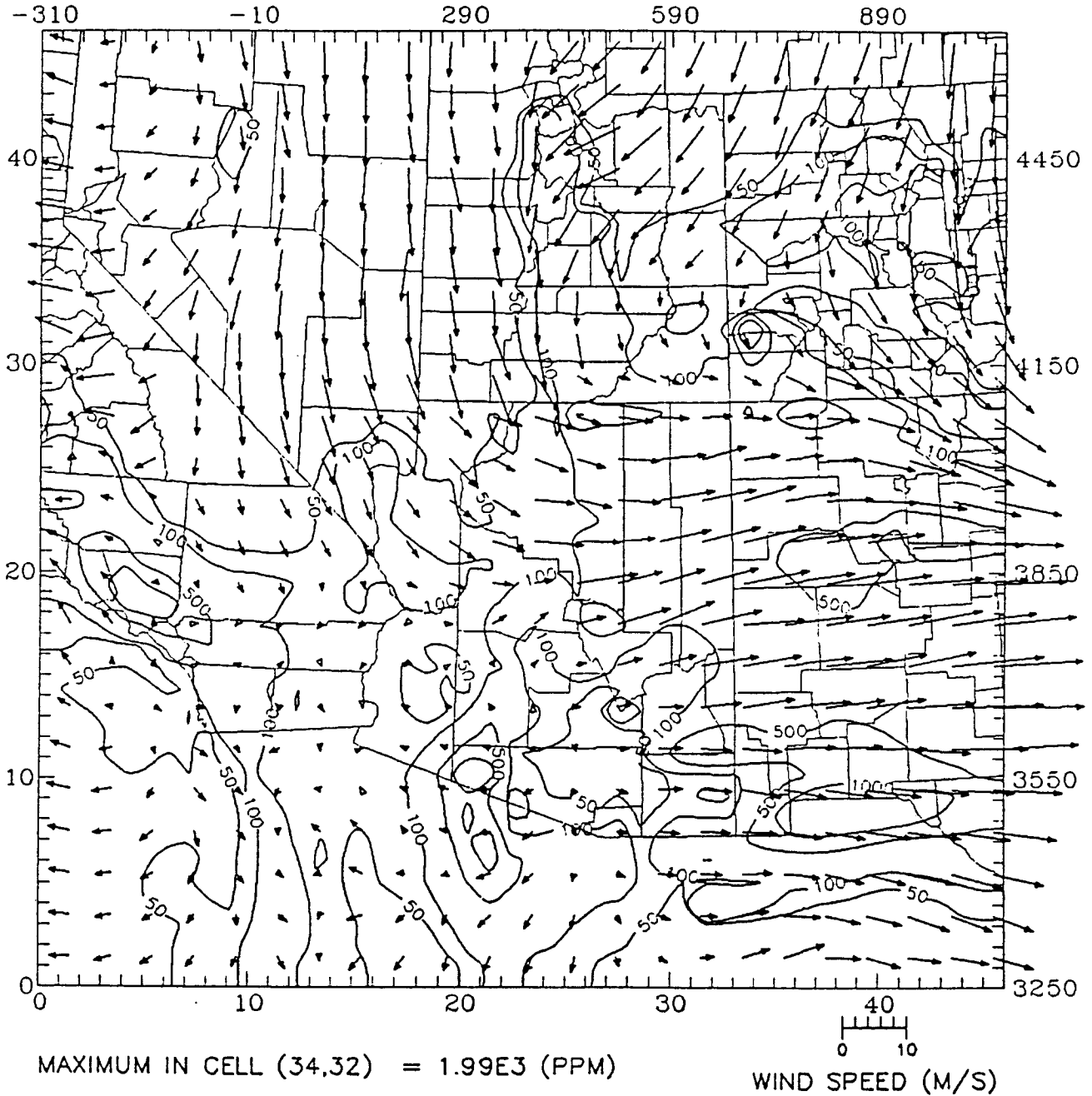


Figure 8-1. SO₂ Concentrations Predicted by Inert SO₂ Model Showing Wind Vectors for 2300 Hours 19 January 1990.

SO2 (PPM)*1.0E-5 WITH WIND VECTORS AT LEVEL 4
1100 MST 900120

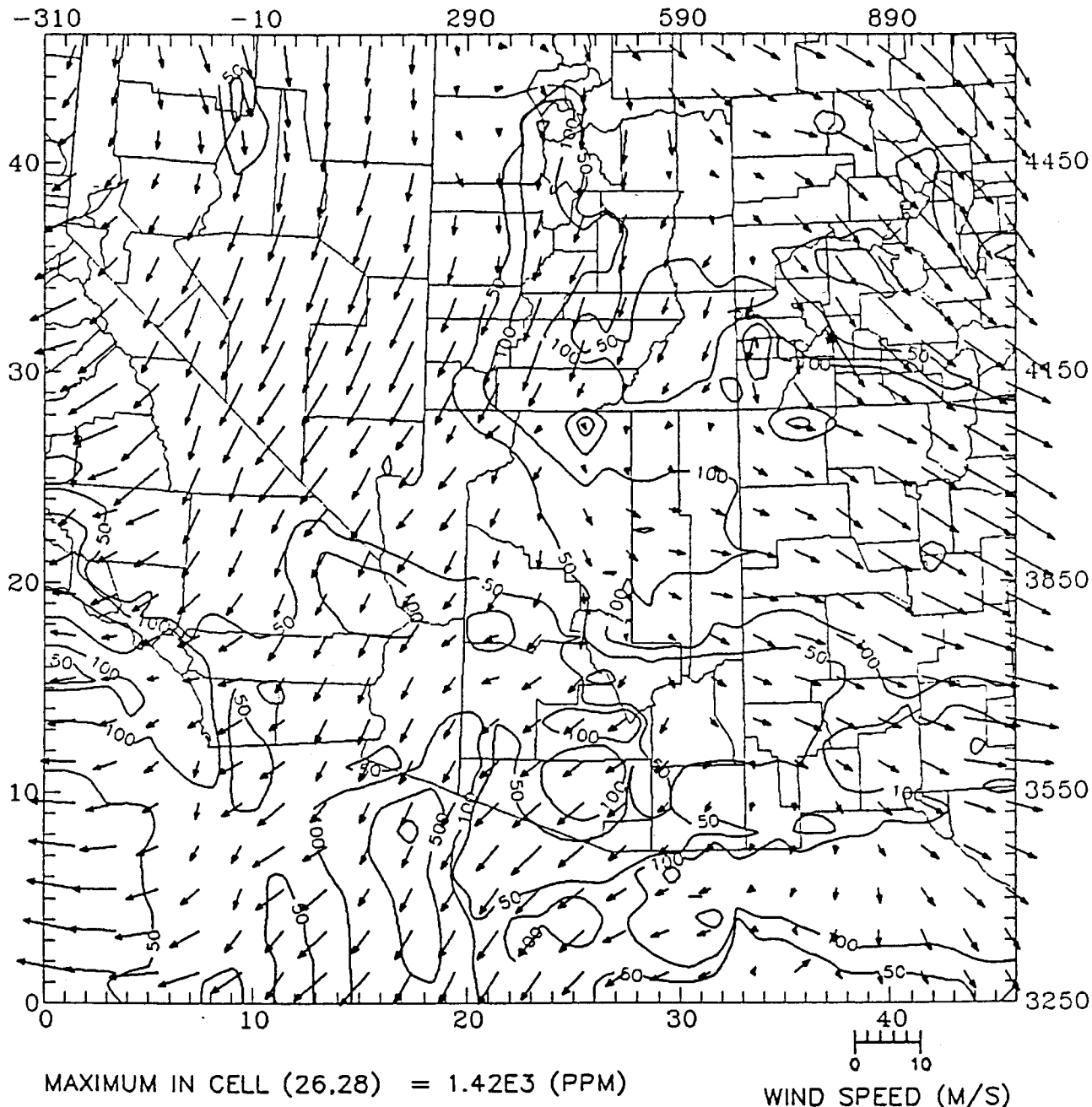


Figure 8-2. SO₂ Concentrations Predicted by Inert SO₂ Model Showing Wind Vectors for 1100 Hours 20 January 1990.

SO₂ (PPM)*1.0E-5 WITH WIND VECTORS AT LEVEL 4
2300 MST 900120

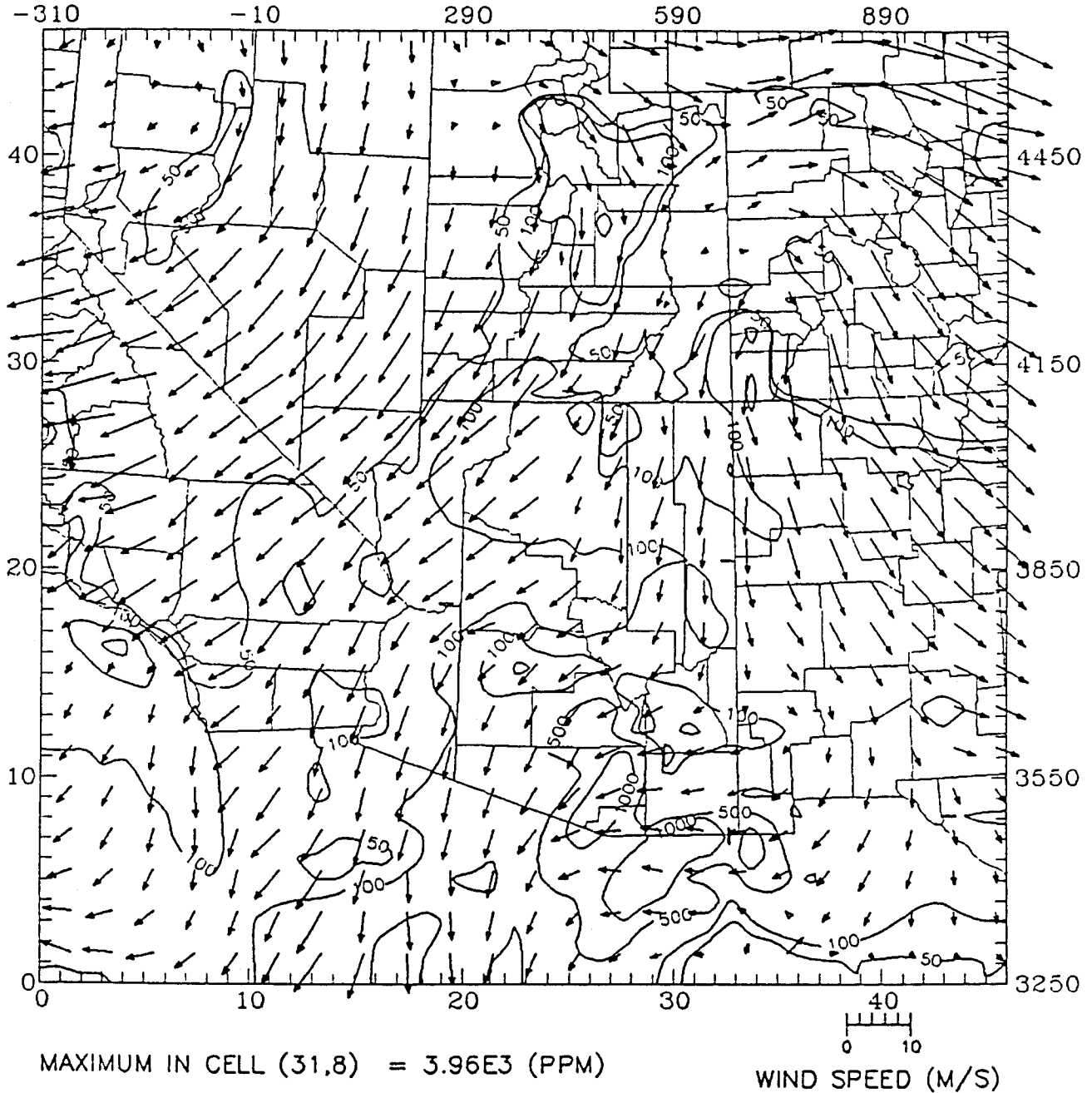


Figure 8-3. SO₂ Concentrations Predicted by Inert SO₂ Model Showing Wind Vectors for 2300 Hours 20 January 1990.

The inert model was also run with the NGS SO₂ emissions turned off to detect the impact of NGS emissions. Figure 8-4a shows the results of these model runs. NGS contributed about 20 percent of the emittants reaching Hopi Point early on January 19. However, this time period was not marked with an increase in measured sulfate and, as can be seen on Figure 5-4, the particle light scattering was very low. Later in the morning, the measured sulfate levels rose and light scattering increased markedly; however, by noon the modeled contribution of emittants due to NGS was only 3 percent.

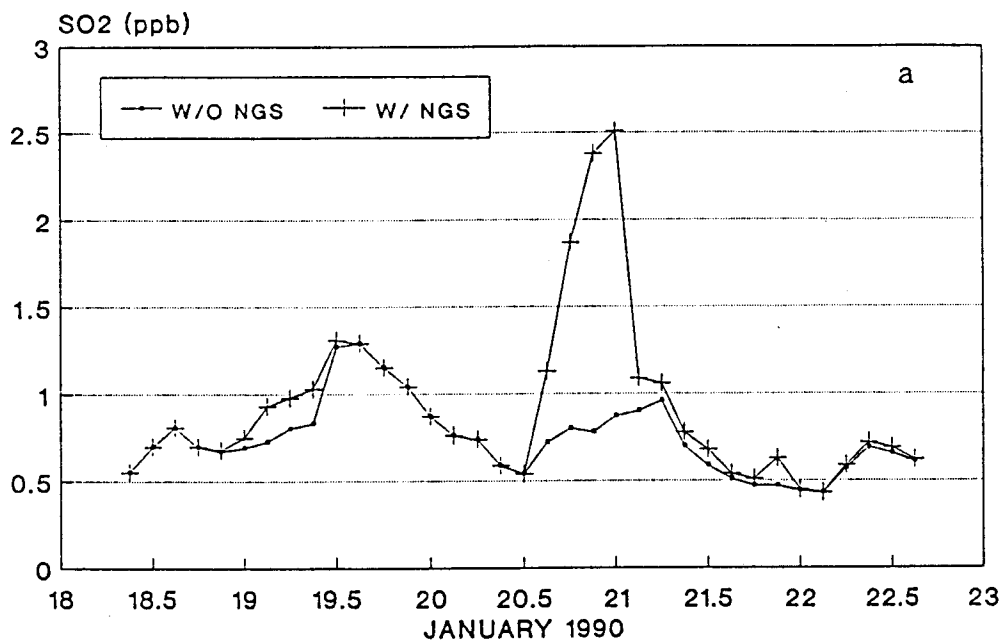
Between noon of January 19 and noon of January 20, the sulfate concentration at Hopi Point was roughly constant at about 1.5 µg/m³ (ranging from 1.2 to 1.7). During this time there was no impact due to NGS, yet the particle light scattering was observed to be at its peak (for this five-day episode).

After noon on January 20, the shift began to carry air masses from NGS south and southwest toward Hopi Point. Figure 8-4 shows a large impact due to NGS emissions during the latter half of January 20 and early on January 21 (over 65 percent of the "inert" SO₂ was from NGS during the last few hours of January 20). Two other observations can also be made during this period. First, sulfate concentrations increased to about 2.5 µg/m³ at the end of January 20 (see Figure 8-4b). Second, particle light scattering decreased rapidly between noon on January 20 and noon on January 21 (see Figure 5-4) with a small secondary peak occurring late on January 20. The high level of sulfate which arrived at the same time that particle light scattering was low is an indication of non-aqueous phase sulfate formation. It can be seen on Figure 5-7 that humidity levels at Hopi Point decreased substantially during this period.

For the remainder of this modeling episode, NGS contributed a small or negligible fraction of the SO₂ emittants reaching Hopi Point (see Figure 8-4a). A second, lower, sulfate peak was observed during January 22 (also seen at Desert View); however, NGS contributed very little and the light scattering due to particles was very low. The model results were also examined at Desert View with similar conclusions (see Figure 8-5).

The model was also exercised with a simple linear chemical mechanism to account for the transformation of SO₂ "emittants" into sulfate. Although the chemical mechanism is a much simpler version of the detailed chemical mechanism, results from these model runs (including the effects of deposition) for this episode indicate very good agreement between observed and predicted sulfate concentrations, especially at Hopi Point (see Figure 8-6b). Figure 8-6a shows the effects of removing NGS SO₂ emissions on sulfate concentrations at Hopi Point. The increase in sulfate which was observed late on January 20 had a significant contribution from NGS. At about 1600 MST on January 20, the sulfate prediction with NGS emittants included begins to deviate markedly from the predicted sulfate without NGS emittants, reaching a peak near the end of January 20. The NGS contribution decreased rapidly so that by the daylight hours on January 21, the contribution was very low. At the peak, the NGS contribution to Hopi Point sulfate concentrations was between 50 and 60 percent, however this high level of NGS contribution was only present for a few hours late on January 20. The average NGS contribution

INERT SO₂ MODEL Hopi Point



SO₄ OBSERVED Hopi Point

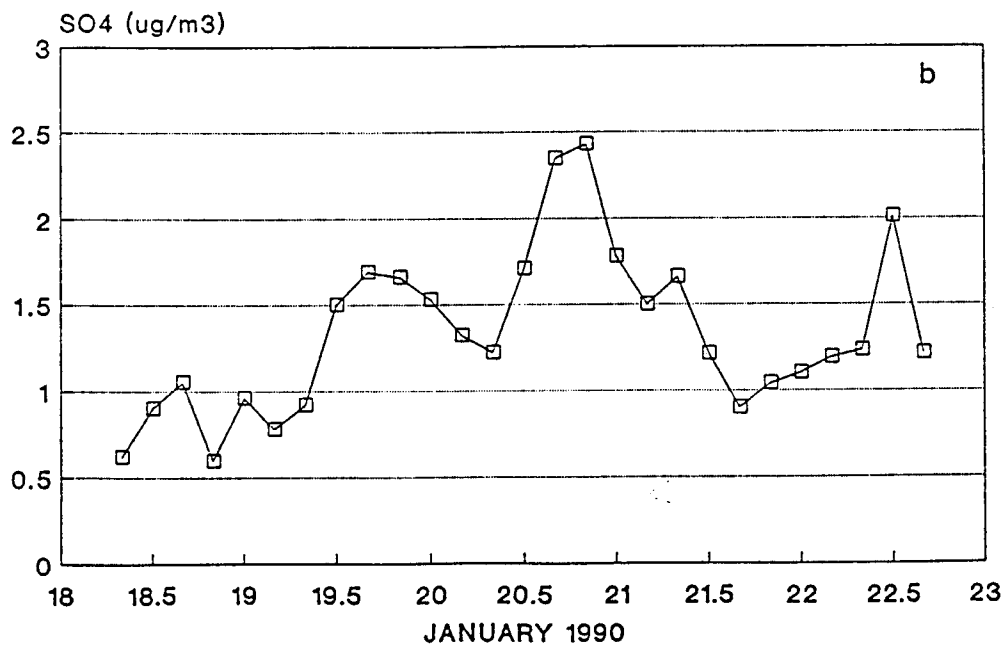
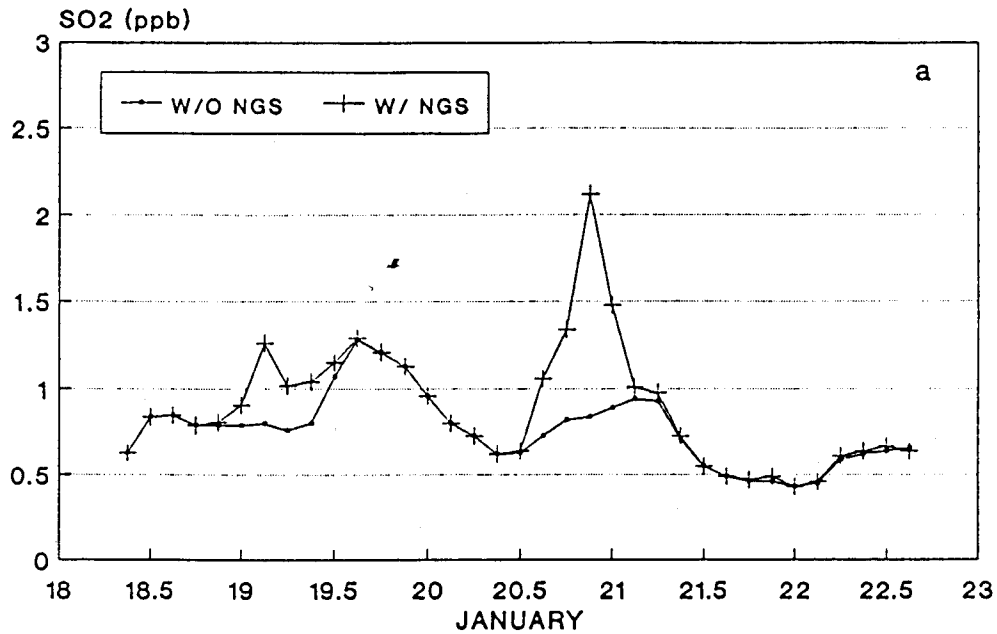


Figure 8-4. (a) SO₂ Concentrations Predicted by Inert SO₂ Model at Hopi Point: With and Without NGS SO₂ Emissions; (b) SO₄ Measured at Hopi Point (AVS1 Sampler).

INERT SO₂ MODEL Desert View



SO₄ OBSERVED Desert View

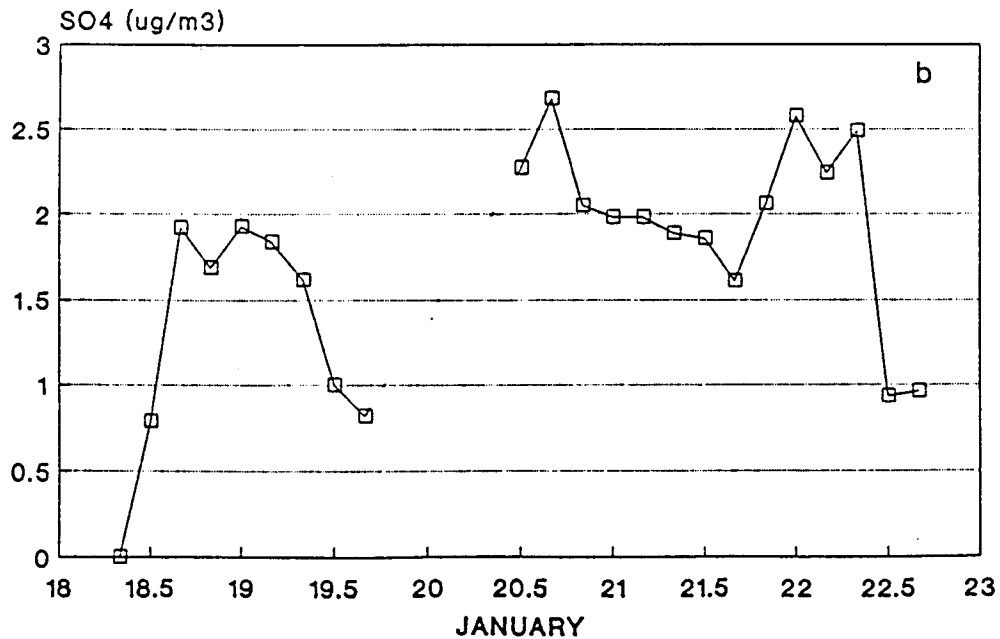


Figure 8-5. (a) SO₂ Concentrations Predicted by Inert SO₂ Model at Desert View With and Without NGS SO₂ Emissions; (b) SO₄ Measured at Desert View (AVS1 Sampler).

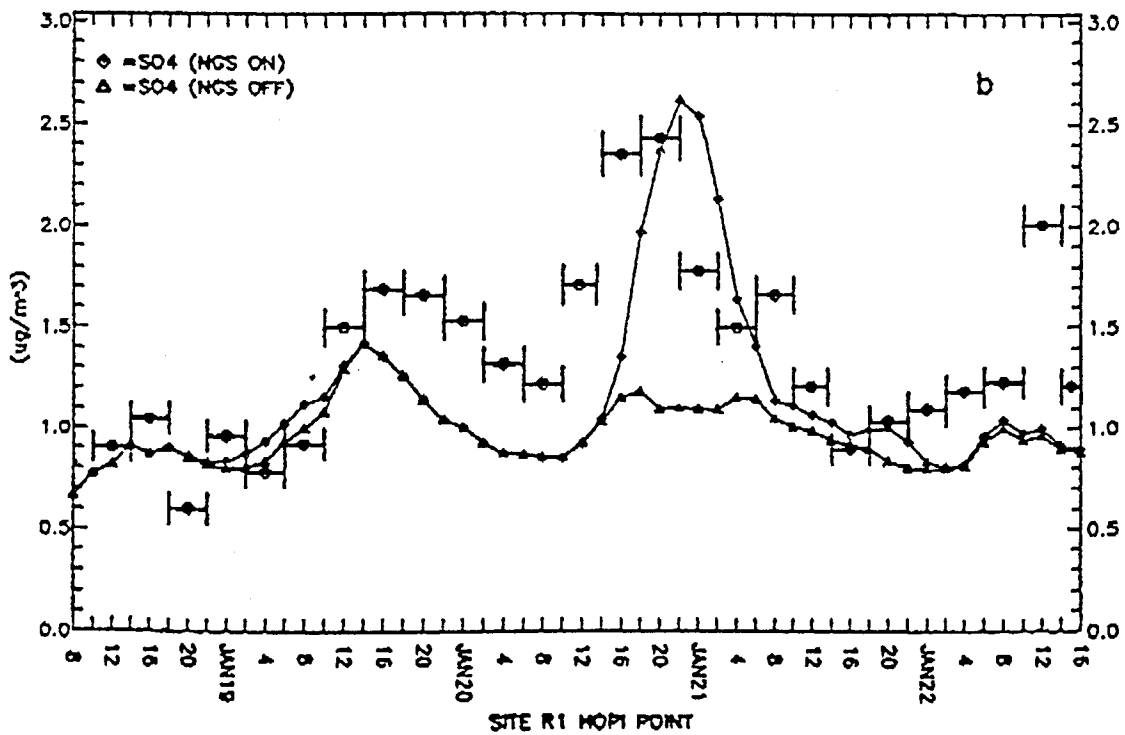
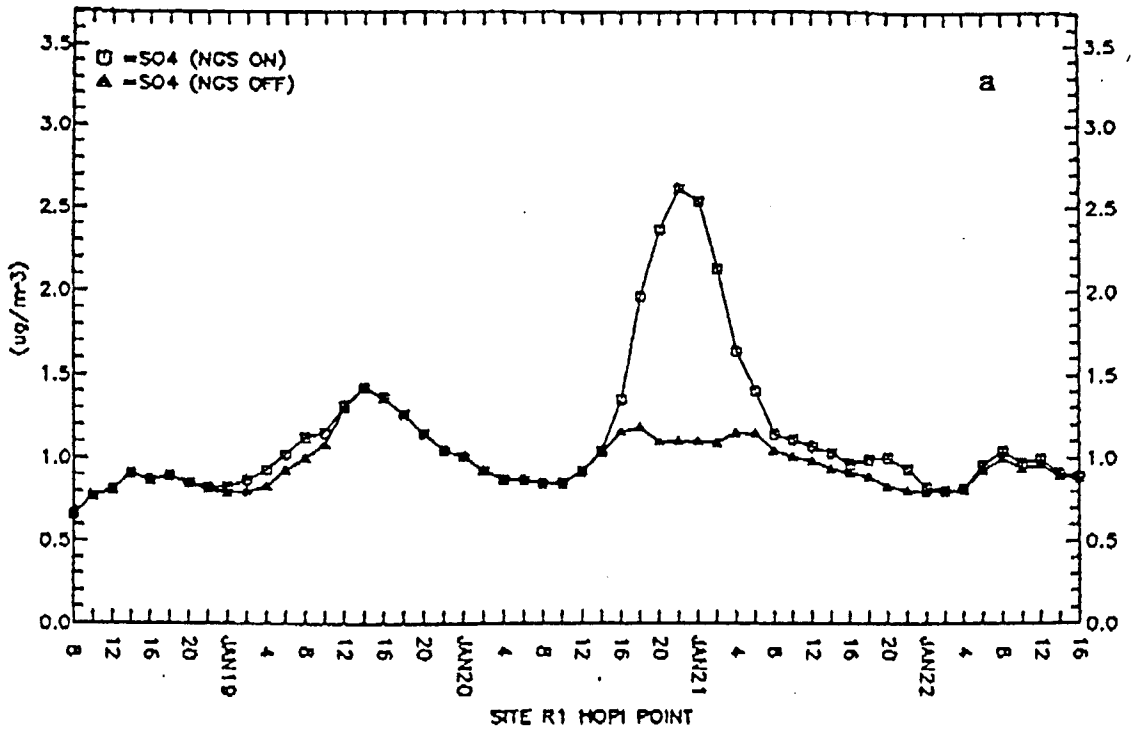


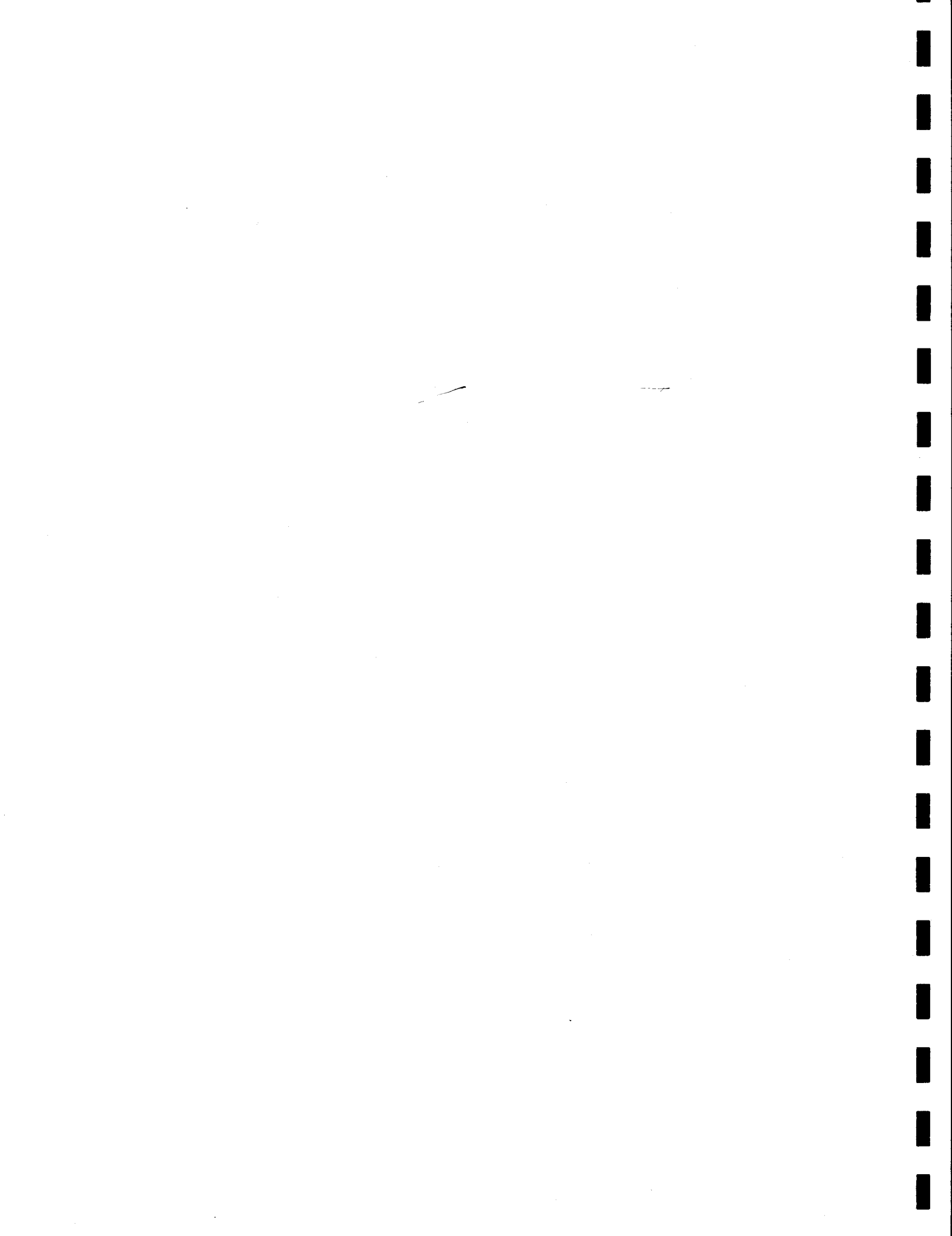
Figure 8-6. (a) Sulfate Concentrations Predicted by Linear Chemistry Model at Hopi Point With and Without NGS SO_2 Emissions; (b) Same as (a), Except Including SO_4 Measured at Hopi Point (AVS1 Sampler). Vertical bars represent measurement uncertainty; horizontal bars indicate averaging period for measurement.

to sulfate during the 24-hour period beginning on noon of January 20 was less than 30 percent of the total sulfate at Hopi Point.

A more detailed chemical mechanism, accounting for the "full" chemistry in the atmosphere, will be incorporated into the model to further refine the estimate of the contribution to sulfate concentrations due to NGS emissions. When the full chemistry model runs are completed, the effect of controlling NGS SO₂ emissions on sulfate concentrations at Hopi Point will be determined for this January modeling episode and also for a second episode (February 26 to March 5).

From the deterministic modeling to date of the January 18 to 23, 1990 episode and by comparison of the model results with the measured sulfate concentration at Hopi Point, several observations can be made.

- During all but one day during the episode between January 18 and 23, 1990, SO₂ emissions from NGS had little impact on sulfate levels at Hopi Point.
- NGS contributed about 20 percent of the "inert" SO₂ emittants that arrived at Hopi Point early on January 19; however, measured sulfate levels were not observed to increase during this time and particle light extinction remained low.
- The SO₂ emissions from NGS contributed a large portion of the emittants that arrived at Hopi Point during only one period, between noon on January 20 and early on January 21. Emissions from NGS contributed up to between 50 and 60 percent of the peak sulfate levels observed late on January 20. The level of NGS contribution to sulfate at Hopi Point was much lower for much of this period, with an average contribution for the 24-hour period beginning on noon of January 20 of less than 30 percent.
- While sulfate levels were observed to increase about 40 percent during the aforementioned period, light scattering by particles was observed to decrease rapidly. This indicates that the sulfate was formed outside of clouds and had a much smaller effect on light extinction than sulfate formed in clouds.
- Results from the model with linear chemistry indicate good agreement between model sulfate predictions and observations.



9. QUALITY ASSURANCE AND UNCERTAINTIES

The data analysis has included work to evaluate the accuracy and precision of the data. Some preliminary results of these analyses are presented here.

Performance and system audits were performed for most measurements as part of the field program, and are listed in the August Status Report.

9.1 PERFLUOROCARBON TRACER DATA

The perfluorocarbon tracer (PFT) release, sampling, and gas chromatographic analysis included many quality assurance and quality control steps. A partial list of them follows:

- The rate of PFT release was determined both from flow measurements and from changes in the weight of the supply cylinder.
- Grab samples of flue gases were collected and analyzed for both sulfur dioxide and tracer.
- Tracer sampling was conducted near NGS to check for fugitive leaks.
- Dynamic blanks were prepared in San Diego, analyzed, shipped to the field and placed in the samplers, then returned for analysis.
- Quality Assurance spiked samples were mixed with the field samples.
- Collocated samplers were operated at three sites: Hopi Point, Desert View, and Glen Canyon.
- Additional hour-average samples were collected at Hopi Point at selected times.
- Lot blank and lot reference samples were analyzed with each lot to assure the blank and span calibrations of the analytical equipment.
- Three percent of the samples are being re-analyzed. Half of these were selected randomly and half will be selected to obtain replicate data during times of special interest.
- Quality assurance audits were performed during the field operations.

These procedures are producing a large data base which will be used to quantify the accuracy and precision of the PFT data. This work is still in progress, so only preliminary information is presented here.

Figures 9-1 and 9-2 show scatter diagrams for the PFT concentrations measured by the collocated samplers at Hopi Point. For all four tracers, the side-by-side samplers gave results which are not correlated with each other. Similar results were obtained at Desert View, where the observed PFT

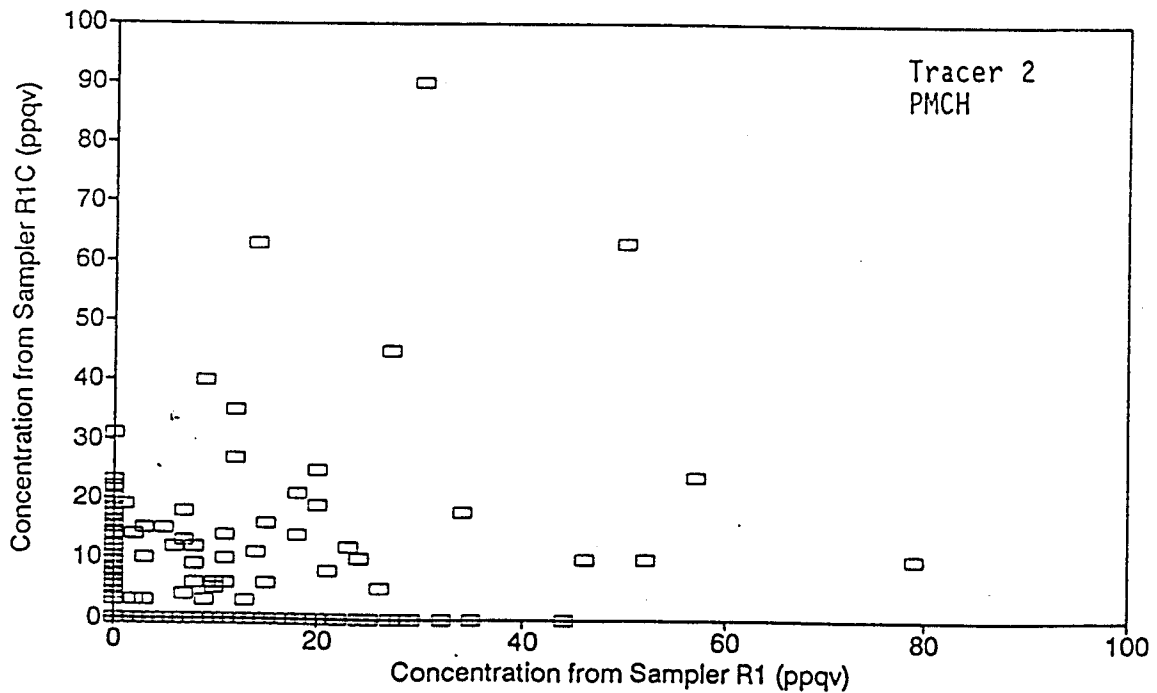
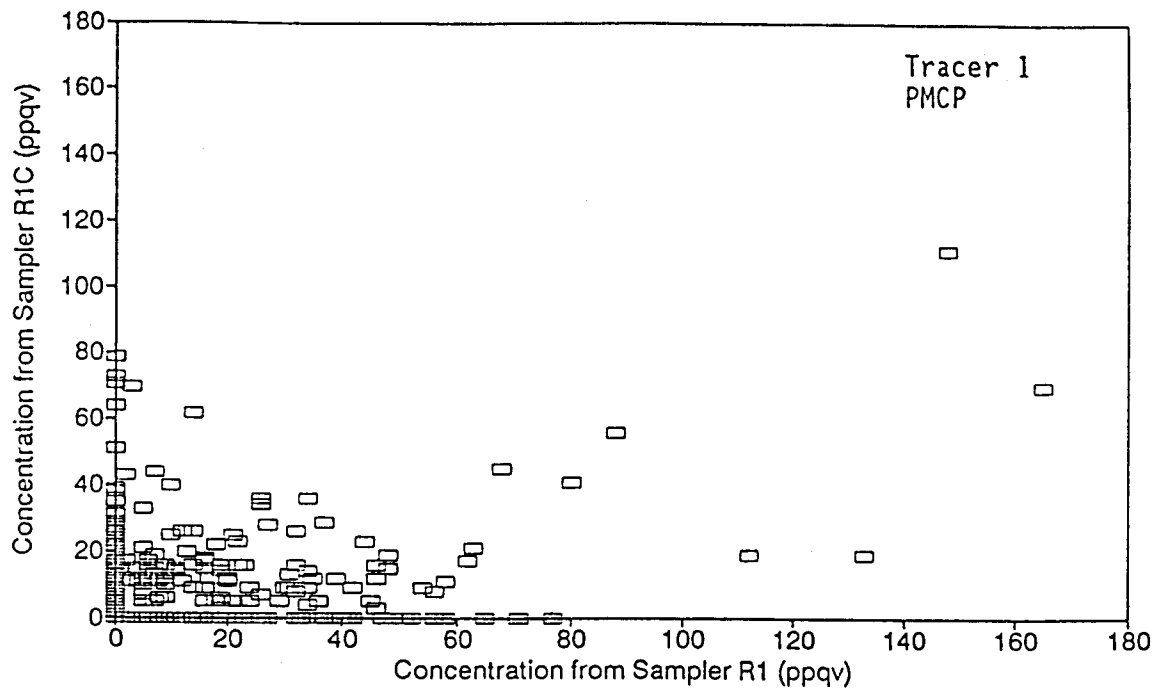


Figure 9-1. Scatter Diagrams Comparing Perfluorocarbon Tracer Concentrations Measured by Collocated Samplers at Hopi Point for Tracer 1, PMCP, and Tracer 2, PMCH.

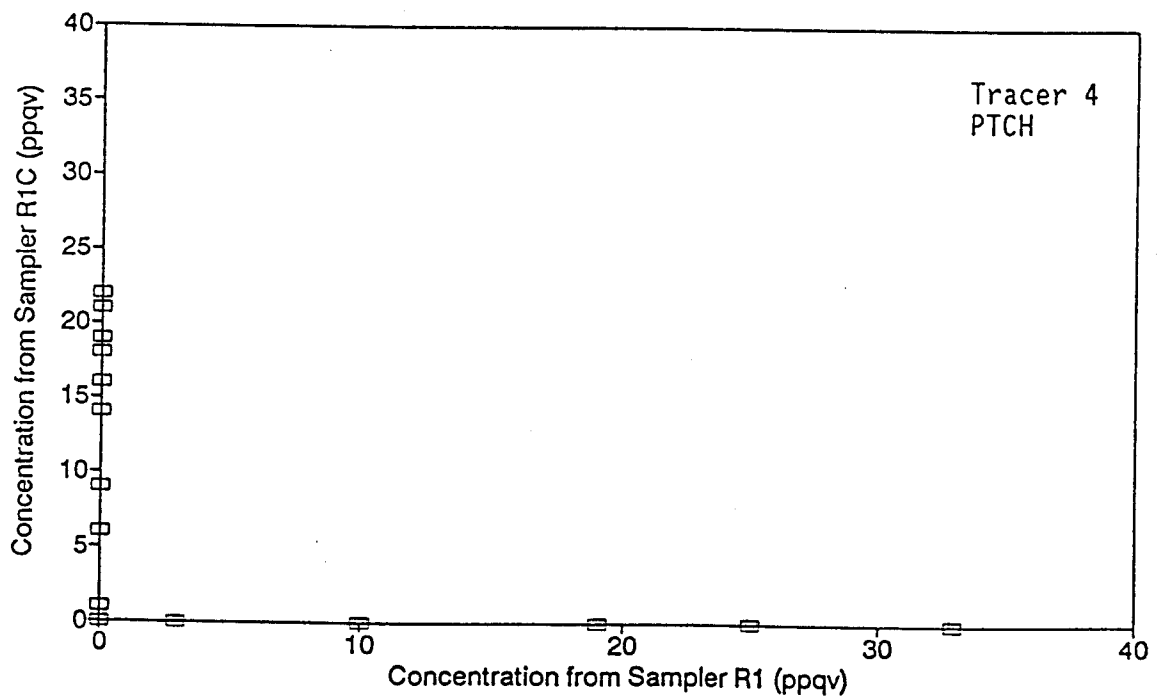
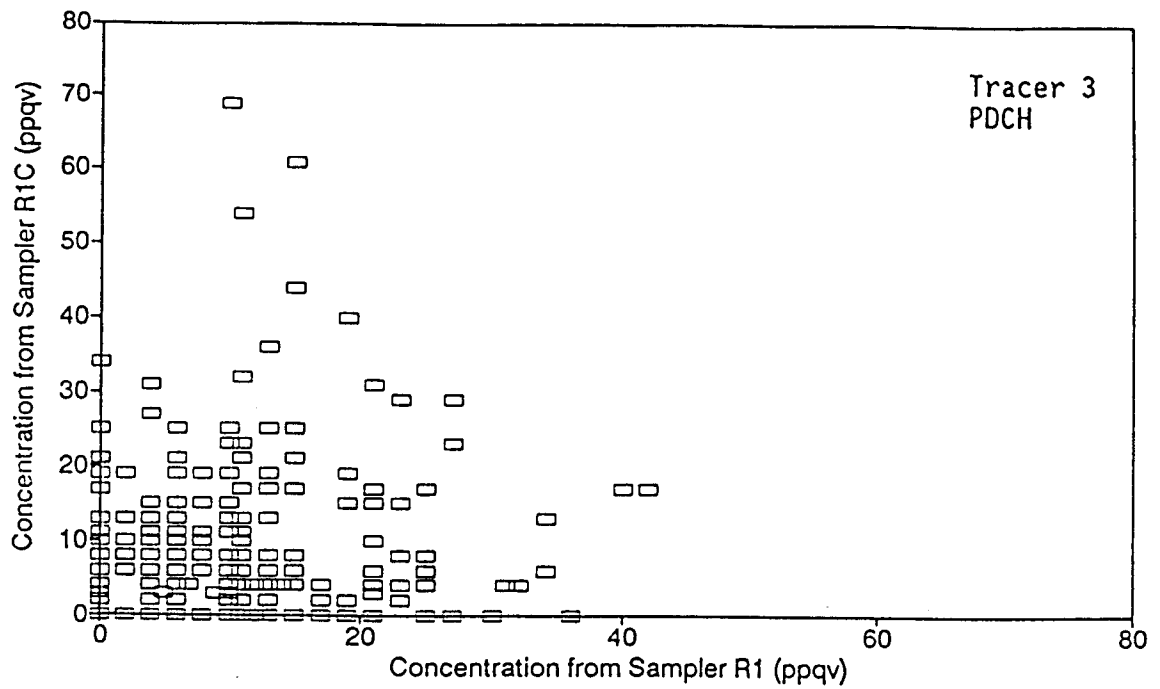


Figure 9-2. Scatter Diagrams Comparing Perfluorocarbon Tracer Concentrations Measured by Collocated Samplers at Hopi Point for Tracer 3, PDCH, and Tracer 4, PTCH.

concentrations fell in a similar range. Tracer concentrations extending up to about 800 ppqv were observed at Glen Canyon, where it was found that the collocated PFT concentrations showed good agreement for concentrations above 100 to 400 ppqv, depending on the tracer. These data indicate that individual measurements of the PFT concentrations cannot be used to quantify the concentrations of the NGS emittants at Hopi Point.

The animation described in Section 4 shows that non-zero PFT concentrations are frequently observed at the Receptor Sites when the NGS emissions are certainly being transported elsewhere. Since the NGS emittants are probably present at Hopi Point about 21% of the time, this indicates a positive bias PFT data.

Further evidence for the positive bias can be found in the cumulative frequency distribution of χ/Q values for the dilution of the NGS emittants derived from the PFT data at Hopi Point during the Category 3 periods, when the emittants probably were not present at Hopi Point. These data are shown in Figure 5-10. The similarity between the χ/Q curves for times when the NGS emittants were probably absent and probably present at Hopi Point indicates that all the PFT data at Hopi Point probably contain a positive bias from noise.

The finding that the collocated sampler data are not correlated and the likelihood of a positive bias in the PFT data indicates that single data points for the PFT concentrations cannot be used in attribution calculations such as the DMB analysis used in WHITEX. The possibility that averages of the tracer data and averages which include other data, such as sulfur dioxide concentrations, can be used for attribution calculations is now being examined.

In contrast to these shortcomings, the PFT data sometimes appear to provide an excellent quantification of the concentrations of the NGS emittants down to concentrations below 50 ppqv. Examples appear in Chapter 11 of the August Status Report (Richards et al., 1990). Therefore, it appears that accurate PFT concentration measurements are embedded within the noise.

Uses of the tracer data which are believed to be valid include:

- Confirmation of the meteorological calculations of the locations of the NGS emittants. When combined with the meteorological and sulfur dioxide data in the animation, the tracer data play a crucial role in confirming the validity of the classification of the measurement periods according to the presence or absence of NGS emittants at Hopi Point.
- Quantification of the concentrations of the emittants when the PFT concentrations are above a threshold which has yet to be determined. Preliminary estimates are that the thresholds will be different for the different tracers, and may be in the 100 to 300 ppqv range.

The possibility of lowering these thresholds through averaging the data is being explored.

9.2 SURFACE AIR QUALITY AND OPTICAL DATA

The surface particle and gaseous air quality data and optical data collected during the NGS Visibility Study have been submitted to independent quality assurance audits and various internal quality control checks throughout the project. Estimates of precision are being entered in the surface database. The data have been processed and are continuing to be validated through Level II.

9.2.1 QC/QA Tests

The following tasks were performed during the field study to minimize uncertainties in particle and continuous data:

- AVS sampler system check before dispatching the samplers to the monitoring stations;
- "Shakedown test" and data analysis performed during the period from December 18 to December 22, 1989 at seven sites, including Hopi Point, Meadview, Hanksville, Glen Canyon, Vermillion Cliffs, Tusayan and Kaiparowits Plateau. During the shakedown, the field and laboratory operation in Flagstaff were audited internally and by the QA contractors;
- Pre- and post-study calibrations;
- External QA audits three times;
- SRP's independent QC checks periodically during the field study;
- Internal QC, in which all sites were visited 3-5 times each during the study period;
- Cross comparison of laboratory analysis data and review of laboratory blanks and replicate analyses;
- Collocated particle samplers at Hopi Point (R-1) and Indian Gardens (R-2), and 24-hour samplers at Hopi Point;
- Manifold Leak Tests on each filter manifold at the Flagstaff field laboratory after filter loading;
- Special tests of flowrate, and particle and gas loss to evaluate measurement uncertainties. Particle loss and cut-size efficiency at a flowrate lower than the original design rate was investigated. The cut-size of the fine particle samplers was estimated to be approximately 3.7 μm ;
- Internal audit for filter and data processing; and
- Contracted QA audit on filter handling and data processing. A senior member of the external QA team conducted performance audits for filter loading, manifold leak check systems and filter handling at the

Flagstaff field operation center during the field study. He also audited data management and processing.

9.2.2 Validation and Estimation of Precision

The data have been processed using detailed field logs and have been flagged against Level I screening criteria. Precision of particle data has been estimated using collocated sampling data and other quality control test data. Table 9-1 is a summary of the precision estimates for several of the key surface variables. The particle data precision was estimated for the four-hour samplers which have the greatest variability and uncertainty. Precision has been estimated for each particulate observable using collocated data collected at sites R-1 and R-2. The collocated data for sulfur (XRF-S) and SO₂ are displayed graphically in Figures 9-3 through 9-6. The data shown have been screened for those values lying outside of three standard deviations of the collocated differences.

Of 664 paired XRF-S observations in the Hopi Point and Indian Garden data sets, 11 were identified as outliers and are now being investigated. For mass, 18 of 693 pairs are outliers and for SO₂ there are 23 of 650. Some of these pairs repeat among the different variables; many do not. These data will be flagged after investigation either as "valid following Level II investigation," "suspect without evidence to invalidate," or "invalid for reasons discovered during the investigation." If there is no evidence that a screened value is invalid, it will be included in the final collocated precision calculation.

For continuous gas data, uncertainty was estimated using the data derived from EPA-recommended procedures for precision checks. For the nephelometer (b_{sp}) data, precision was derived from Freon-12 and zero checks throughout the study. Resulting precision estimates are shown in Table 9-1.

Table 9-1. Estimated Precision in Surface Air Quality and Optical Data

Measurement	Sites	Estimated Precision
Light Scattering by Particles, b_{sp}	R1 Hopi Point	0.6 Mm^{-1} + 10% of reading
	R2 Indian Gardens ^a	2 Mm^{-1} + 9% of reading
	R3 Desert View	0.7 Mm^{-1} + 9% of reading
Gas (O_3, SO_2, NO_x)	R1-R3	< 10%
SO_2 (filter)	All	30% ^b
XRF-Sulfur	All	12% ^b

a. No zero data were available at this site. Consequently, more uncertainty is introduced into those measurements.

b. Calculated using mean collocated value.

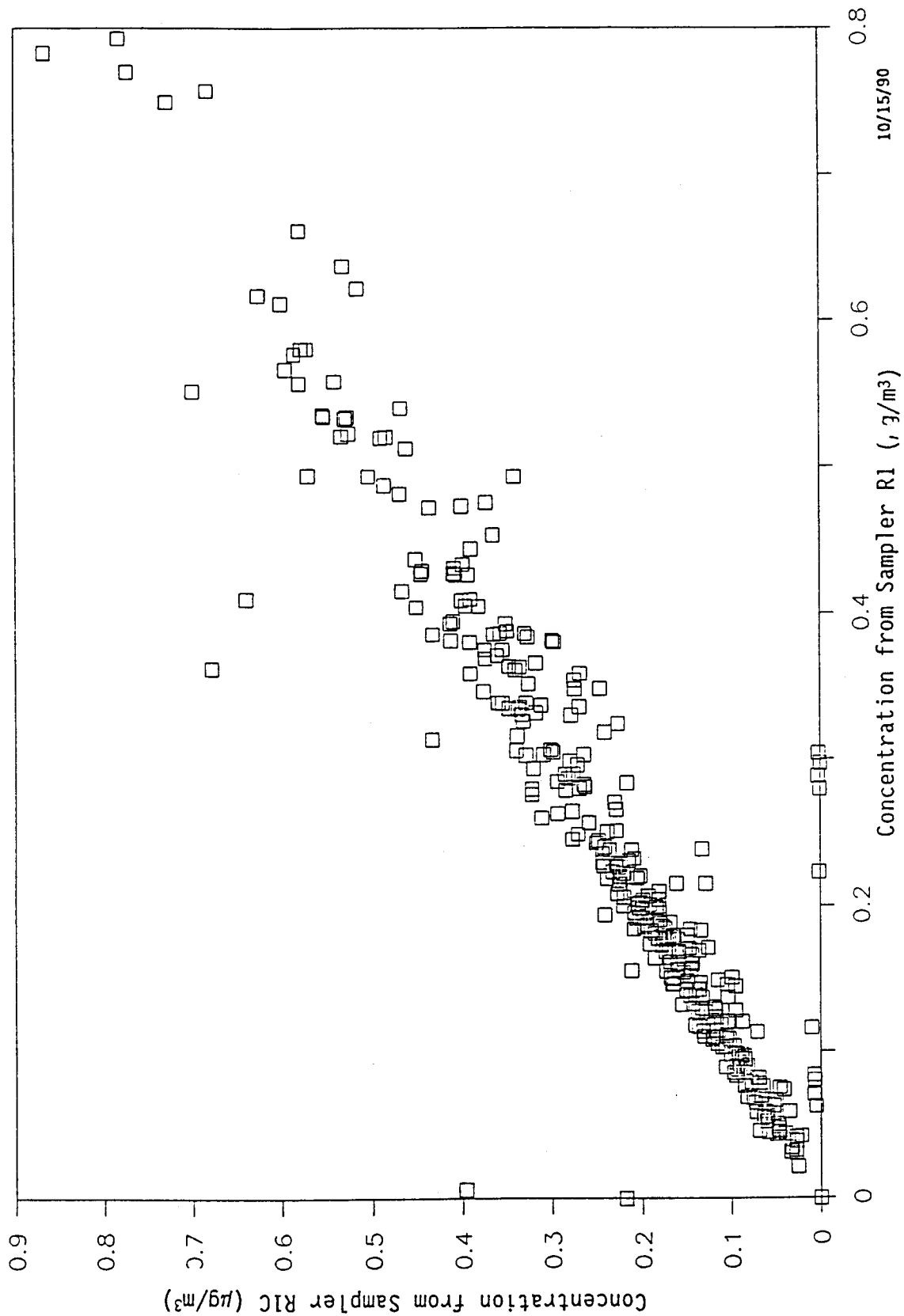


Figure 9-3. Scatter Diagram Comparing Fine-Particle Sulfur Concentrations Measured by Collocated Samplers at Hopi Point.

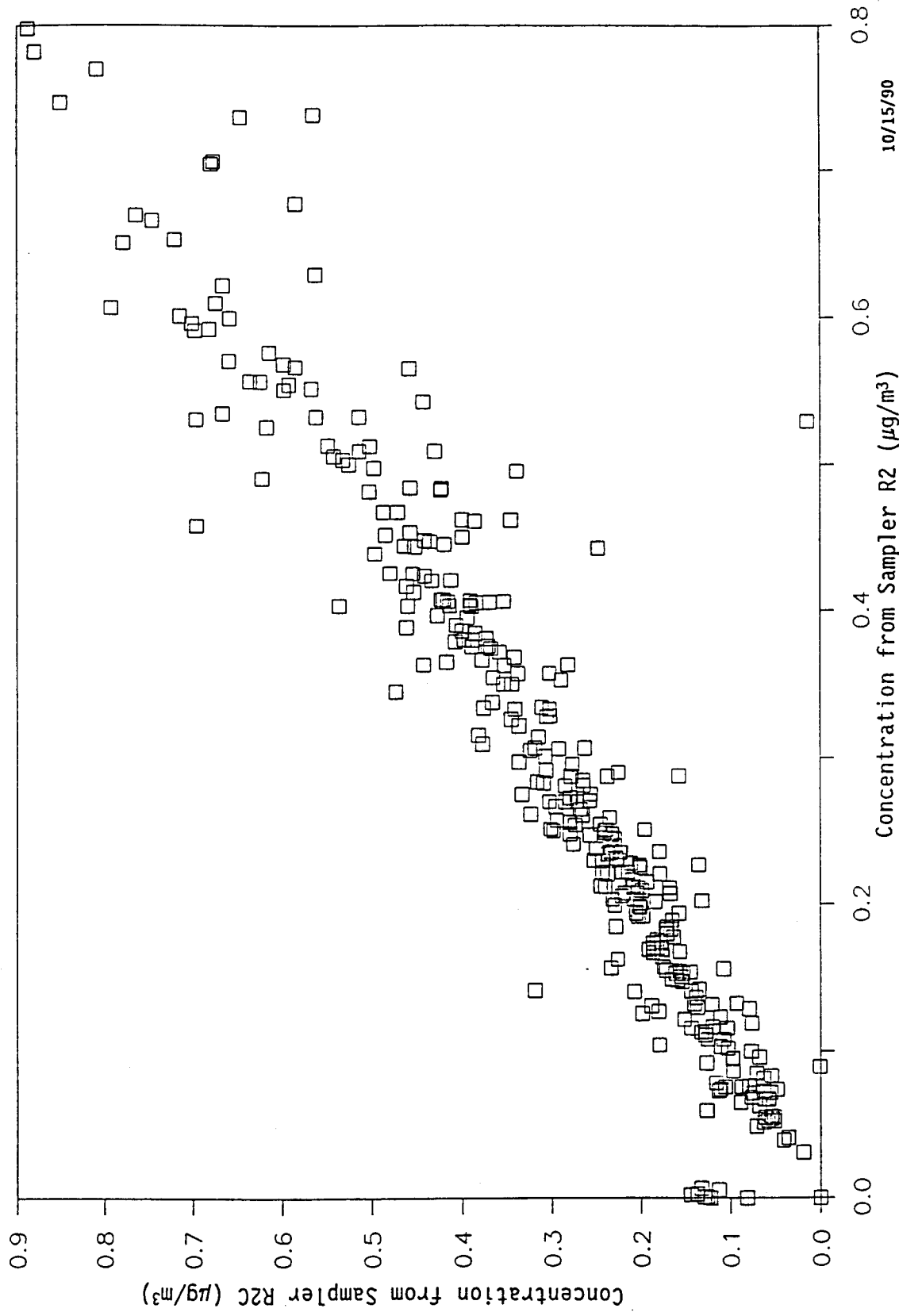


Figure 9-4. Scatter Diagram Comparing Fine-Particle Sulfur Concentrations Measured by Collocated Samplers at Indian Gardens.

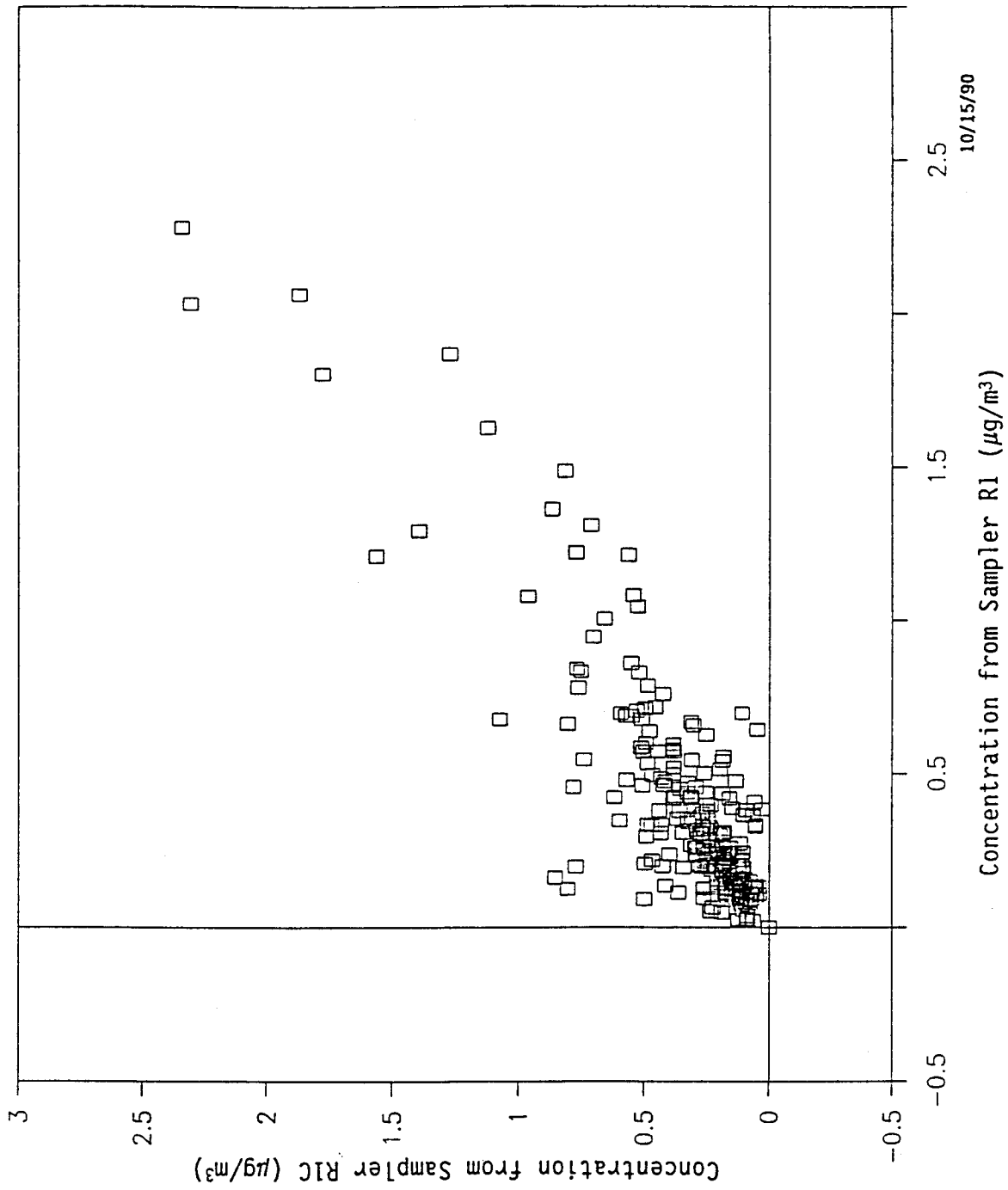


Figure 9-5. Scatter Diagram Comparing Sulfur Dioxide Concentrations Measured by Collocated Filter Samplers at Hopi Point.

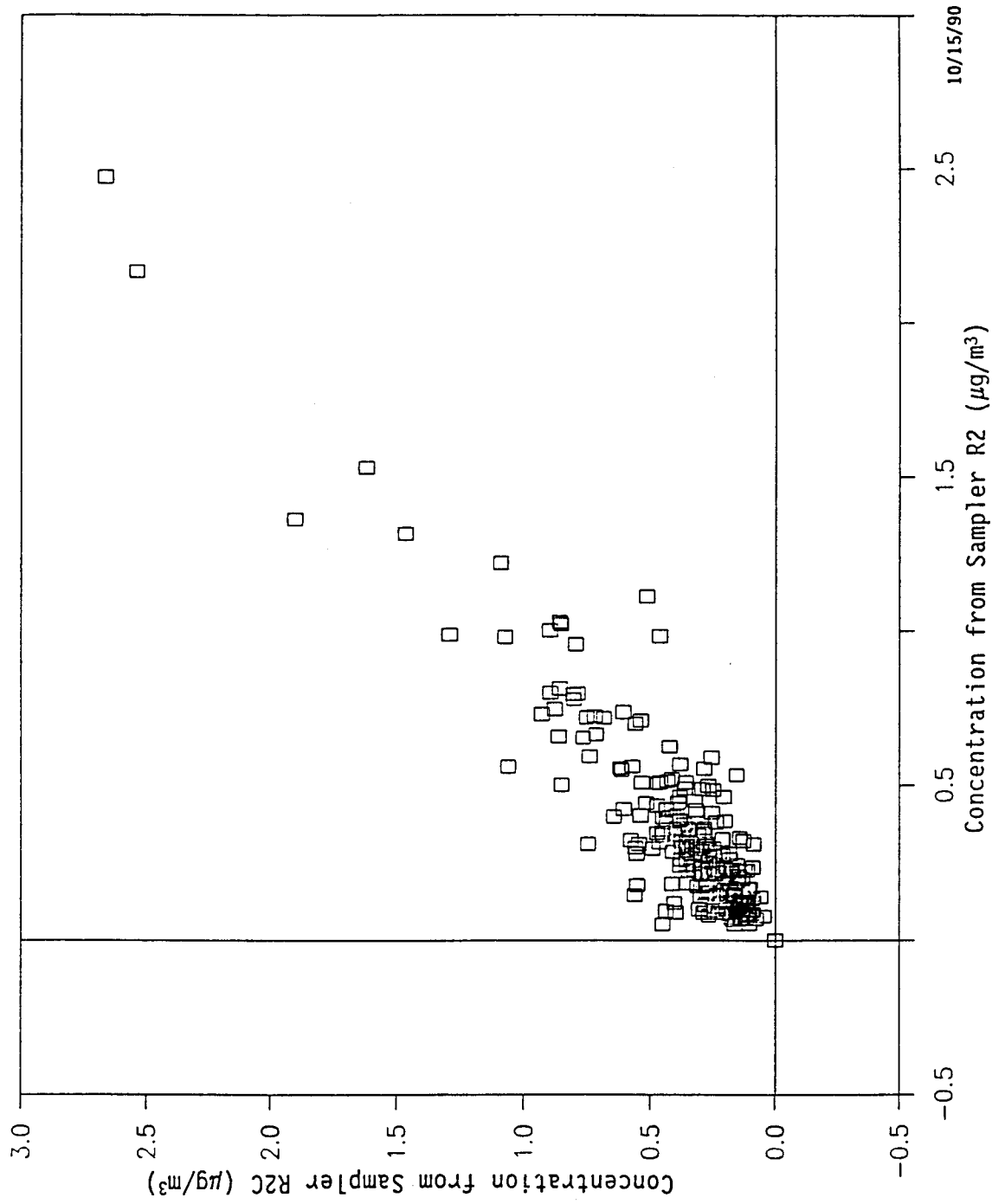


Figure 9-6. Scatter Diagram Comparing Sulfur Dioxide Concentrations Measured by Collocated Filter Samplers at Indian Gardens.



10. REFERENCES

- Anderson, J.A. and R.G.M. Hammarstrand (1988) Airborne Background Characterizations Upwind of the Page, Arizona Area: Program Summary and Data Presentation: Draft Final Report, STI #97020-805-FR, Prepared for Salt River Project, Phoenix, Arizona, April 1988.
- Covert, D.S., J. Heintzenberg, and H.C. Hansson Aerosol Sci. Technol. 12: 446-456.
- Davis, R.E. (1990) A Discriminant Analysis of January, 1989 to April, 1990 Rawinsonde Observations in the Western United States, Final Report. Submitted to Salt River Project by Depart. of Environmental Sciences, University of Virginia.
- Fang, C.P., P.H. McMurry, V.A. Marple, and K.L. Rubow (1990) Aerosol Sci. Technol. (in press).
- Friedlander, S.K. (1977) Smoke, Dust and Haze: Fundamentals of Aerosol Behavior, Wiley Interscience, New York.
- Goodin, William R., G.J. McRae and J.H. Seinfeld (1980) An Objective Analysis Technique for Constructing Three-Dimensional Urban-Scale Wind Field. J. Appld. Meteor. 19:98-108.
- Heisler, S.L. and S.K. Friedlander (1977) Atmos. Environ. 11:157-168.
- Hering, S.V. and S.K. Friedlander (1982) Atmos. Environ. 16:2647-2656.
- Hering, S.V. and P.H. McMurry (1990) Atmos. Environ. (in press).
- Hering, S.V., J.L. Bowen, J.G. Wengert, and L.W. Richards (1981) Atmos. Environ. 15:1999-2009.
- Kalkstein, L.S. and S.R. Webber (1990) A Synoptic Evaluation of the Winters of the WHITEX and NGS Study Periods: Are They Typical? Submitted to Salt River Project by the Center for Climatic Research, University of Delaware.
- Malm, W., K. Gebhart, D. Latimer, T. Cahill, R. Eldred, R. Pielke, R. Stocker, and J. Watson (1989) National Park Service Report on the Winter Haze Intensive Tracer Experiment, Final Report, December 1989.
- McMurry, P.H. and D. Grosjean (1985) Atmos. Environ. 19:1445-1451.
- McMurry, P.H. and M.R. Stolzenburg (1989) On the Sensitivity of Particle Size to Relative Humidity for Los Angeles Aerosols, Atmos. Environ. 23: 497-507.
- McMurry, P.H. and J.C. Wilson (1982) Atmos. Environ. 16:121-134.
- McMurry, P.H. and J.C. Wilson (1983) J. Geophys. Res. 88:5101-5108.

- Mie, G. (1908) Beitrage zur Optik trüber Medien, speziell kolloidaler Metallösungen. Ann. Physik 25, 377-445.
- Muller, R.A., G.E. Faiers, and J.M. Grymes (1990) Interpretation of Weather Types Over Northcentral Arizona January-February 1987 January-March 1990, Preliminary Report. Submitted to the Water Resources Management Office, Salt River Project.
- NRC (1990) Haze in the Grand Canyon: An Evaluation of the Winter Haze Intensive Tracer Experiment, National Academy Press, Washington, D.C.
- Ouimette, J. and R.C. Flagan (1982) Atmos. Environ. 16:2405-2419.
- Richards, L.W. and D.L. Blumenthal, ed., et al. (1990) Navajo Generating Station Visibility Study Status Report, Working Draft Number 4, STI-99281-1001-WD4. Prepared for Salt River Project, Phoenix, AZ, August 1990.
- Smith, T.B. (1981) Some Observations of Pollutant Transport Associated with Elevated Plumes. Atmos. Environ. 15:2197-2203.
- Vossler, T.L. and E.S. Macias (1986) Environ. Sci. Tech. 20:1235-1243.
- Wall, S.M., W. John, and J.L. Ondo (1988) Atmos. Environ. 22:1649-1656.

APPENDIX A

SELECTED DATA FOR THE FOUR-HOUR MEASUREMENT PERIODS

A number of the analyses in this report are based on the data in the following listing. The sources of the data are:

Light Scattering by Particles: Four-hour average of the integrating nephelometer reading at Hopi Point. Data release date: June 25, 1990.

Relative Humidity: Four-hour average of the hourly relative humidity measured by the meteorological surface measurements at Hopi Point. Data release date: June 25, 1990.

Fine Sulfur: Fine particle sulfur reported as sulfur. Four-hour filter samples were collected by the AVS1 filter sampler with a 3.7 μm cutpoint inlet and were analyzed by x-ray fluorescence. Data release date: September 30, 1990.

Light Extinction: Three transmissometers operated in the Grand Canyon during this study. Date release date: July 5, 1990. The sight paths were:

NPS South Rim:	Transmitter at Lippan Point Receiver at Grandview Point
NPS In-Canyon:	Transmitter at Phantom Ranch Receiver at Yavapai Museum
AV In-Canyon:	Transmitter at Indian Gardens Receiver at Kolb Studio (Near Hopi Point)

The data from the AV In-Canyon transmissometer are available at validation level 1 and were released on July 5, 1990. Raw data from the NPS transmissometers were made available daily during the study for use in forecasting and are used in this table. In this report, the transmissometer readings are used to indicate when clouds or precipitation are present in the sight paths, so accurately calibrated data are not necessary.

The categories listed in the third column are described at the beginning of Section 4. The further breakdown of Category 2 required for the analyses in Section 6 led to the introduction of the following categories:

- 2P: Uncertain, additional analysis may assign period to "probably present" category.
- 2A: Uncertain, additional analysis likely to assign period to "probably absent" category.

Date	Start Hour (MST)	Category	Four Hour Average Values at Hopi Point			Maximum One-Hour Transmissometer Reading During Four Hour Period (Mm ⁻¹)		
			Light Scattering by Particles (Mm ⁻¹)	Relative Humidity (%)	Fine Sulfur (µg/m ³)	NPS South Rim	NPS In Canyon	AV In Canyon
1/10/90	200	3	.6	27	-99.000*	-99	-99	-99
1/10/90	600	3	1.2	26	-99.000	-99	-99	-99
1/10/90	1000	3	.3	21	-99.000	-99	-99	-99
1/10/90	1400	3	.6	21	-99.000	-99	-99	-99
1/10/90	1800	3	.9	29	-99.000	-99	-99	-99
1/10/90	2200	3	.8	30	.038	-99	-99	-99
1/11/90	200	3	.9	30	.030	13	31	-99
1/11/90	600	3	.7	32	.034	14	32	-99
1/11/90	1000	3	.4	19	.019	14	34	-99
1/11/90	1400	3	2.7	16	.034	19	30	-99
1/11/90	1800	3	2.6	18	.036	16	29	-99
1/11/90	2200	3	6.5	22	.047	19	31	-99
1/12/90	200	3	12.9	38	.134	28	32	-99
1/12/90	600	3	6.0	38	.143	200	33	-99
1/12/90	1000	3	3.9	32	.128	22	35	-99
1/12/90	1400	3	3.4	39	.199	21	35	-99
1/12/90	1800	3	2.3	46	.177	18	31	-99
1/12/90	2200	3	2.9	57	.179	75	28	-99
1/13/90	200	3	5.9	71	.277	50	30	-99
1/13/90	600	3	10.0	69	.372	36	35	-99
1/13/90	1000	3	14.6	62	.396	41	40	-99
1/13/90	1400	3	3.9	49	.184	37	41	-99
1/13/90	1800	3	5.5	72	.274	27	24	-99
1/13/90	2200	3	15.0	89	-99.000	35	31	-99
1/14/90	200	3	19.7	95	-99.000	77	33	-99
1/14/90	600	3	17.2	89	.187	44	33	-99
1/14/90	1000	3	9.2	74	.289	31	34	-99
1/14/90	1400	3	8.5	86	.215	183	113	-99
1/14/90	1800	3	.2	99	-99.000	525**	1000**	-99
1/14/90	2200	3	.8	99	-99.000	525	490	-99
1/15/90	200	3	2.2	99	-99.000	525	105	-99
1/15/90	600	3	7.6	98	-99.000	525	45	-99
1/15/90	1000	3	11.9	98	.079	40	29	-99
1/15/90	1400	3	9.5	97	.096	38	293	-99
1/15/90	1800	3	10.8	98	.099	288	186	-99
1/15/90	2200	3	9.9	98	.096	525	189	-99
1/16/90	200	3	9.4	97	.095	525	413	-99
1/16/90	600	3	13.0	96	.080	195	25	-99
1/16/90	1000	3	10.5	89	.101	96	32	-99
1/16/90	1400	3	9.0	89	.121	56	124	-99
1/16/90	1800	3	11.6	95	.131	525	42	-99
1/16/90	2200	3	16.8	97	.179	525	720	-99
1/17/90	200	3	18.1	95	-99.000	525	73	-99
1/17/90	600	3	17.2	89	.214	393	42	-99
1/17/90	1000	3	12.9	84	.220	525	800	-99
1/17/90	1400	3	7.2	86	.265	525	245	-99
1/17/90	1800	3	5.0	97	.259	525	1000	-99
1/17/90	2200	3	4.6	97	.272	525	1000	-99
1/18/90	200	3	6.8	97	.220	525	35	-99
1/18/90	600	3	6.7	95	.205	525	424	-99
1/18/90	1000	3	6.3	92	.300	525	167	-99
1/18/90	1400	2A	7.6	84	.352	525	37	-99
1/18/90	1800	1	5.9	96	.198	525	109	-99

* -99.000 = Missing Data

** The full-scale reading for the NPS South Rim transmissometer is 525 Mm⁻¹ and 1000 Mn⁻¹ for the other two transmissometers.

Date	Start Hour (MST)	Category	Four Hour Average Values at Hopi Point			Maximum One-Hour Transmissometer Reading During Four Hour Period (Mm ⁻¹)		
			Light Scattering by Particles (Mm ⁻¹)	Relative Humidity (%)	Fine Sulfur (μg/m ³)	NPS South Rim	NPS In Canyon	AV In Canyon
1/18/90	2200	1	7.5	97	.320	525	136	-99
1/19/90	200	1	11.5	97	.259	525	423	-99
1/19/90	600	1	18.4	96	.306	525	388	-99
1/19/90	1000	1	29.2	91	.498	525	54	-99
1/19/90	1400	1	23.4	95	.563	302	200	-99
1/19/90	1800	1	24.0	96	.555	525	293	-99
1/19/90	2200	1	26.2	95	.511	177	368	-99
1/20/90	200	2A	26.2	95	.441	525	209	-99
1/20/90	600	2A	30.0	95	.406	525	48	-99
1/20/90	1000	1	18.0	83	.571	244	49	-99
1/20/90	1400	1	15.0	71	.782	36	35	-99
1/20/90	1800	1	19.2	81	.809	34	35	-99
1/20/90	2200	1	16.2	76	.592	28	33	-99
1/21/90	200	1	12.9	72	.501	30	31	-99
1/21/90	600	1	12.8	67	.555	28	32	-99
1/21/90	1000	1	7.9	47	.405	27	32	-99
1/21/90	1400	1	4.0	37	.300	21	24	-99
1/21/90	1800	1	4.3	42	.348	20	28	-99
1/21/90	2200	1	6.8	50	.365	27	29	-99
1/22/90	200	1	7.3	51	.397	24	30	-99
1/22/90	600	1	7.7	51	.411	24	33	-99
1/22/90	1000	1	6.1	39	.670	20	35	-99
1/22/90	1400	1	3.9	37	.404	14	39	-99
1/22/90	1800	1	4.2	39	.316	15	41	-99
1/22/90	2200	1	3.9	37	.280	12	40	-99
1/23/90	200	1	2.6	35	.358	10	43	-99
1/23/90	600	1	6.1	47	.167	10	44	-99
1/23/90	1000	1	1.8	19	-99.000	12	43	-99
1/23/90	1400	3	2.0	21	-99.000	14	35	-99
1/23/90	1800	3	2.4	27	-99.000	12	32	-99
1/23/90	2200	3	1.6	30	-99.000	10	30	-99
1/24/90	200	3	2.0	38	-99.000	10	30	-99
1/24/90	600	3	2.0	37	-99.000	13	30	-99
1/24/90	1000	3	1.5	25	-99.000	14	32	-99
1/24/90	1400	3	1.1	19	-99.000	12	29	-99
1/24/90	1800	3	1.0	21	-99.000	9	26	-99
1/24/90	2200	3	.9	25	-99.000	8	25	-99
1/25/90	200	2A	1.2	30	-99.000	9	25	-99
1/25/90	600	2A	1.2	21	-99.000	9	26	-99
1/25/90	1000	2A	1.3	13	.066	11	28	-99
1/25/90	1400	3	1.1	13	.095	13	27	-99
1/25/90	1800	3	1.0	21	.052	9	26	-99
1/25/90	2200	3	1.0	20	.075	9	25	-99
1/26/90	200	3	1.2	18	.073	9	25	-99
1/26/90	600	3	2.4	16	.059	10	27	-99
1/26/90	1000	3	2.1	17	.062	13	30	-99
1/26/90	1400	3	2.7	21	.070	14	30	-99
1/26/90	1800	3	2.8	25	.080	13	30	-99
1/26/90	2200	3	2.7	30	.083	13	28	-99
1/27/90	200	3	3.5	45	.116	40	55	-99
1/27/90	600	3	4.5	54	-99.000	36	55	-99
1/27/90	1000	1	2.4	40	.068	16	34	-99
1/27/90	1400	1	2.1	33	.103	17	36	-99
1/27/90	1800	1	1.2	47	.103	12	27	-99
1/27/90	2200	1	.7	40	.057	13	26	-99
1/28/90	200	1	.3	31	.031	8	23	-99
1/28/90	600	2A	-99.0	28	.032	7	23	-99

Date	Start Hour (MST)	Category	Four Hour Average Values at Hopi Point			Maximum One-Hour Transmissometer Reading During Four Hour Period (Mm ⁻¹)		
			Light Scattering by Particles (Mm ⁻¹)	Relative Humidity (%)	Fine Sulfur (μg/m ³)	NPS South Rim	NPS In Canyon	AV In Canyon
1/28/90	1000	3	.5	21	.044	10	26	-99
1/28/90	1400	3	.8	20	.057	12	28	-99
1/28/90	1800	3	1.1	24	.045	10	27	-99
1/28/90	2200	3	1.3	20	.057	11	26	-99
1/29/90	200	3	1.8	23	.058	12	27	-99
1/29/90	600	3	1.9	28	-99.000	12	28	-99
1/29/90	1000	3	1.6	21	-99.000	15	29	-99
1/29/90	1400	3	1.3	21	-99.000	15	29	-99
1/29/90	1800	3	1.0	22	-99.000	434	26	-99
1/29/90	2200	3	1.1	23	.081	439	26	-99
1/30/90	200	3	1.0	25	.069	436	25	-99
1/30/90	600	3	1.1	22	.082	441	27	-99
1/30/90	1000	3	1.1	15	.054	427	28	-99
1/30/90	1400	3	1.4	20	.069	15	29	-99
1/30/90	1800	3	5.3	28	.114	18	34	-99
1/30/90	2200	3	5.5	33	.152	91	34	-99
1/31/90	200	3	6.5	75	.108	525	78	-99
1/31/90	600	3	2.3	98	.151	-99	-99	-99
1/31/90	1000	3	3.0	99	-99.000	-99	-99	-99
1/31/90	1400	3	5.2	100	.094	-99	-99	-99
1/31/90	1800	3	8.7	99	.129	-99	-99	-99
1/31/90	2200	3	8.4	99	.120	-99	-99	-99
2/01/90	200	3	14.8	98	.168	69	64	-99
2/01/90	600	3	9.8	98	.177	70	266	-99
2/01/90	1000	3	1.8	98	.089	525	1000	-99
2/01/90	1400	3	13.5	97	.138	525	1000	-99
2/01/90	1800	3	7.0	96	.151	525	129	-99
2/01/90	2200	3	4.5	97	.090	525	319	-99
2/02/90	200	3	1.2	96	.034	525	529	-99
2/02/90	600	3	1.1	92	.043	525	23	-99
2/02/90	1000	3	1.0	72	.046	12	24	10
2/02/90	1400	3	1.3	53	.048	11	24	16
2/02/90	1800	3	1.2	61	.047	11	25	16
2/02/90	2200	3	1.0	58	.063	9	22	17
2/03/90	200	1	1.1	58	.076	10	21	18
2/03/90	600	1	1.2	45	.085	12	22	17
2/03/90	1000	1	2.7	24	.109	14	25	17
2/03/90	1400	1	2.7	28	.150	14	25	17
2/03/90	1800	1	3.5	34	.148	12	24	22
2/03/90	2200	1	4.5	32	.169	13	25	23
2/04/90	200	2A	3.0	27	.103	12	25	19
2/04/90	600	2A	3.6	22	.092	16	27	20
2/04/90	1000	2A	4.5	16	-99.000	18	30	20
2/04/90	1400	3	4.8	32	-99.000	21	30	24
2/04/90	1800	3	6.2	46	-99.000	18	30	23
2/04/90	2200	3	5.9	50	-99.000	15	28	22
2/05/90	200	1	5.4	60	-99.000	525	27	21
2/05/90	600	1	5.8	61	-99.000	16	28	22
2/05/90	1000	1	5.5	42	-99.000	18	30	22
2/05/90	1400	1	4.6	37	-99.000	21	1000	20
2/05/90	1800	1	4.0	46	-99.000	16	1000	19
2/05/90	2200	2A	3.8	52	-99.000	14	1000	20
2/06/90	200	2A	4.9	73	.149	14	1000	19
2/06/90	600	2A	6.8	64	-99.000	14	1000	32
2/06/90	1000	2A	3.5	32	.215	19	1000	27
2/06/90	1400	2A	3.7	32	.186	22	23	19
2/06/90	1800	2A	6.1	54	.348	22	26	26

Date	Start Hour (MST)	Category	Four Hour Average Values at Hopi Point			Maximum One-Hour Transmissometer Reading During Four Hour Period (Mm ⁻¹)		
			Light Scattering by Particles (Mm ⁻¹)	Relative Humidity (%)	Fine Sulfur (μg/m ³)	NPS South Rim	NPS In Canyon	AV In Canyon
2/06/90	2200	2A	9.0	57	.493	18	27	27
2/07/90	200	2A	6.6	51	.335	14	24	22
2/07/90	600	2A	5.2	53	.324	17	25	22
2/07/90	1000	2A	5.1	41	.206	20	25	22
2/07/90	1400	2A	4.6	39	.210	22	24	20
2/07/90	1800	2A	4.8	53	.219	20	22	23
2/07/90	2200	2A	6.8	68	.302	28	25	25
2/08/90	200	2A	13.2	92	.358	525	1000	1000
2/08/90	600	2A	12.0	98	.426	525	1000	1000
2/08/90	1000	3	15.3	95	.385	525	320	132
2/08/90	1400	3	7.2	72	.173	525	24	26
2/08/90	1800	3	5.7	63	.154	17	21	21
2/08/90	2200	3	6.2	69	.138	14	21	22
2/09/90	200	3	3.9	53	.105	13	19	18
2/09/90	600	3	2.4	43	.113	11	18	20
2/09/90	1000	3	1.9	29	.108	13	20	17
2/09/90	1400	3	2.0	37	.098	14	18	16
2/09/90	1800	3	1.4	48	.097	10	16	16
2/09/90	2200	3	1.6	47	.064	10	16	15
2/10/90	200	3	.3	43	.030	10	16	14
2/10/90	600	2A	.5	47	.042	14	19	16
2/10/90	1000	2A	.7	37	.038	16	18	15
2/10/90	1400	2A	.6	37	.039	15	18	14
2/10/90	1800	2A	1.2	51	.045	12	16	19
2/10/90	2200	2A	1.1	56	.043	10	17	19
2/11/90	200	1	.8	56	.041	10	16	21
2/11/90	600	1	.8	53	.050	15	17	24
2/11/90	1000	1	.7	41	.079	17	18	30
2/11/90	1400	1	.9	38	.076	17	18	-99
2/11/90	1800	1	1.3	46	.085	14	15	-99
2/11/90	2200	1	1.6	52	.089	14	17	-99
2/12/90	200	1	1.6	59	.083	14	17	-99
2/12/90	600	3	2.2	59	.123	14	18	-99
2/12/90	1000	3	3.4	54	.137	27	19	-99
2/12/90	1400	3	5.1	44	.095	14	21	17
2/12/90	1800	3	10.1	47	.110	19	26	23
2/12/90	2200	3	31.8	70	.302	27	46	56
2/13/90	200	3	37.0	75	.284	40	48	51
2/13/90	600	3	29.8	66	.245	32	49	52
2/13/90	1000	3	13.6	37	.155	25	45	48
2/13/90	1400	3	7.8	27	.118	25	34	31
2/13/90	1800	3	12.7	63	.264	25	33	34
2/13/90	2200	3	24.4	74	.427	40	44	44
2/14/90	200	3	17.5	81	.330	525	1000	1000
2/14/90	600	3	12.8	93	.289	525	1000	1000
2/14/90	1000	3	8.1	91	.226	525	1000	1000
2/14/90	1400	3	4.2	89	.146	525	1000	1000
2/14/90	1800	3	7.0	85	.281	42	294	34
2/14/90	2200	3	8.9	73	.370	23	31	32
2/15/90	200	3	11.9	70	.381	26	65	53
2/15/90	600	3	15.5	72	.476	38	60	68
2/15/90	1000	3	11.5	48	-99.000	36	44	48
2/15/90	1400	3	8.5	40	-99.000	28	33	36
2/15/90	1800	3	6.8	50	-99.000	19	32	34
2/15/90	2200	3	4.6	44	-99.000	14	22	27
2/16/90	200	3	5.7	53	-99.000	11	18	24
2/16/90	600	3	5.8	45	-99.000	14	22	27

Date	Start Hour (MST)	Category	Four Hour Average Values at Hopi Point			Maximum One-Hour Transmissometer Reading During Four Hour Period (Mm ⁻¹)		
			Light Scattering by Particles (Mm ⁻¹)	Relative Humidity (%)	Fine Sulfur (μg/m ³)	NPS South Rim	NPS In Canyon	AV In Canyon
2/16/90	1000	3	7.1	30	.179	16	25	-99
2/16/90	1400	3	6.1	28	.188	16	25	-99
2/16/90	1800	3	5.4	38	.172	13	22	13
2/16/90	2200	3	3.7	38	.117	7	20	18
2/17/90	200	3	2.8	36	.130	8	15	-99
2/17/90	600	3	3.1	39	.132	36	17	16
2/17/90	1000	3	3.0	37	.283	11	19	17
2/17/90	1400	3	2.5	51	-99.000	227	361	587
2/17/90	1800	3	4.6	67	-99.000	525	251	200
2/17/90	2200	3	7.7	86	-99.000	525	1000	1000
2/18/90	200	3	5.9	94	-99.000	525	1000	1000
2/18/90	600	3	5.9	97	-99.000	525	1000	457
2/18/90	1000	3	4.8	80	.239	91	28	27
2/18/90	1400	3	7.1	72	.266	145	89	101
2/18/90	1800	3	4.5	98	.178	525	1000	1000
2/18/90	2200	3	-99.0	98	.021	525	1000	1000
2/19/90	200	3	1.1	97	-99.000	525	1000	1000
2/19/90	600	3	1.6	95	.078	274	1000	821
2/19/90	1000	3	3.0	95	.128	525	1000	1000
2/19/90	1400	3	7.3	95	.251	525	378	899
2/19/90	1800	3	6.9	96	.190	525	52	82
2/19/90	2200	3	8.9	97	.383	525	481	59
2/20/90	200	3	16.8	96	.661	525	48	40
2/20/90	600	3	10.6	97	.433	305	36	38
2/20/90	1000	2P	8.9	96	.374	27	35	40
2/20/90	1400	2P	9.7	74	.431	27	32	29
2/20/90	1800	2P	13.0	78	.381	23	33	32
2/20/90	2200	2P	10.7	71	.362	20	34	32
2/21/90	200	2P	6.2	52	.286	15	28	26
2/21/90	600	2P	4.0	36	.204	15	27	26
2/21/90	1000	2P	3.3	31	.179	15	27	25
2/21/90	1400	2P	4.0	41	.188	16	25	18
2/21/90	1800	2P	3.0	56	.129	12	20	18
2/21/90	2200	2P	2.2	57	.110	9	18	19
2/22/90	200	1	1.7	52	.098	9	18	16
2/22/90	600	1	2.4	56	.089	11	17	16
2/22/90	1000	1	1.7	34	.144	13	19	16
2/22/90	1400	1	1.8	32	.099	13	18	13
2/22/90	1800	2P	2.0	50	.087	10	16	23
2/22/90	2200	2P	2.2	55	.095	9	16	17
2/23/90	200	1	2.4	59	.098	11	16	19
2/23/90	600	1	1.9	34	.096	11	17	17
2/23/90	1000	1	2.3	26	.146	14	19	13
2/23/90	1400	1	2.4	24	.148	17	19	15
2/23/90	1800	1	2.5	33	.171	47	16	16
2/23/90	2200	1	2.3	29	.118	10	16	15
2/24/90	200	1	2.3	30	.166	10	18	14
2/24/90	600	1	2.9	37	.236	14	18	16
2/24/90	1000	1	3.5	31	.315	17	21	16
2/24/90	1400	1	3.4	21	.227	149	21	16
2/24/90	1800	1	3.2	19	.170	10	19	19
2/24/90	2200	1	3.0	15	.118	11	19	22
2/25/90	200	1	3.4	25	.160	11	19	22
2/25/90	600	2P	3.8	19	.156	10	20	22
2/25/90	1000	2P	3.2	16	.271	12	23	21
2/25/90	1400	2P	3.6	19	.379	14	43	17
2/25/90	1800	2P	4.5	28	.392	13	39	23

Date	Start Hour (MST)	Category	Four Hour Average Values at Hopi Point			Maximum One-Hour Transmissometer Reading During Four Hour Period (Mm ⁻¹)		
			Light Scattering by Particles (Mm ⁻¹)	Relative Humidity (%)	Fine Sulfur (μg/m ³)	NPS South Rim	NPS In Canyon	AV In Canyon
2/25/90	2200	2P	5.4	32	.363	12	35	21
2/26/90	200	2P	5.1	31	.444	14	34	21
2/26/90	600	2P	5.5	29	.473	14	36	26
2/26/90	1000	3	5.6	31	.351	15	35	21
2/26/90	1400	3	4.7	33	.329	16	35	20
2/26/90	1800	3	5.5	49	.363	16	33	22
2/26/90	2200	3	5.8	54	.386	14	30	25
2/27/90	200	3	6.2	56	-99.000	14	30	19
2/27/90	600	3	6.4	51	.365	15	31	22
2/27/90	1000	3	5.3	38	.426	16	34	22
2/27/90	1400	3	5.7	36	.409	17	26	19
2/27/90	1800	3	7.0	48	.005	15	22	20
2/27/90	2200	3	9.9	62	.520	15	22	28
2/28/90	200	3	10.7	68	.622	16	23	22
2/28/90	600	3	9.9	60	.637	22	26	23
2/28/90	1000	2P	8.8	47	.617	28	28	24
2/28/90	1400	2P	9.9	45	.792	24	29	25
2/28/90	1800	2P	12.0	57	.783	20	25	30
2/28/90	2200	2P	12.4	65	.749	18	23	28
3/01/90	200	2P	14.1	67	.770	18	24	26
3/01/90	600	2P	11.9	60	.756	19	26	29
3/01/90	1000	2P	7.5	42	.612	23	27	24
3/01/90	1400	2P	6.7	40	.487	17	25	23
3/01/90	1800	2P	7.4	48	.512	15	21	28
3/01/90	2200	2P	9.2	52	.539	15	21	28
3/02/90	200	2P	9.2	52	.558	18	22	23
3/02/90	600	2P	9.5	51	.580	18	24	27
3/02/90	1000	2P	10.3	44	.580	22	32	26
3/02/90	1400	2P	10.8	42	.493	23	28	27
3/02/90	1800	2A	11.2	50	.519	23	28	31
3/02/90	2200	2A	13.6	56	.532	25	28	33
3/03/90	200	3	13.6	73	.429	125	76	43
3/03/90	600	3	27.3	96	.535	525	1000	77
3/03/90	1000	3	17.6	76	.576	130	36	49
3/03/90	1400	3	13.8	56	.522	28	33	34
3/03/90	1800	3	15.1	65	.566	29	30	38
3/03/90	2200	3	18.7	78	.533	30	32	33
3/04/90	200	3	18.3	71	.556	40	32	34
3/04/90	600	3	24.2	67	.520	50	37	42
3/04/90	1000	3	20.2	52	.386	43	39	39
3/04/90	1400	3	10.0	47	.360	30	37	38
3/04/90	1800	3	15.1	64	.392	39	33	36
3/04/90	2200	3	33.7	72	.494	70	50	60
3/05/90	200	3	23.0	61	.415	50	65	74
3/05/90	600	3	12.7	72	.293	51	666	1000
3/05/90	1000	3	6.2	95	.194	525	1000	1000
3/05/90	1400	3	3.6	95	.110	525	1000	1000
3/05/90	1800	3	6.0	97	.161	525	284	1001
3/05/90	2200	3	2.8	98	.065	525	264	467
3/06/90	200	3	2.3	96	.044	11	58	99
3/06/90	600	3	2.1	84	.054	9	15	21
3/06/90	1000	3	1.7	59	.068	10	16	21
3/06/90	1400	3	2.4	51	.110	12	17	21
3/06/90	1800	3	3.6	53	.184	14	19	24
3/06/90	2200	3	4.2	59	.176	12	17	22
3/07/90	200	3	4.5	63	.204	11	16	23
3/07/90	600	3	4.8	58	.199	13	16	36

Date	Start Hour (MST)	Category	Four Hour Average Values at Hopi Point			Maximum One-Hour Transmissometer Reading During Four Hour Period (Mm ⁻¹)		
			Light Scattering by Particles (Mm ⁻¹)	Relative Humidity (%)	Fine Sulfur (µg/m ³)	NPS South Rim	NPS In Canyon	AV In Canyon
3/07/90	1000	3	4.8	43	.257	16	18	25
3/07/90	1400	3	4.1	41	.202	13	19	21
3/07/90	1800	3	3.5	47	.183	10	16	18
3/07/90	2200	3	4.2	51	.197	10	17	16
3/08/90	200	3	4.0	53	.186	11	17	16
3/08/90	600	3	3.8	44	.178	10	18	17
3/08/90	1000	3	4.0	30	.164	13	20	14
3/08/90	1400	3	2.7	22	.139	13	20	14
3/08/90	1800	3	3.3	-99	.229	13	20	16
3/08/90	2200	3	5.3	-99	.358	15	21	19
3/09/90	200	3	5.6	-99	.394	13	22	19
3/09/90	600	3	4.7	-99	.298	15	23	22
3/09/90	1000	3	4.3	-99	.260	17	24	19
3/09/90	1400	3	5.9	-99	.302	19	28	23
3/09/90	1800	3	4.6	-99	.279	18	26	23
3/09/90	2200	3	2.2	-99	.127	44	19	19
3/10/90	200	3	1.5	-99	.091	10	15	13
3/10/90	600	3	2.7	-99	.142	12	17	16
3/10/90	1000	3	4.2	-99	.240	17	23	23
3/10/90	1400	2A	5.8	-99	.427	45	28	29
3/10/90	1800	2A	12.7	-99	.533	30	33	-99
3/10/90	2200	2A	12.7	-99	.305	522	48	-99
3/11/90	200	2A	8.5	-99	.191	525	24	-99
3/11/90	600	3	8.9	94	.227	57	29	-99
3/11/90	1000	3	2.5	89	.055	114	971	-99
3/11/90	1400	3	2.8	97	.063	525	1000	-99
3/11/90	1800	3	7.8	96	.210	525	1000	-99
3/11/90	2200	3	10.8	88	.198	525	150	-99
3/12/90	200	3	7.5	70	.150	205	56	-99
3/12/90	600	3	7.2	66	.185	28	29	-99
3/12/90	1000	3	7.3	52	.250	50	28	26
3/12/90	1400	3	8.0	56	.347	525	556	783
3/12/90	1800	3	12.0	83	.303	525	85	218
3/12/90	2200	3	11.7	82	.288	30	23	30
3/13/90	200	3	9.8	87	.297	114	27	88
3/13/90	600	3	6.0	83	.279	320	295	179
3/13/90	1000	3	4.9	56	.348	15	75	30
3/13/90	1400	3	3.6	36	.241	12	30	25
3/13/90	1800	3	5.4	59	.296	12	18	20
3/13/90	2200	3	4.9	47	.321	11	17	18
3/14/90	200	3	4.8	47	.361	9	16	18
3/14/90	600	3	4.6	46	.326	9	17	19
3/14/90	1000	3	4.0	40	.309	13	18	20
3/14/90	1400	3	3.6	37	.239	13	17	18
3/14/90	1800	3	3.4	41	.205	10	15	18
3/14/90	2200	3	3.4	48	.199	9	15	17
3/15/90	200	3	4.0	50	.215	9	16	17
3/15/90	600	2A	3.2	48	.154	9	16	18
3/15/90	1000	2A	2.2	34	.120	11	27	18
3/15/90	1400	2A	1.8	25	.088	12	21	22
3/15/90	1800	2A	1.8	34	.120	8	14	16
3/15/90	2200	2A	2.3	44	.147	7	13	16
3/16/90	200	1	2.0	53	.127	7	13	17
3/16/90	600	1	3.2	43	.198	10	14	18
3/16/90	1000	1	3.3	28	-99.000	11	17	17
3/16/90	1400	1	3.0	22	.385	13	18	15
3/16/90	1800	1	3.8	31	.380	9	16	23

Date	Start Hour (MST)	Category	Four Hour Average Values at Hopi Point			Maximum One-Hour Transmissometer Reading During Four Hour Period (Mm ⁻¹)		
			Light Scattering by Particles (Mm ⁻¹)	Relative Humidity (%)	Fine Sulfur (μg/m ³)	NPS South Rim	NPS In Canyon	AV In Canyon
3/16/90	2200	1	2.8	30	.336	8	15	17
3/17/90	200	1	2.6	27	.289	8	15	17
3/17/90	600	1	2.5	24	.249	8	15	19
3/17/90	1000	1	2.6	19	.218	12	19	19
3/17/90	1400	1	2.0	17	.183	13	20	15
3/17/90	1800	1	1.9	21	.206	9	17	14
3/17/90	2200	1	2.0	28	.168	9	15	17
3/18/90	200	1	1.8	30	.114	7	14	14
3/18/90	600	1	1.9	31	.137	10	16	16
3/18/90	1000	1	2.6	24	.304	12	19	17
3/18/90	1400	1	2.1	21	.408	11	18	15
3/18/90	1800	1	1.3	27	.222	8	15	17
3/18/90	2200	1	1.6	33	.142	7	14	16
3/19/90	200	1	2.3	37	.177	8	15	16
3/19/90	600	2P	3.3	35	.223	11	17	18
3/19/90	1000	2P	2.8	26	.231	12	19	20
3/19/90	1400	2P	2.9	20	.178	13	18	16
3/19/90	1800	2P	3.1	26	.190	12	17	22
3/19/90	2200	2P	3.3	30	.228	11	17	22
3/20/90	200	2P	4.3	35	.280	11	17	20
3/20/90	600	2P	3.8	30	.283	11	18	28
3/20/90	1000	2P	2.9	21	-.000	13	21	27
3/20/90	1400	2P	2.7	21	-.99.000	13	22	20
3/20/90	1800	2P	2.5	24	.220	12	19	19
3/20/90	2200	2P	2.5	29	.201	10	19	18
3/21/90	200	1	2.5	31	.155	11	18	20
3/21/90	600	1	2.4	26	.223	12	18	21
3/21/90	1000	1	2.3	20	.191	14	21	23
3/21/90	1400	1	1.9	15	.146	13	19	18
3/21/90	1800	1	2.1	21	.161	9	17	18
3/21/90	2200	1	2.3	26	.132	9	17	19
3/22/90	200	1	2.5	30	.168	8	16	21
3/22/90	600	1	2.6	23	.156	11	18	24
3/22/90	1000	1	2.8	17	.192	15	21	20
3/22/90	1400	2P	3.2	15	.246	15	22	20
3/22/90	1800	2P	5.7	19	.374	19	26	26
3/22/90	2200	2A	7.4	18	.404	17	25	26
3/23/90	200	2A	14.9	22	.313	34	33	27
3/23/90	600	2A	19.9	25	.437	38	36	37
3/23/90	1000	2A	14.5	19	.306	29	37	38
3/23/90	1400	3	4.9	13	.200	20	26	25
3/23/90	1800	3	7.5	16	.220	17	25	28
3/23/90	2200	3	5.6	14	.199	15	22	22
3/24/90	200	3	4.7	17	.181	11	20	20
3/24/90	600	3	4.9	16	.173	15	21	26
3/24/90	1000	3	7.3	14	.232	19	26	31
3/24/90	1400	3	7.0	12	.177	19	27	26
3/24/90	1800	3	7.1	13	.179	17	24	26
3/24/90	2200	2A	7.6	19	.201	16	23	28
3/25/90	200	2A	10.0	28	.331	17	27	31
3/25/90	600	3	10.0	30	.472	22	29	34
3/25/90	1000	3	9.2	18	.338	21	34	33
3/25/90	1400	3	8.3	16	.345	22	32	32
3/25/90	1800	3	7.6	21	.335	19	26	30
3/25/90	2200	3	7.9	30	.387	17	32	28
3/26/90	200	3	7.4	37	.334	15	24	27
3/26/90	600	3	6.9	32	.325	16	25	32

Date	Start Hour (MST)	Category	Four Hour Average Values at Hopi Point			Maximum One-Hour Transmissometer Reading During Four Hour Period (Mm ⁻¹)		
			Light Scattering by Particles (Mm ⁻¹)	Relative Humidity (%)	Fine Sulfur (μg/m ³)	NPS South Rim	NPS In Canyon	AV In Canyon
3/26/90	1000	3	4.7	16	.257	16	26	30
3/26/90	1400	3	5.1	15	.208	17	26	29
3/26/90	1800	3	4.6	20	.195	16	25	28
3/26/90	2200	3	6.3	34	.333	21	25	27
3/27/90	200	3	5.4	35	.276	13	23	27
3/27/90	600	3	4.3	36	.238	13	22	29
3/27/90	1000	3	4.4	30	.263	17	26	31
3/27/90	1400	3	4.9	17	.184	40	25	28
3/27/90	1800	3	8.3	33	.338	42	27	32
3/27/90	2200	3	13.6	44	.481	53	38	39
3/28/90	200	3	11.9	49	.405	53	35	40
3/28/90	600	3	14.4	50	.404	56	38	44
3/28/90	1000	3	10.1	34	.368	48	48	41
3/28/90	1400	3	6.3	30	.243	169	30	35
3/28/90	1800	3	12.4	57	.337	33	35	40
3/28/90	2200	3	20.7	80	.453	37	34	43
3/29/90	200	3	27.1	96	.408	128	121	1000
3/29/90	600	3	11.6	87	.238	151	175	1000
3/29/90	1000	3	10.2	68	.279	525	34	37
3/29/90	1400	3	7.4	66	.215	23	28	33
3/29/90	1800	3	8.4	93	.184	37	47	76
3/29/90	2200	3	7.4	99	.129	38	79	1000
3/30/90	200	3	12.6	99	.199	79	147	1000
3/30/90	600	3	17.7	94	.296	193	81	1000
3/30/90	1000	3	10.5	62	.353	219	103	39
3/30/90	1400	3	7.4	47	.318	38	24	32
3/30/90	1800	3	8.3	88	.215	525	22	76
3/30/90	2200	3	13.2	95	.230	525	301	1000
3/31/90	200	2P	23.3	92	.410	34	32	48
3/31/90	600	1	21.7	86	.551	525	49	48
3/31/90	1000	1	18.1	60	-99.000	525	40	48
3/31/90	1400	1	11.4	42	-99.000	26	28	35
3/31/90	1800	1	11.4	60	-99.000	176	29	35
3/31/90	2200	1	9.9	76	-99.000	17	22	32

APPENDIX B

MATRIX OF SELECTED MEASUREMENTS FROM THE 1990 NGS WINTER STUDY

LEGEND:

- All times are MST.
- IOP is Intensive Operations Period.
 - "-A" = Aircraft only
 - "-B" = Blind*
 - "-M" = Meteorology only
 - "-M-ROU" = Modified routine days
- Tracer was released from 6:00 PM of previous day to 6:00 PM of date shown.
- Tracer and air quality values are maxima of 3 daytime 4-hour samples (0600-1800 MST).
- Hopi Point-Indian Gardens stability is D if lapse rate is less than -0.5 C/100m.
- If Page mixing depth is less than the altitude of Hopi Point, symbol is "<HP."
- Hopi Point surface winds are vector averages from 6:00 AM to 10:00 AM and from 2:00 PM to 6:00 PM.
- Hopi Point relative humidity is averaged from 6:00 AM to 10:00 AM and from 2:00 PM to 6:00 PM.
- Precipitation is for 24-hour period beginning at 3:00 PM of previous day.
- Kalkstein surface weather type is preliminary due to frequency of PAC3 surface weather types.

* Four days of data were originally sequestered as "blind" days for the analysts and modelers. These data were recently released and will be included in subsequent analyses.

APPENDIX B:

MATRIX OF SELECTED MEASUREMENTS FROM THE 1990 NGS WINTER STUDY

DATE	IOP STATUS	* PRELIMINARY * HOPI POINT DAILY MAX TRACER CONCENTRATION					HOPI POINT DAILY MAX 4 HOUR			BRYCE CANYON
		TRACER	PMCP	PMCH	POCH	PTCH	MASS	AMSULF	B-SP	DAY MAX B-SP
		(----- f1/1 -----)					(- ug/m3 -)	(1/Mm)	(1/Mm)	
11090		NA	NA	NA	NA	NA	NA	NA	1	3
11190	IOP	NA	NA	NA	NA	NA	2.68	0.14	3	2
11290	IOP	POCH	NA	NA	8	NA	4.11	0.59	6	6
11390		POCH	NA	NA	25	NA	4.68	NA	15	16
11490		PTCH	NA	NA	17	0	1.73	1.19	17	12
11590		PMCP	9	NA	17	0	1.43	0.39	12	5
11690		PTCH	5	NA	27	0	2.25	0.50	13	7
11790		PMCP	22	NA	21	0	3.23	0.94	17	12
11890		PMCH	15	13	27	0	2.65	1.25	8	6
11990		POCH	25	21	19	0	3.75	2.32	29	42
12090	IOP	PTCH	NA	NA	NA	NA	3.78	3.22	30	37
12190		PMCP	31	11	11	0	2.82	2.29	13	8
12290	IOP-M	PMCH	19	6	10	0	4.62	2.76	8	4
12390	IOP	POCH	7	0	8	0	2.50	0.69	6	1
12490	IOP-M	PTCH	5	2	10	0	1.91	1.41	2	1
12590		PMCP	46	10	6	0	2.06	0.39	1	2
12690		PMCH	34	7	6	0	1.64	0.29	3	3
12790		POCH	NA	NA	NA	NA	8.82	0.52	5	2
12890	IOP-M	PTCH	NA	NA	NA	NA	0.60	0.18	1	1
12990	IOP-A	PMCP	14	4	10	0	1.35	0.18	2	1
13090		PMCH	42	18	15	0	2.00	0.28	2	4
13190		POCH	11	20	21	0	1.80	0.62	5	11
20190		PTCH	0	8	11	0	2.16	0.73	13	6
20290	IOP	PMCP	5	0	17	0	2.18	0.20	1	4
20390	IOP	PMCH	16	17	21	0	3.69	0.45	3	2
20490	IOP-B	POCH	NA	NA	NA	NA	3.18	0.38	5	2
20590	IOP-B	PTCH	NA	NA	NA	NA	2.68	NA	6	17
20690		PMCP	26	11	8	0	2.24	NA	7	3
20790	IOP	PMCH	20	7	6	0	2.77	0.86	5	9
20890		POCH	3	2	8	0	2.48	1.76	15	2
20990		PTCH	3	2	13	0	2.22	1.59	2	1
21090		PMCP	40	20	13	0	0.31	NA	1	1
21190	IOP	PMCH	37	79	21	0	0.97	NA	1	1
21290	IOP	POCH	3	11	6	0	3.67	0.39	5	3
21390	IOP	PTCH	1	11	6	0	7.11	1.01	30	18
21490		PMCP	4	0	6	0	2.32	1.19	13	12
21590	IOP-B	PMCH	NA	NA	NA	NA	6.84	1.96	16	14
21690	IOP-B	POCH	NA	NA	NA	NA	2.43	NA	7	7
21790		PTCH	0	2	8	0	1.70	NA	3	5
21890		PMCP	0	0	19	0	1.68	1.10	7	4
21990		PMCH	12	35	0	0	0.75	1.04	7	10
22090	IOP	POCH	0	0	27	0	2.20	1.79	11	20
22190	IOP	PTCH	0	0	11	0	2.24	0.84	4	5
22290	IOP	PMCP	21	10	4	0	2.91	0.41	2	9
22390	IOP	PMCH	19	0	0	0	0.88	0.39	2	3

DATE	HOPI PT. - IND. GARD. PASQUILL STABILITY MIXING			HOPI POINT METEOR. DATA						CEDAR RIDGE WINDS BELOW 500 M	
	8AM	4PM	PAGE 4 PM DEPTH	06-10		14-18		AM	PM	8AM	4PM
	(m/s)	(m/s)		DIR	SPD	DIR	SPD	RH	RH	(m/s)	(m/s)
					(m/s)	(m/s)	(%)				
11090	E	E	< HP	238	1.3	293	1.2	26	21	NA	NA
11190	E	E	< HP	237	0.8	94	1.2	32	16	NA	NE/3
11290	E	E	< HP	176	2.3	206	3.9	38	39	NA	NA
11390	E	D	>= HP	195	2.8	227	4.7	69	49	S/7	SW/12
11490	D	D	>= HP	198	3.2	202	4.9	89	86	S/12	S/8
11590	D	D	< HP	226	2.0	233	1.9	98	97	S/4	SW/6
11690	D	D	< HP	204	1.2	204	2.0	96	89	S/2	NA
11790	D	D	>= HP	141	3.0	72	3.1	89	86	NA	NA
11890	D	D	>= HP	72	4.0	74	1.4	95	84	NE/7	SE/6
11990	D	D	>= HP	274	3.2	250	1.7	96	95	NA	NA
12090	D	D	>= HP	311	0.7	70	0.7	95	71	NW/5	N/12
12190	E	D	< HP	84	2.8	83	3.9	67	37	NE/3	N/3
12290	E	E	< HP	77	1.9	238	2.4	51	37	SE/4	S/5
12390	E	E	< HP	208	1.5	263	3.5	47	20	S/6	SW/7
12490	E	E	>= HP	0	0.8	95	0.7	37	19	NW/12	NW/7
12590	E	E	< HP	233	0.6	272	1.1	21	13	SE/5	NA
12690	E	D	< HP	229	5.5	244	5.2	16	21	NA	NA
12790	D	E	>= HP	75	0.7	82	1.1	54	33	NA	NA
12890	E	E	< HP	336	0.4	264	2.1	28	20	NA	NA
12990	D	D	>= HP	230	5.2	276	2.1	28	21	SW/10	W/5
13090	E	D	< HP	205	4.1	224	5.3	22	20	SE/9	NA
13190	D	D	< HP	198	3.5	234	2.6	98	100	SW/8	S/5
20190	D	D	< HP	191	3.5	232	5.9	98	97	S/10	SW/11
20290	D	D	>= HP	302	2.0	261	1.8	92	53	NW/14	NW/10
20390	E	D	< HP	88	2.0	83	1.5	45	28	SE/2	SE/5
20490	E	D	< HP	97	1.7	163	1.6	22	32	SE/10	E-SE/6
20590	D	D	>= HP	302	0.8	262	3.5	61	37	NW/9	SW/3
20690	E	E	>= HP	180	1.3	226	3.5	64	32	S/7	S/5
20790	D	D	< HP	196	3.2	240	4.6	53	39	NA	SW/6
20890	D	D	>= HP	245	3.4	266	2.2	98	72	NW/4	SW/5
20990	E	E	< HP	297	0.4	260	1.8	43	37	NW/4	N/3
21090	E	E	< HP	291	1.5	315	0.2	47	37	NW/10	NW/6
21190	E	D	>= HP	85	3.6	87	2.7	53	38	NE/3	E/3
21290	D	D	< HP	227	4.7	226	5.1	59	44	S/7	SW/15
21390	D	D	>= HP	200	4.0	227	9.1	66	27	SW/21	SW/22
21490	D	D	>= HP	244	4.3	305	1.9	93	89	NA	NA
21590	D	D	>= HP	283	1.7	270	1.3	72	40	NA	NA
21690	D	D	>= HP	203	2.7	224	4.2	45	28	NA	NA
21790	D	D	< HP	200	5.4	218	5.4	39	51	NA	NA
21890	D	D	>= HP	207	3.9	208	3.9	97	72	NA	NA
21990	D	D	< HP	165	2.4	264	2.5	95	95	NA	NA
22090	NA	NA	>= HP	292	1.1	290	1.9	97	74	NA	NA
22190	NA	NA	>= HP	298	1.5	292	1.3	36	41	NA	NW/12
22290	NA	NA	>= HP	83	1.5	31	0.5	56	32	N/6	NW/5
22390	NA	NA	< HP	87	1.3	79	1.4	34	24	W/2	NW/2

* PRELIMINARY *
BRIGGS NGS
PLUME WIND

WINSLOW
700 MB WIND

NWS
GRAND CANYON
PRECIP SNOW

KALKSTEIN
WEA. TYPE:
SFC UPPER

DATE	4AM		4PM		5AM		5PM		PRECIP (in.)	SNOW (in.)	WEA. TYPE:	
	DIR	SPD (m/s)	DIR	SPD (m/s)	DIR	SPD (m/s)	DIR	SPD (m/s)			SFC	UPPER
11090	233	4.6	207	3.4	345	2	290	4	0	0	FAC3	NW3
11190	209	1.7	182	4.4	230	4	275	4	0	0	FAC3	NW3
11290	117	3.9	182	3.6	190	7	220	10	0	0	FAC3	NW3
11390	199	4.6	232	9.1	225	16	245	14	0	0	A2	MU3
11490	203	11.1	209	13.2	230	22	215	12	0	0	C1	SW3
11590	284	9.8	NA	NA	230	9	235	7	0.39	0	A2	SW1
11690	323	1.7	184	4.7	200	4	245	8	0.03	0.5	FAC3	SW1
11790	200	10.7	93	3.4	215	13	165	9	0.05	0.5	A2	SW1
11890	64	8.2	35	5.9	160	14	.	.	0.17	1.0	A2	MU1
11990	287	1.0	291	7.2	265	6	280	11	0.26	3.0	C1	W1
12090	305	5.2	33	5.0	305	4	20	4	0.06	0.5	FAC3	W1
12190	74	4.1	91	2.0	60	7	100	8	0	0	FAC2	SW2
12290	70	2.4	192	2.2	.	.	245	9	0	0	FAC3	SW4
12390	NA	NA	160	2.7	310	9	285	10	0	0	FAC3	SW4
12490	325	17.2	337	7.0	320	13	15	13	0	0	A3	W2
12590	286	3.9	191	6.5	360	11	300	9	0	0	FAC3	NW2
12690	249	3.7	235	13.0	260	13	305	21	0	0	FAC3	NW3
12790	72	4.0	80	1.2	.	.	325	5	0	0	A3	NW4
12890	304	5.0	195	3.3	340	11	325	9	0	0	FAC3	W2
12990	292	3.2	274	7.4	260	12	295	14	0	0	FAC3	W2
13090	198	1.8	183	6.6	280	7	220	16	0	0	FAC1	W2
13190	240	8.8	222	5.1	225	20	250	8	0.18	0	C2	SW1
20190	237	7.4	NA	NA	190	8	230	21	0.11	1.0	C1	SW1
20290	6	6.0	5	5.0	290	8	.	.	0.36	4.0	FAC1	SW1
20390	322	1.0	123	2.5	20	13	35	4	0	0	MS1	NW1
20490	161	7.1	166	6.8	.	.	210	17	0	0	FAC3	SW2
20590	47	6.1	288	4.0	215	9	320	9	0	0	FAC1	SW1
20690	271	0.6	164	1.8	260	4	235	10	0	0	FAC3	NW2
20790	255	4.4	229	9.1	230	13	230	12	0.22	3.0	FAC3	SW3
20890	284	6.0	305	2.6	230	23	245	7	0	0	A2	SW3
20990	300	4.4	218	3.5	290	8	320	7	0	0	FAC3	SW2
21090	270	2.9	328	6.4	.	.	355	7	0	0	FAC3	SW2
21190	59	1.1	63	3.4	.	.	240	5	0	0	FAC3	NW3
21290	214	6.2	237	8.6	250	16	245	19	0	0	C1	SW4
21390	219	7.5	233	5.2	250	21	240	27	0	0	C1	SW3
21490	269	9.6	295	9.0	225	30	235	16	0.21	4.0	P2	SW1
21590	300	9.2	268	5.1	270	12	295	8	0	0	NA	W1
21690	265	3.0	190	8.5	275	5	265	11	0	0	A1	W1
21790	217	17.1	NA	NA	245	22	220	13	0	0	MS1	MU1
21890	207	13.7	210	14.3	235	22	225	21	0.17	2.0	MS1	SW1
21990	NA	NA	NA	NA	190	27	250	8	1.41	16.5	MS1	SW1
22090	338	7.8	301	8.2	.	.	345	12	0	0	FAC3	W1
22190	297	6.7	323	6.8	325	9	360	15	0	0	FAC3	NW2
22290	304	4.3	282	2.9	25	9	15	9	0	0	FAC2	NW2
22390	303	3.9	184	2.5	15	5	350	6	0	0	FAC3	NW3

		* PRELIMINARY *					HOPI POINT			ERYCE
		HOPI POINT DAILY MAX					DAILY MAX 4 HOUR			CANYON
		TRACER CONCENTRATION					MASS AMSULF B-SP			DAY MAX
DATE	IOP	TRACER	FMCP	PMCH	PDCH	PTCH	(- ug/m3 -)	(1/Mm)	(1/Mm)	B-SP
	STATUS	(----- f1/1 -----)								(1/Mm)
22490		PDCH	14	50	10	0	3.34	1.30	3	3
22590		PTCH	0	12	13	0	4.48	1.56	4	3
22690		FMCP	58	24	15	0	3.55	1.95	6	3
22790	IOP	PMCH	80	21	21	0	3.55	1.69	6	6
22890	IOP	PDCH	8	0	30	0	4.99	3.26	10	16
30190	IOP	PTCH	3	0	12	0	4.22	3.12	12	7
30290	IOP	FMCP	39	8	10	0	4.12	2.52	11	13
30390	IOP	PMCH	9	0	4	0	3.78	2.37	27	24
30490	IOP	PDCH	1	0	6	0	5.25	2.14	24	23
30590		PTCH	5	15	8	0	3.83	1.21	13	17
30690		FMCP	16	10	10	0	2.05	0.45	2	7
30790		PMCH	14	0	6	0	3.69	1.06	5	15
30890		PDCH	0	6	11	0	2.12	0.73	4	4
30990		PTCH	0	0	8	0	4.50	1.25	6	4
31090	IOP-M	FMCP	10	6	11	0	4.22	1.76	6	4
31190		PMCH	16	10	13	0	1.73	0.94	9	8
31290		PDCH	0	0	13	0	3.37	1.03	8	6
31390		PTCH	0	0	15	0	4.23	1.44	6	9
31490		FMCP	0	0	0	0	3.76	1.34	5	5
31590		PMCH	35	32	21	0	1.90	0.63	3	3
31690	IOP	PDCH	0	0	19	0	2.61	1.59	3	4
31790	IOP	PTCH	0	0	15	0	2.06	1.03	3	2
31890	IOP	FMCP	148	27	25	0	1.73	1.68	3	3
31990		PMCH	68	29	4	0	1.62	0.95	3	3
32090	M-ROU	PDCH	0	20	4	0	2.30	1.17	4	7
32190	M-ROU	PTCH	0	8	25	0	4.70	0.92	2	11
32290	M-ROU	FMCP	47	8	17	25	2.12	1.01	3	13
32390	M-ROU	PMCH	47	1	15	33	5.45	1.80	20	12
32490	M-ROU	PDCH	0	0	34	10	2.58	0.73	7	14
32590	M-ROU	PTCH	0	0	27	0	5.26	1.95	10	21
32690	M-ROU	FMCP	26	15	15	0	3.55	1.34	7	19
32790	M-ROU	PMCH	19	17	34	0	5.58	1.08	5	13
32890	M-ROU	PDCH	0	34	8	0	5.82	1.67	14	34
32990	M-ROU	NA	0	0	6	0	3.69	1.15	12	25
33090	M-ROU	NA	4	0	19	0	2.07	1.46	18	58
33190	M-ROU	NA	0	0	4	0	NA	NA	22	48

DATE	HOPI PT. - IND.GARD. PAGE PASQUILL 4 PM STABILITY MIXING			HOPI POINT METEOR. DATA						CEDAR RIDGE WINDS BELOW 500 M	
	8AM	4PM	DEPTH	06-10 DIR	SPD (m/s)	14-18 DIR	SPD (m/s)	AM RH	PM RH	8AM (m/s)	4PM (m/s)
								(%)			
22490	NA	NA	>= HP	89	3.6	51	0.5	37	21	SE/4	SE/4
22590	E	E	< HP	116	1.0	228	2.2	19	19	SE/3	SW/3
22690	E	D	< HP	153	1.9	235	1.4	29	33	S/5	S/3
22790	E	D	>= HP	81	0.4	307	0.5	51	36	S/3	NW/5
22890	E	D	>= HP	87	1.5	NA	NA	60	45	NE/3	N/4
30190	NA	NA	>= HP	NA	NA	NA	NA	60	40	S/3	S/2
30290	D	D	>= HP	206	1.0	233	2.8	51	42	L&V	S/5
30390	D	D	< HP	210	1.0	251	2.8	96	56	S/3	SW/8
30490	D	D	< HP	204	2.1	211	3.6	67	47	S/6	S/8
30590	D	D	< HP	215	4.0	236	3.8	72	95	SW/15	W/9
30690	D	D	>= HP	288	2.8	320	1.5	83	51	NW/11	NW/10
30790	E	E	>= HP	100	0.6	267	1.6	58	41	NW-N/3S/4	
30890	E	D	>= HP	104	0.9	226	1.0	44	22	S/5	S/6
30990	NA	NA	>= HP	NA	NA	NA	NA	NA	NA	SE/5	S/7
31090	NA	NA	>= HP	NA	NA	NA	NA	NA	NA	S/8	S/9
31190	D	D	< HP	213	4.4	235	6.1	94	97	S/9	SW/18
31290	D	D	>= HP	225	3.7	238	2.6	66	56	SW/6	SW/4
31390	D	D	>= HP	313	1.7	2	1.4	83	36	NW/8	NW/13
31490	D	D	>= HP	309	1.4	283	2.5	46	37	NW/8	NW/8
31590	D	D	>= HP	358	1.8	323	1.6	48	25	NW/13	NW/8
31690	E	D	>= HP	62	1.7	68	0.9	43	22	N/8	NE/8
31790	E	D	< HP	75	0.8	314	1.3	24	17	SE/3	SE-S/4
31890	E	E	>= HP	77	1.2	54	0.7	31	21	NA	N/6
31990	E	E	>= HP	85	2.2	75	1.4	35	20	NA	SE/3
32090	E	D	>= HP	153	0.9	296	0.8	30	21	SE/5	S-SW/3
32190	E	D	>= HP	285	0.6	296	1.2	26	15	NW/3	W/5
32290	E	D	>= HP	195	0.9	259	2.0	23	15	SW/3	SW/6
32390	D	D	>= HP	259	2.2	345	0.5	25	13	W/6	W/7
32490	E	D	>= HP	213	0.2	306	0.7	16	12	SW/2	NA
32590	E	D	>= HP	211	2.0	243	3.6	30	16	SW/5	SW/5
32690	E	D	>= HP	165	2.3	219	3.3	32	15	S/7	S/5
32790	D	D	>= HP	221	2.7	237	3.9	36	17	S/7	SW/9
32890	D	D	>= HP	205	2.9	223	3.6	50	30	S/6	SW/8
32990	D	D	>= HP	172	1.5	249	1.0	87	66	SE/2	NW/5
33090	D	D	>= HP	257	0.8	358	0.5	94	47	W/2	SW/1
33190	D	D	>= HP	85	1.8	66	1.4	86	42	NA	NA

DATE	* PRELIMINARY * BRIGGS NGS PLUME WIND				WINSLOW 700 MB WIND				NWS GRAND CANYON		KALKSTEIN	
	4AM		4PM		5AM		5PM		PRECIP	SNOW	WEA.	TYPE:
	DIR	SPD (m/s)	DIR	SPD (m/s)	DIR	SPD (m/s)	DIR	SPD (m/s)	(in.)	(in.)	SFC	UPPER
22490	84	1.7	207	1.9	130	2	220	7	0	0	FAC3	NW3
22590	131	2.2	179	1.6	250	8	200	5	0	0	FAC3	NW3
22690	127	2.1	203	8.1	230	8	130	4	0	0		AZ SW4
22790	32	1.4	312	3.6	325	7	335	8	0	0	FAC3	SW2
22890	162	0.2	252	1.5	295	4	320	3	0	0	FAC3	SW2
30190	184	0.8	219	2.5	310	1	315	5	0	0		
30290	191	4.8	248	3.1	290	3	240	4	0	0		
30390	240	5.5	213	5.2	250	4	255	9	0.04	0		
30490	272	3.1	206	7.0	235	5	225	5	0	0		
30590	215	11.8	247	8.2	230	25	215	14	0.29	4.5		
30690	292	12.9	310	13.2	315	12	295	10	0.07	T		
30790	346	3.3	216	4.5	315	6	290	6	0	0		
30890	211	2.4	173	4.9	260	7	195	8	0	0		
30990	222	3.5	188	4.6	195	15	220	8	0	0		
31090	243	5.2	199	6.9	195	7	190	5	T	0		
31190	231	11.8	NA	NA	225	13	220	20	0.12	0.5		
31290	241	10.2	250	7.5	225	19	215	12	0.40	2.0		
31390	280	7.7	295	13.3	250	14	295	11	0.02	0		
31490	329	4.9	NA	NA	345	10	305	10	0	0		
31590	312	9.9	56	5.3	340	13	340	14	0	0		
31690	30	7.3	53	4.1	5	8	.	.	0	0		
31790	239	2.9	262	1.0	0	0		
31890	20	2.6	8	3.4	.	.	355	6	0	0		
31990	86	4.2	202	6.6	50	4	205	9	0	0		
32090	221	3.8	313	3.5	205	23	215	6	0	0		
32190	310	3.5	264	4.0	270	10	250	4	0	0		
32290	135	0.9	221	4.0	210	3	240	6	0	0		
32390	255	8.0	280	9.2	270	7	270	7	0	0		
32490	293	4.7	226	4.9	285	6	260	6	0	0		
32590	269	4.2	195	5.2	255	11	260	8	0	0		
32690	233	5.0	192	3.2	235	15	220	6	0	0		
32790	249	4.1	214	10.2	215	10	235	13	0	0		
32890	227	11.7	214	6.7	225	16	220	12	0	0		
32990	235	2.7	346	3.6	235	6	.	.	0.06	0		
33090	50	1.5	34	5.9	.	.	330	2	T	0		
33190	140	1.5	NA	NA	210	3	135	3	0.04	0		